

8788

NACA TN 2490

0065586

TECH LIBRARY KAFB, NM

NATIONAL ADVISORY COMMITTEE FOR AERONAUTICS

TECHNICAL NOTE 2490

FLIGHT INVESTIGATION OF SOME FACTORS AFFECTING THE
CRITICAL TAIL LOADS ON LARGE AIRPLANES

By Harvey H. Brown

Ames Aeronautical Laboratory
Moffett Field, Calif.



Washington
September 1951

AFMTC
TECHNICAL LIBRARY
AFL 2811



0065586

1

NACA TN 2490

TABLE OF CONTENTS

	<u>Page</u>
SUMMARY	1
INTRODUCTION	1
SYMBOLS	2
DESCRIPTION OF TEST AIRPLANE	5
DESCRIPTION OF INSTRUMENTATION	6
DESCRIPTION OF TESTS	8
Pitching Maneuvers	8
Yawing Maneuvers	8
Rolling Pull-Out Maneuvers	9
RESULTS AND DISCUSSION	9
Pitching Maneuvers	9
Test results	9
Pilot effort and airplane response	9
Pilot effort	9
Airplane response	11
Rates of control motion	12
Angular acceleration	12
Comparison between computed and measured quantities during pull-ups	16
Yawing Maneuvers	18
Test results	18
Pilot effort and airplane response	19
Pilot effort	19

	<u>Page</u>
Airplane response	20
Rates of control motion	21
Rolling Pull-Outs.	21
Structural Deflections	23
Fuselage bending deflections	23
Horizontal-tail distortion	24
Vertical-tail distortion	25
CONCLUSIONS	26
Pitching Maneuvers	26
Yawing Maneuvers	27
Rolling-Pull-Out Maneuver	27
Structural Deflections	27
APPENDIX	28
REFERENCES	29
TABLES	30
FIGURES	33

NATIONAL ADVISORY COMMITTEE FOR AERONAUTICS

TECHNICAL NOTE 2490

FLIGHT INVESTIGATION OF SOME FACTORS AFFECTING THE CRITICAL TAIL LOADS ON LARGE AIRPLANES

By Harvey H. Brown

SUMMARY

An investigation of the maneuvering tail load requirements was conducted using a Lockheed Constitution airplane. The forces exerted by the pilot, the control motions, and the airplane response were analyzed for a series of maneuvers.

The motion of the airplane in its plane of symmetry as calculated using aerodynamic parameters from wind-tunnel tests and the measured elevator motion agreed closely with the measured airplane motion. Analysis showed that some terms in the equations of motion (such as those involving $dC_L/d\delta_e$) which may be neglected for the case of small airplanes should be considered when treating large airplanes.

For rapid maneuvers the time lag between a control motion and the resulting airplane response was more noticeable than for smaller airplanes. This lag required anticipatory motions and forces on the part of the pilot and caused "overshoot" in striving for a particular flight condition.

Pilots were inclined to allow the controls to return to neutral at a higher rate than obtained in the initial deflection, producing tail loads of which they had no physical awareness. The maximum negative angular accelerations in pitch were of the same magnitude as the maximum positive accelerations. Comparison was made with various methods of estimating this quantity. The rolling pull-out was found to be a particularly severe maneuver and the comments of the pilots indicate that it may occur in practice.

Structural deflections of the fuselage, horizontal stabilizer, and vertical stabilizer were found to be of moderate importance.

INTRODUCTION

The prediction of the maneuvering tail loads on an airplane has long been a vexing problem to the designer. A solution to the problem

requires a knowledge of the control exerted by the pilot as well as a knowledge of the motion of the airplane resulting from the pilot's effort. Two basic methods have been used to solve the problem. One method involves a statistical evaluation of past maneuvers, adjusting this evaluation on the basis of size, wing loading, type, etc. A second method is to estimate control forces or control motions likely to be produced by the pilot, and then to calculate the motions of the airplane and the tail loads which will result from these control motions.

No matter which method is employed, as airplanes increase in size and weight, experimental data must be obtained to evaluate current design requirements and to assist in extrapolation to airplanes of yet greater size. This need for data comes about because of the variation in response of the airplane as size increases, and also because a pilot's mental attitude and his control actions will vary according to the size and type of airplane. At the present time there exists a scarcity of flight-test results concerning the maneuvering of large airplanes. It was for the purpose of helping to fill this gap that the Bureau of Aeronautics made available to the National Advisory Committee for Aeronautics a Lockheed Constitution for flight-testing. This airplane was instrumented by the NACA but the maintenance and operation of the airplane was performed by the Navy Department.

It was believed that if the elevator deflection and airplane attitude were known, the tail load could be calculated or determined from wind-tunnel test results. Therefore, the flight tests were primarily concerned with the determination of the motions of the airplane, and also with the action of the pilot which produced the airplane motion, although some pressure-distribution measurements were made.

The flight tests consisted of pull-up push-down longitudinal maneuvers, rudder-kick directional maneuvers, and a few rolling pull-outs. Although the various maneuvers were rather carefully restricted to prevent exceeding the design loads, it is considered that the results give an indication of the most severe maneuvers which an experienced pilot would intentionally employ.

The tests consisted of nine flights carried out over a period of two weeks. All the maneuvers were performed by Navy pilots regularly assigned to this type of airplane.

SYMBOLS

B	empirical constant
C, C ₂	arbitrary constants
C _D	airplane drag coefficient

C_L	airplane lift coefficient
C_{L_H}	lift coefficient of horizontal tail
ΔC_l	increment in rolling moment due to aileron deflection
C_{l_p}	$\frac{\partial C_l}{\partial \left(\frac{pb}{2V} \right)}$
C_N	airplane normal-force coefficient $\left(\frac{nW}{Sq} \right)$
C_m	airplane pitching-moment coefficient
C_n	airplane yawing-moment coefficient
C_{n_β}	$\frac{\partial C_n}{\partial \beta}$
F_a	aileron control force, pounds
F_e	elevator control force, pounds
F_r	rudder control force, pounds
I_y	airplane moment of inertia about Y axis, slug-feet squared
J	parameter defined in text, radian per second per second
K	empirical constant denoting ratio of damping moment of complete airplane to damping moment of tail alone
K_1, K_2, K_3	constants occurring in the differential equations of airplane motion
L	lift on airplane in Z direction, pounds
S	wing area, square feet
S_H	horizontal-tail area, square feet
V	true airspeed, miles per hour
V_i	indicated airspeed, miles per hour
W	airplane gross weight, pounds
X, Y, Z	standard airplane axes
b	wing span, feet

c	chord length, feet
\bar{c}	wing mean aerodynamic chord, feet
f_b	bending stress in main beam of vertical stabilizer, tension in port beam cap positive, pounds per square inch
g	acceleration due to gravity, 32.2 feet per second per second
h_p	pressure altitude, feet
k_y	radius of gyration $\left(\sqrt{\frac{I_y}{m}}\right)$, feet
l_H	horizontal-tail length, feet
m	airplane mass $\left(\frac{W}{g}\right)$, slugs
n	airplane load factor $\left(\frac{L}{W}\right)$
Δn	increment in load factor $(n-1)$
p	rolling velocity (same as $\dot{\phi}$), radians per second
Δp	pressure difference between orifices at a given chordwise station in upper and lower surface of airfoil, pounds per square foot
q	dynamic pressure, pounds per square foot
t	time, seconds
x	distance from leading edge, feet
α	angle of attack of airplane, degrees
$\Delta\alpha$	increment in angle of attack from trim angle, degrees
α_H	angle of attack of the horizontal tail, degrees
β	angle of sideslip, degrees
γ	angle between tangent to flight path and horizontal plane, radians
δ_a	total aileron angle, degrees
δ_{aL}	left aileron angle, degrees

δ_{aR}	right aileron angle, degrees
δ_e	elevator angle, degrees
$\Delta\delta_e$	increment in elevator angle from trim position, degrees
δ_r	rudder angle, degrees
ϵ	angle of downwash at the horizontal tail, degrees
η_t	tail efficiency factor
θ	angle between airplane longitudinal axis and horizontal plane, radians
ρ	air density, slugs per cubic foot
ϕ	angle between airplane lateral axis and horizontal plane, radians
ψ	angle of yaw, radians
$\left(\frac{dC_m}{d\alpha} \right)_{W+F}$	pitching-moment coefficient of airplane without horizontal tail
$d\delta_e/dt$	rate of elevator motion, degrees per second
$d\delta_r/dt$	rate of rudder motion, degrees per second
$\dot{\alpha}, \dot{\theta}, \dot{\phi}, \dot{\psi}, \dot{\gamma}$	equivalent notations for $\frac{d\alpha}{dt}, \frac{d\theta}{dt}, \frac{d\phi}{dt}, \frac{d\psi}{dt}, \frac{d\gamma}{dt}$, radians per second
$\ddot{\theta}$	equivalent notation for $\frac{d^2\theta}{dt^2}$, radians per second per second

DESCRIPTION OF TEST AIRPLANE

The tests were carried out using a Lockheed Constitution, XR60-1, No. 85164, a four-engine transport-type airplane shown in figures 1 and 2. Figure 3 is a three-view drawing of the test airplane.

One of the distinguishing features of this airplane was its control system. The elevator, ailerons, and rudder (which had no aerodynamic balances or servo tabs) were operated by hydraulic boost. Three independent hydraulic systems were provided: one of which could operate all three controls as well as flaps, landing gear, etc., a second which could operate elevator and aileron, and a third which could operate elevator and rudder.

The boost ratios were as follows:

Elevator	45.5:1
Aileron	19:1
Rudder	21:1

The maximum rates of control motion as a function of control force, when deflecting the control from neutral as determined from tests on the ground,¹ are shown in figure 4. These data represent the conditions of zero aerodynamic loading.

The pertinent dimensions of the airplane, derived principally from reference 1, are listed in table I.

The airplane gross weight during the tests varied from 153,500 pounds to 145,000 pounds primarily because of fuel consumption. The corresponding variation in center of gravity was 22.7 to 25.4 percent of the mean aerodynamic chord. The airplane moment of inertia about the Y axis for the gross weight during the tests, based on information in reference 1, was considered to be 3.5×10^8 slug-feet squared.

DESCRIPTION OF INSTRUMENTATION

The instruments for the tests of the XR60-1 airplane were concentrated mainly on the lower deck between the front and rear wing beams. Photographs of these instruments are shown in figure 5. A few of the instruments such as the airspeed and altitude recorder, recording manometer, and various control-surface-position recorders were located in various other portions of the airplane.

A free-swivelling airspeed head mounted on a boom extending forward from the port wing tip approximately one chord length was used in measuring the static and dynamic pressures. These pressures were recorded on a standard NACA recording instrument in the wing near the tip. Experience has indicated that, for airspeed heads located this distance ahead of the wing leading edge, the measured static pressure is within 2 percent of the free-stream static pressure. Therefore values of airspeed and altitude presented in this report were not corrected for position error.

The normal acceleration was measured at a position close to the center of gravity and recorded on a standard NACA instrument. The angular velocities about all three airplane axes were similarly recorded.

¹The ground test runs were made with hydraulic pressure supplied by the electrical auxiliary pump and also with the pressure supplied by the engine-driven pumps. No significant difference was noted.

A Statham angular accelerometer was used to measure angular acceleration about the Y axis. Unfortunately, the voltage regulator used with this instrument failed during the tests so that the calibration factor varied as a function of the airplane voltage. The calibration of the instrument used in reducing the flight data was that corresponding to a value of the airplane regulated voltage measured after flight. A comparison of the angular accelerations as measured by the accelerometer and those derived from the slopes of the turnmeter records indicated a 14-percent difference. Thus there exists a possibility that the values of angular acceleration measured by the accelerometer and presented in this report may be too high by this percentage.

The control forces were measured by means of strain-gage pickups and registered on recording galvanometers.

Small vanes mounted on a boom extending forward from the starboard wing tip were used to sense the angles of attack and sideslip. This information was transmitted to the recorder by means of selsyns. The output of the sideslip-angle selsyn transmitter was also fed to a sideslip indicator on the pilot's instrument panel. Unfortunately this system of recording angles proved to have considerable time lag. In addition, the recorded value of angle of attack had $\pm 0.2^\circ$ hysteresis and the angle of yaw $\pm 1.5^\circ$ hysteresis.

It was realized that in a maneuver with angular accelerations present, the normal acceleration in the pilot's compartment could be different from the normal acceleration at the center of gravity. Therefore, the pilot was furnished with an instrument which indicated the normal acceleration at the center of gravity.

The pressures at the orifices on the horizontal and vertical stabilizer were recorded by an NACA 60-cell recording manometer in the afterpart of the fuselage.

Strain gages were installed on the main beam caps of the vertical stabilizer at the 13.4-percent-span station. Their output was used to operate an indicator on the pilot's instrument panel which afforded him an indication of the bending stress in the vertical stabilizer. This information was also recorded.

Bending deflection of the fuselage in flight was determined by two 16-mm gun-sight cameras; one positioned on top of the fuselage above the wing and pointed aft, the other in the dorsal and shooting forward. Similar cameras were used to photograph the elastic distortion of the vertical and horizontal stabilizers. To measure twist of the elevator and rudder relative to the fixed surface the control-surface angles were measured at both ends of the control surface.

DESCRIPTION OF TESTS

Tests were made at various speeds in straight unaccelerated flight to establish power and tab settings for trim. These settings are noted in table II. All subsequent runs were made with these same settings.

The remaining flight tests consisted of pitching maneuvers, yawing maneuvers, and a few aileron rolls. These maneuvers were performed at approximately 5,000 feet and 20,000 feet altitude.

Pitching Maneuvers

Steady turns were made in which the pilot attempted to maintain load factors of 1.5, 2.0, and 2.5 at each of the speeds listed in table II.²

Pull-up push-down maneuvers were performed at these same airspeeds. The pilot, after trimming for straight level flight, moved the control column aft and then forward at various rates. The pilots were instructed to attain load factors of only 1.5 to 2.0 in these maneuvers since it was expected that some overshoot would occur.

Yawing Maneuvers

Only two speeds ($V_1 = 145$ and 204 mph) at the two altitudes were used for the directional tests. The power and tab settings shown in table II were used. The airplane was flown in a steady sideslip and then slowly rolled to a wings-level attitude while holding constant rudder angle. This maneuver was repeated for various initial angles of sideslip. The pilot was furnished a sideslip indicator as well as a meter which indicated the bending stress in the main beam of the vertical stabilizer. Maximum angles of sideslip requested were 12° at 145 miles per hour and 9° at 204 miles per hour. Because of large control forces the maximum angle of sideslip reached at 204 miles per hour was about 6° .

Rudder kicks were performed in which the pilot deflected the rudder and then returned the control using various rates of control motion. The pilots were instructed not to release the rudder abruptly for angles of sideslip greater than $8\text{--}1/2^\circ$ at 145 miles per hour or 4° at 204 miles per hour. In addition, the pilots were cautioned never to exceed an indicated stress corresponding to 80 percent of the limit design stress.

²Because of the possibility of stalling the airplane, the maximum acceleration attempted at $V_1 = 145$ miles per hour was 1.9g.

Rolling Pull-Out Maneuvers

Rolling pull-out maneuvers were made in which the pilot rolled out of a steady turn while attempting to hold a constant normal acceleration. The rudder was held fixed and the airplane was allowed to yaw. In this maneuver the pilots were instructed to restrict the vertical stabilizer bending stress to 80 percent of the limit stress as in the rudder-kick maneuvers. These rolling pull-out maneuvers were performed only at 20,000 feet altitude.

RESULTS AND DISCUSSION

Pitching Maneuvers

Test results.— The measured variations of elevator control force and elevator angle with load factor during turning flight are shown in figures 6 and 7. The considerable scatter of the data was occasioned principally by the difficulty in producing steady turns, especially with only the power required for unaccelerated flight. With such a large airplane a period of time is required to attain steady speed after a change in flight angle. Similarly, an interval of time occurs between the application of an increment of elevator angle and the subsequent change in normal acceleration. Under these conditions it was difficult to produce the desired stable conditions.

Approximately fifty pitching maneuvers were performed during the tests. These maneuvers included a wide variation in the degree of abruptness of the pull-ups and push-downs. The time histories of pitching maneuvers shown in figures 8 through 17 are typical, in general, of the most abrupt maneuvers performed. Because these time histories constitute only a portion of the complete test results, much of the subsequent analysis is based on test results not shown in the time histories.

Examples of the chordwise distribution of loading at a single span station on the horizontal stabilizer during a pull-up push-down maneuver have been included in figure 9(b). The time history of angle of attack is shown for only a few maneuvers because the time lag associated with the recording of this quantity makes its value dubious.

Pilot effort and airplane response.— A study of the airplane motion has two aspects, the action of the pilot and the response of the airplane. These aspects will be considered separately.

Pilot effort.— The pilot, in maneuvering an airplane in pitch, is primarily aware of normal acceleration. It has long been recognized that the pilot's physical awareness of normal acceleration is not entirely adequate in restricting loads

in a maneuver: first, because there can be a considerable time lag between a control motion and the resulting change in normal acceleration, and second, because the maneuvering loads on the tail may be quite independent of normal acceleration.

Thus, in maneuvering an airplane, especially a large one, the pilot must anticipate the subsequent action of the airplane and operate his controls accordingly. The extent of this anticipation may be observed in the time histories shown in figures 8 through 17. The time lag usually increases with airplane size because, although aerodynamic maneuvering moments increase roughly as the third power of the aircraft dimensions, the moments of inertia increase as the fourth power (for constant wing loading), thus effectively slowing the response of the airplane.

The pilots, in performing the pull-up push-down maneuvers, were instructed to "shoot for" a load factor of 1.5 to 2.0. On the push-down portion of the maneuver the limit set was zero load factor. In general, load factors obtained in excess of these limitations may be considered to have been unintentional.³ In the pull-up there was considerable overshoot except at the lowest and highest speeds (fig. 18). At the lowest speed the buffeting near the stall effectively warned the pilot to limit his effort. At the highest speed, which involved a moderate dive, the pilots were naturally cautious. In regard to the push-down portion of the maneuver it may be seen that there was very little overshoot. The pilots, in general, were much more cautious in applying push forces than in applying pull forces.

Because the pilot is quite responsive to normal acceleration, it is interesting to plot concurrent variation of elevator control force with airplane load factor (fig. 19) for various speeds. These data more or less define a regime within which the pilots acted. It may be observed that the pilot was able to apply large pull forces before the airplane load factor increased. In addition, push forces were encountered at or near the maximum load factor. These forces, especially the push forces at maximum load factor, represent sizable maneuvering tail loads of which the pilot is usually not aware. In figure 20 are shown the maximum pull forces which occurred near a load factor of 1.0 and also the maximum push forces occurring near the maximum load factor.

In figure 21 are shown the minimum time intervals in which various pull forces were developed. It may be seen that the

³ It should be noted that the overshoot referred to is not that due to low damping of the short-period oscillations. The short-period oscillation of this airplane is very nearly "dead beat."

pilot in one maneuver applied a maximum force, about 88 pounds, in a little over 0.4 of a second. The maximum rate was considerably higher. In general, it was found that at least 0.35 second was required to complete a given control-force change, regardless of its magnitude.

From conversations with the pilots it was concluded that a pilot's physical awareness of acceleration is somewhat dependent upon the duration of the acceleration. Thus they considered that a steady turn subjected the airplane to higher loads than a quick pull-up push-down maneuver which attained the same acceleration.

Because the pilot is some distance (approximately 52 feet) from the airplane center of gravity, he is subjected to normal accelerations due to angular accelerations. In the present tests this normal acceleration amounted to 1.6g per radian per second squared angular acceleration. In an abrupt pull-up there was a phase relationship between the incremental normal acceleration due to angular acceleration and the airplane normal acceleration which served to decrease the time lag between the maximum elevator deflection and the maximum load factor apparent to the pilot. In other words, because of the pilot's location forward of the center of gravity, the airplane appeared to respond more quickly than it actually did. In addition, the maximum load factor apparent to the pilot was slightly less than that occurring at the center of gravity. This may partially account for the pilots' comments in regard to differing awareness of normal acceleration in steady turns and in quick pull-ups.

Airplane response.- It has been shown by various investigators (references 2 and 3) that the forces on and the motion of small- and moderate-sized airplanes may be calculated for a given elevator motion from a knowledge of the aerodynamic parameters. It will be shown later that this also holds true for a large airplane. The point to be made is that the primary unknown to be investigated in regard to design values of maneuvering horizontal-tail loads is the elevator motion or the pilot's action in maneuvering.

In figure 22 are presented concurrent variations of elevator angle with airplane load factor. The difference between the elevator angle during the pull-up push-down maneuver and the steady-turn value is taken to be the maneuvering increment.⁴ The

⁴This increment is exact for the initial values obtained at $n = 1.0$. For other load factors, an error is introduced because the pull-up push-down maneuvers were performed mostly with wings level; whereas, the turns were performed with some bank. The bank affects the pitching velocity, and therefore the elevator angle, associated with a given load factor.

envelopes of this maneuvering increment for various speeds for both altitudes were converted to positive and negative increments of pitching-moment coefficients using elevator effectiveness results from reference 1. Multiplying these incremental coefficients by the dynamic pressure produces a parameter which is a function of horizontal-tail load due to elevator deflection. In figure 23 this parameter ΔC_{mq} is shown as a function of airplane load factor. The positive values correspond to downward tail loads, and the maximum downward maneuvering tail load occurred at or very near a load factor of one. Inspection of the negative values indicates that the maximum upward tail load due to elevator deflection occurred at load factors just below the maximum.

Rates of control motion.— The rate of control deflection influenced the rate of change of maneuvering tail load, and is therefore of interest.

As previously described, the airplane control system utilized full power boost. The range of pilot forces employed during the maneuvers was below that corresponding to maximum output of the boost. The boost mechanism produces a rate of elevator deflection which is a function of the force exerted by the pilot as well as of the aerodynamic hinge moment. The rates obtained during the ground tests (corresponding to zero aerodynamic moments) shown in figure 4(a) were corrected for the effect of the weight of the elevator and included in figure 24. In figure 24 are also shown various maximum instantaneous rates of elevator deflection obtained during the flight tests as a function of control force. As expected, the aerodynamic hinge moment restricted the rate of elevator deflection from trim position but greatly assisted in returning the elevator toward the trim position. As a consequence, large forces were required to produce sizable positive rates of elevator deflection, but negative rates of the same magnitude were achieved with zero control force. In view of the fact that the pilots actually pushed in returning the control to trim, somewhat higher rates of control motion very probably would have been measured in these tests were it not for the nonlinear characteristic of the boost system in the push direction (see fig. 4(a)).

No significant variation in the maximum rate of change of elevator angle used in the maneuvers was noted with change in airspeed up to 240 miles per hour, as may be seen by inspection of figure 25. Most of the effect of airspeed occurred above 240 miles per hour and it has already been pointed out that the pilots were more cautious at the highest speeds.

Angular acceleration.— The airplane angular acceleration is directly a function of maneuvering tail load; thus maneuvering horizontal-tail loads may be defined in terms of angular acceleration. Equations have been suggested in references 5 and 6

for predicting the maximum angular acceleration to be expected in a pitching maneuver for which the peak load factor may have any value but for which the variation of load factor with time is typical of that for a rapid pull-up push-down maneuver. These equations have been based on experimental data for small or moderately large airplanes. It becomes of importance, therefore, to check the validity of these equations for a large airplane.

The maximum positive and negative angular accelerations measured during the various flight tests are shown in figure 26. Except for the highest speed (about 290 mph) there appears to have been no marked trend due to speed. As pointed out previously, the pilots had a more cautious attitude toward pull-ups at this highest speed. There does seem to have been a tendency toward larger values of angular acceleration at the higher altitude.

Included in figure 26 are some values of angular acceleration computed from results contained in reference 4. These values were obtained during structural demonstrations consisting of pull-ups to the limit load factor. Much higher values of angular acceleration were obtained in the maneuvers of the present investigation than were obtained in the demonstration tests.

The equation of reference 5 for estimating maximum angular accelerations is

$$\ddot{\theta} = BJ$$

where

$$J = \left[\left(\frac{d\delta_e}{dt} \right) \frac{\left(\frac{dC_{L_H}}{d\alpha_H} \right)}{\left(\frac{dC_L}{d\alpha} \right)} \left(\frac{d\alpha_H}{d\delta_e} \right) \left(\frac{S_H l_H}{I_y} \right) \left(\frac{nW}{S} \right) \left(\frac{1}{V_1} \right) \right]^{\frac{1}{2}}$$

and B is an empirically derived factor for which Bouton, the author, suggests values⁵ of +2.5 and -3.5. In figure 27 are shown, as a function of J, the maximum values of $\ddot{\theta}$ obtained in the present investigation.⁶ It will be observed that, in

⁵These values are derived in an unpublished paper based on test results of fighter-type airplanes with 6,500 to 12,000 pounds gross weight.

⁶Also included are values derived from structural demonstration flight tests reported in reference 4. The agreement between these results and the subject flight-test results is good in regard to evaluation of B.

general, for a given value of J the angular accelerations are higher for the higher airspeeds. On the basis of these flight tests the maximum values of B obtained were +1.5 and -1.7, which are considerably below the values of +2.5 and -3.5 reported in reference 5 for the smaller airplanes.

In reference 6, design values of angular acceleration based upon the maneuvering load factor Δn and airplane gross weight were suggested. These were empirically derived from tests of airplanes having gross weights less than 72,000 pounds. These suggested values are

$$\ddot{\theta}_{\max} = \frac{40,000}{W}$$

and

$$\ddot{\theta}_{\max} = \frac{125}{\sqrt{W}} \Delta n$$

Application of the design value of $\frac{40,000}{W}$ produces values of $\ddot{\theta}_{\max}$ from 0.26 to 0.27, which were greatly exceeded in the present investigation. In figure 28, the maximum values of $\frac{\ddot{\theta}_{\max}}{\Delta n}$ obtained in the present flight tests are shown as a function of gross weight. It may be seen that the suggested value of $125 W^{-1/2}$ is also lower than some values obtained in the tests.

The Civil Aeronautics Administration (reference 7) lists the following design specifications for a checked pull-up maneuver:⁷

$$\dot{\theta} = - \frac{30}{V_A} n(n-1.5)$$

at the design load factor, where

V_A design maneuvering speed (approximately 180 mph for the test airplane)

n design load factor

and also

$$\dot{\theta} = + \frac{45}{V_D} n(n-1.5) \text{ at unit load factor}$$

and

$$\dot{\theta} = - \frac{30}{V_D} n(n-1.5) \text{ at design load factor}$$

⁷A checked pull-up maneuver is considered to be the same as a pull-up, push-down maneuver.

where

V_D the design dive speed (approximately 300 mph for the test airplane)

These equations presenting angular acceleration in terms of design load factor and airspeed are based in part, at least, upon experimental results for small and moderately sized airplanes. The present tests afforded an opportunity to check these equations for a large airplane. The design values appropriate to the test airplane are shown in figure 29(a).

These equations are used to specify a component of tail load associated with a checked pull-up to the design load factor, usually at the maximum gross weight. The flight tests failed to satisfy these assumed conditions on three counts: (1) none of the pull-ups had a maximum load factor equal to the minimum load factor specified, (2) the flight speeds differed somewhat from the design speeds, and (3) the airplane weight during the tests, was only about 80 percent of the maximum allowable. In view of the wide range of values that the parameters of an airplane of a given weight may have, however, the effect of the airplane reduced weight was not considered of particular significance and only corrections for (1) and (2) above were attempted.

In figure 30 the maximum angular accelerations obtained from the flight tests at various speeds are presented as a function of maximum load factor. The values specified by the CAA for a design load factor of 2.5 are also shown. Considerable extrapolation is required to compare the positive flight values at the highest speed with the pertinent specification of the CAA, but extrapolating in accordance with the trends shown for the lower speeds indicates that the specification is satisfactory. When one performs a similar comparison for the negative angular acceleration it is at once obvious that the specifications are inadequate by a considerable amount.

A set of equations specifying maximum angular accelerations, which is quite similar to that of reference 7, is given in reference 8 (ICAO). For a large transport airplane, these are (figure 29(b))

$$\ddot{\theta} = \frac{+50 (n-1.0)^2}{V} \text{ at load factor of one}$$

and

$$\ddot{\theta} = \frac{-50 (n-1.0)^2}{V} \text{ at load factor of } n$$

where n is design load factor (2.5 minimum), and V has values of V_A and V_D of reference 7 (approximately 180 and 300 mph, respectively, for test airplane).

The positive values obtained by use of these equations at $n = 2.5$ will be the same as those of reference 7 and the resulting agreement with flight values as indicated in figure 30 is satisfactory. The negative values specified will be larger than those specified by reference 7 and agreement with flight results was considered satisfactory.

The Navy specifications regarding angular accelerations are based on selected values for each category of aircraft. Values for the test (transport) airplane at positive values of load factor are shown in figure 29(c). These values, together with values obtained in the present flight tests for approximately the specified airspeeds, are tabulated below:

<u>Navy specifications</u>	<u>Flight-test results</u>	
$\ddot{\theta} = 2 \text{ rad/sec}^2 \text{ at } n = 1.5$	$\ddot{\theta} = 0.37$	} $V_1 = 170$
$\ddot{\theta} = -2 \text{ rad/sec}^2 \text{ at } n = 3.0$	$\ddot{\theta} = -.50$	
$\ddot{\theta} = 1 \text{ rad/sec}^2 \text{ at } n = 1.5$	$\ddot{\theta} = 0.15$	} $V_1 = 290$
$\ddot{\theta} = -1 \text{ rad/sec}^2 \text{ at } n = 3.0$	$\ddot{\theta} = -.29$	

On the basis of this comparison, the Navy specifications would appear to be conservative.

In addition to a knowledge of the maximum values of pitching angular acceleration, it is essential, of course, to know at what part of the maneuver they are attained. Inspection of the records indicated that the maximum positive angular accelerations were obtained at a load factor of approximately 1.0 and that the maximum negative values were obtained near the maximum load factor. This, of course, agrees with conclusions previously reached, based on the elevator angle results shown in figure 23.

Comparison between computed and measured quantities during pull-ups.—As previously stated, it has been shown for the case of smaller airplanes that, given a time history of elevator motion and a knowledge of the airplane parameters, the angle of attack of the tail and therefore the tail load is readily calculable. In order to ascertain whether the above may be true for a large airplane, such as used in the flight tests, the motion of the airplane was computed using two selected experimental time histories of elevator motion. The required aerodynamic parameters were obtained

from reference 1 and the equations of motions employed are listed in the appendix. The results of the computations, which were carried out at Ames Laboratory using the Reeves Electronic Analogue Computer (REAC), as well as the experimental results, are shown in figure 31. The agreement between computed and flight-test results may be seen to be very good except for the angular acceleration at the higher speed maneuver. As will be pointed out later, this discrepancy may be explained as an effect of tail flexibility.

Reference 9 presents a convenient method of estimating the tail load based on an assumed variation of load factor with time. The load factor is considered to be represented by

$$\Delta n = at^b e^{-ct}$$

where a , b , and c are empirically derived constants.

The values of angular acceleration and angular velocity computed using this method are also shown in figure 31. It may be observed that for the present tests the method overestimates the angular velocities and angular accelerations. Since in reference 9 these angular velocities and accelerations were derived from the assumed load-factor time history, it is apparent that the fundamental error lies in the shape of the load factor curve.

Calculations which were made of the airplane motion indicated that the term involving $dC_L/d\delta_e$ had a rather large effect upon the shape of the load-factor curve. It is the down tail load due to elevator deflection which produces the initial dip in the load-factor curve which can be observed in any of the abrupt pull-ups presented. When the elevator is returned toward neutral the resulting increment in tail load produces a positive increment in load factor, but this is not as noticeable because it occurs nearly coincident with the peak of the load-factor curve.

It should be noted that this effect of tail load on airplane load factor is inconsequential except if the tail loads are defined in terms of the load-factor curve; also the importance of this term increases with the size of the airplane, being unimportant for small airplanes, and should become relatively important for airplanes larger than the Constitution. This situation comes about because the airplane moment of inertia relative to the airplane mass increases with an increase in airplane size. Thus the translational effects of the tail load compared to the rotational effects are greater for a large airplane than for a small airplane.

Reference 9 also contains a method for estimating the time to reach the maximum load factor, as a function of the time to reach

maximum elevator angle, assuming the elevator deflection is increased linearly to a maximum and returned to neutral at the same rate. There were several pull-ups in the present flight tests that involved approximately this type of elevator input. In figure 32 is shown the time required to reach the maximum load factor as a function of the time to attain the maximum elevator angle for these particular maneuvers. Shown too is the relationship presented in reference 9. Due to the large value of moment of inertia the data from the present tests fall slightly outside the scope of reference 9 but agree fairly well nevertheless. It is suggested that in using this relationship for large airplanes the actual values of δK_2 be employed.

Yawing Maneuvers

Test results.— Both steady sideslips and wings-level sideslips were performed in the hope that analysis would allow a determination of the relationship between yawing velocity and rudder deflection. However, due to the low side-force gradient present in the test aircraft, there was very little difference between these two sideslip conditions.

The variation of rudder force with angle of sideslip is shown in figure 33. The scatter of the data can be attributed largely to the friction in the control system. For the tests at 204 miles per hour (fig. 33(b)) the maximum steady sideslip attainable was limited to 6.5° by the large control forces. The largest control forces shown, a little over 200 pounds, represent maximum pilot effort. The abrupt change in slope at approximately 136 pounds was caused by the restricted output of the rudder boost system. For greater control force the force output of the boost was constant.

The variation of rudder angle with angle of sideslip is shown in figure 34. The corresponding variation of bending stress in the main beam of the vertical stabilizer at 13.4 percent of the span is shown in figure 35. In figure 36 are shown load distributions obtained at the various sideslip angles.

^aThe value of K_2 as defined in reference 9 is:

$$K_2 = -\frac{q}{m} \left\{ \left(\frac{dC_m}{d\alpha} \right)_{W+F} \frac{S^2}{k_y^2 b} - \frac{dC_{LH}}{d\alpha_H} \eta_t \frac{S l_H}{k_y^2} \left[\left(1 - \frac{d\epsilon}{d\alpha} \right) + \frac{dC_L}{d\alpha} \frac{K}{\sqrt{\eta_t}} \frac{\rho}{2} \frac{S l_H}{m} \right] \right\}$$

It occurs in the equation of motion

$$\ddot{\alpha} + K_1 \dot{\alpha} + K_2 \Delta \alpha = K_3 \Delta \delta_e$$

As previously described, the rudder-kick maneuvers were rather carefully restricted by limiting the angle of sideslip and the bending stress in the stabilizer main beam. Therefore, the most severe maneuvers may not represent the maximum that the pilot would otherwise produce. However, some trends should be evident. Time histories of several typical maneuvers are shown in figures 37 through 46. A total of 27 rudder-kick maneuvers were performed and therefore it should be noted that the subsequent analysis contains data not shown in the time histories presented. One of the most notable characteristics of these maneuvers is the higher rate of control motion in returning to neutral compared to the rate involved in producing the sideslip, even though the pilots were instructed to return the control to neutral at the same rate.

Pilot effort and airplane response.— As in the case of the pitching maneuvers, the yawing maneuvers will be considered first in regard to pilot's action, and second in regard to the airplane motion as a result of the control deflection.

Pilot effort.— In yawing maneuvers the lateral accelerations are comparatively small so the pilot physiologically is not strongly aware of angle of sideslip. He is, therefore, influenced by several factors such as sideslip as indicated by the position of the ball in the inclinometer, angle of bank, rudder-pedal force, changes in heading, etc. However, it is felt that the primary factors in regard to loads are the angle of sideslip and the rudder angle, and that these other factors are of importance only inasmuch as they indicate the angle of sideslip to the pilot.

Thus, in the following analysis, the results are presented primarily as a function of the angle of sideslip. In figure 47 are shown concurrent variation of rudder-control forces with sideslip angle. It can be seen that the pilot was able to apply or to release nearly his maximum force before the airplane changed its angle of sideslip appreciably.

The maximum increments of control force from those required for steady sideslip were as follows:

V_i	^s Maximum positive increment occur- ring near $\beta=0$	^s Maximum negative increment occur- ring near β_{max}
144	125 pounds	116 pounds
200	112 pounds	123 pounds

^sIt may be noted that the action of friction in the control system is to reduce the moment applied to the control surface.

Thus the pilots restricted their control forces to within 125 pounds.

Actually, of course, the pilot could, in returning from steady sideslip, by applying a helping force, greatly increase the negative increment and incidentally greatly increase the vertical-tail load. This action would correspond to the so-called "fish tail" maneuver which is not usually considered in designing transport airplanes. In spite of words of caution, there were maneuvers in which the pilots did apply some small "helping" forces (fig. 42).

The minimum time increments which the pilot required to apply a force are shown in figure 48. A time history of the most abrupt force application is shown. This indicates that the pilot was able to apply 125 pounds in 0.60 second. In one test run on the ground the pilot applied 179 pounds in 0.60 second, which corresponds to $\frac{dF_r}{dt} = 298$ pounds per second..

The period of the directional short-period oscillation for this airplane is about 8 seconds at 144 miles per hour, and about 5 seconds at 205 miles per hour. The damping is rather low and some overshoot did occur. This allows the pilot, for a given force, to attain a greater sideslip in a maneuver than in a steady sideslip.

Airplane response.— The response of the airplane to the rudder motion can be gaged readily from figure 49. In this figure the rudder deflection is plotted as a function of angle of sideslip for several maneuvers. It is readily apparent that large changes in rudder angle can occur before the airplane changes its attitude. The response of the airplane in yaw is slower than in pitch due to the greater moment of inertia about the Z axis, and also because the vertical-tail load per unit rudder deflection is less than the horizontal-tail load per unit elevator angle.

From the data obtained in the maneuvers in which the control was abruptly released, it was possible to determine the variation with sideslip of the rudder angle corresponding to zero hinge moment (zero control force). This has been included in figure 49. Utilizing these data along with the steady-sideslip data of figures 33 and 34 affords an estimation of the variation with sideslip of the rudder deflections corresponding to a 300-pound control force and also for the control force at which the power boost reached its maximum (136 lb). This variation is based on zero yawing velocity and is also included in figure 49.

Rates of control motion.— As for the pitching maneuvers, it is of interest to see if the power boost limits the pilot's ability to move the controls rapidly. In figure 4(b) are shown the rates of control motion obtained in ground tests. The kinetic friction, approximately ± 32 pounds, had a considerable effect upon the rates attainable.

Various maximum rates of rudder motion obtained in the flight tests are presented in figure 50 as a function of control force. Although the maximum rates of right-rudder deflection were not large, in some cases the limit imposed by the boost system time response was reached. In regard to the rates of left-rudder deflection the boost system usually was the restricting influence, the maximum rate usually being a function of hinge moment of the rudder rather than of the control force.

The maximum rates of rudder motion as a function of airspeed are shown in figure 51. There was no significant effect of airspeed or altitude on these maximum rates. The rates of left-rudder deflection involved in releasing the control force were over twice as high as the rates of right-rudder deflection.

The danger involved in the high rates used in returning the rudder to neutral is due to the additive nature of the vertical-tail load due to sideslip and the load produced in returning the rudder. Since it is natural for pilots to associate higher loads with application of control force rather than with release of control force, it is believed that the afore-mentioned dangerous loading condition should be brought to their attention.

Rolling Pull-Outs

In performing the rolling pull-outs the pilots were instructed to roll from a 1.8 to 2.0g steady turn while holding the rudder angle fixed and maintaining constant normal acceleration. The pilots found difficulty in maintaining constant acceleration as the airplane rolled past the wings-level attitude. Therefore, most of the results obtained pertain to airplane load factors of about 1.2.

Time histories of the pertinent quantities measured during two rolling pull-outs are shown in figures 52 and 53. The airplane sideslipped sufficiently to build up quite large vertical-tail loads even though only low load factors ($n = 1.2$) were involved.

Only one rolling pull-out was performed at 145 miles per hour because of the large load produced on the vertical tail. Without the stress indicator the pilot could have inadvertently exceeded the design load.

In reference 10 the following expression is suggested for estimating the maximum sideslip angle attained in a rolling pull-out maneuver:

$$\beta_{\max} = \frac{1}{4} \left(\frac{\Delta C_l}{C_{l_p}} \right) \left(\frac{C_L}{C_{n\beta}} \right)$$

Let

$$\Delta C_l = \frac{\partial C_l}{\partial \delta_a} \delta_a$$

This leads to

$$\beta_{\max} = \frac{\frac{\partial C_l}{\partial \delta_a} \delta_a C_L}{4 C_{l_p} C_{n\beta}}$$

For fixed rudder the bending stress due to the load on the vertical stabilizer may be expressed as:

$$f_b = C \beta_{\max} q = C_2 \delta_a n$$

Thus the vertical-tail load is a function of aileron deflection and load factor. Therefore, it might be expected that the highest loads will be obtained at the lower speeds since larger aileron angles are usually available. This proved true in the flight tests.

In figure 54 the bending stress per unit load factor is shown as a function of total aileron angle. These results indicate that a full deflection of the ailerons ($\delta_a = 35^\circ$) would produce 81 percent of the limit design stress during level flight if the airplane were allowed to yaw.

The aileron control forces involved in the rolling pull-outs are presented in figure 54(a). For both speeds shown the control forces were about 40 pounds at the time the maximum sideslip was attained.

At the present time the Civil Aeronautics Administration and Air Force have no specifications in regard to the rolling pull-out maneuver. The Navy requirements specify designing the vertical tail for full deflection of the ailerons (rudder fixed) at various points on the V-n diagram; the most critical condition for the test airplane would be a

load factor of 2.4 at an indicated airspeed of approximately 160 miles per hour. In view of the reluctance of the pilots to hold a high load factor long enough to allow the airplane to attain a stable angle of yaw, this requirement may be unduly severe.

The pilots, in performing this particular maneuver, were highly impressed by the smallness of the control forces required to produce large vertical-tail loads. Several stated that the rolling pull-out felt quite similar to maneuvers encountered in flying through gusty air. If this is true, then the rolling-pull-out maneuver is not unique to small airplanes and should be considered in the design of large airplanes.

Structural Deflections

Large airplanes, primarily because of their lower limit load factors, usually are relatively more flexible than smaller airplanes. Some measurements of structural deflections were made during the subject flight tests. The purpose was merely to measure the magnitude of the deflections in order to determine whether the deflections were important. No attempt was made to conduct a comprehensive investigation of the deformations.

Fuselage bending deflections.- The bending deflection of the after portion of the fuselage was measured by means of a camera pointing rearward and mounted atop the fuselage above the wing. The angular deflection of the after portion of the fuselage was measured by means of a similar camera mounted within the dorsal fin and pointing forward.

Only bending deflections in the vertical plane were measured. No measurements of sidewise bending deflections or torsional deflections were made. The vertical deflection of the fuselage during the pull-up push-down maneuver for which time histories are shown in figure 16 was found to be less than 1 inch. This maneuver (abrupt pull-up and release with a maximum load factor of 2.55 at 204 mph) was one of the most severe maneuvers performed.

The measured increment in angle of attack of the after portion of the fuselage due to fuselage bending during this same maneuver (fig. 16) was 0.10° . However, this small deflection proved to be in the opposite direction to that expected considering the direction of the aerodynamic load. Apparently the bending deflection due to the mass acceleration effect of the tail assembly outweighed the deflections due to the aerodynamic forces. Measurements over a speed range from 144 miles per hour to 244 miles per hour at a load factor of 1.0 indicated an angular deflection of slightly less than 0.20° . A change in angle of incidence of this magnitude at 300 miles per hour would produce an increment in aerodynamic load of approximately 4 percent of the design tail load.

It was concluded that the effect of fuselage bending on the maneuvering characteristics of the airplane was small and that this was due in part to the balancing of aerodynamic and inertia effects.

Horizontal-tail distortion.- The variation of the bending deflection of the horizontal-stabilizer tip with respect to the fuselage as a function of dynamic pressure is shown in figure 55(a) for unaccelerated flight. These deflections are those produced by the balancing tail load. The measured bending deflections in turning flight are shown in figure 56(a). The results at the two different altitudes coincided except for the larger elevator deflections. In figure 56(a) are indicated certain points which appear to be at variance with the faired curves. Examination of the accelerometer record indicated buffeting had been occurring.

The bending deflections produced during a rather severe pull-up push-down maneuver may be observed in figure 16. Bending deflections due to steady flight and to maneuvering flight were considered to be small.

Though the bending deflections are of interest, in this instance it is the torsional deflections which are of primary importance because twisting affects the spanwise distribution of lift. The twisting deflection of a tail surface is here considered to be composed of a twisting of the stabilizer plus a twisting of the control surface with respect to the stabilizer.

In figures 55(b) and 56(b) are shown the twist of the station at 64.5 percent semispan with respect to the root for unaccelerated and turning flight, respectively. The deflection accompanying a pull-up push-down maneuver is shown in figure 16. In regard to the maneuver, it is rather apparent when one compares the measured twist with the corresponding time histories of elevator deflection and normal acceleration that the twisting was primarily produced by the loading due to elevator deflection rather than by the loading due to the angle of attack.

The twist of the elevator with respect to the stabilizer was determined by measuring the elevator angle at the airplane center line and at the tip of the elevator. The results obtained in unaccelerated and turning flight indicate that at the higher speeds a given elevator angle at the root produced a noticeably smaller elevator angle at the tip. In figure 57 is shown the variation with dynamic pressure of the increment measured at the tip for a given increment in elevator angle at the root.¹⁰

¹⁰It should be noted that the twist between root and tip of the elevator itself was equal to the elevator twist as presented plus the stabilizer twist.

The torsional loading on the elevator and the control force are, of course, related. It is of interest therefore to present the increment in twist produced by an abrupt¹¹ application of an increment in control force. The result (fig. 58(a)) indicates about 1° twist per 40 pounds control force.

The importance of the twisting of the stabilizer was gaged by calculating the increment of angular acceleration associated with the above deflections. The maximum stabilizer twist of the pull-up maneuver shown in figure 16, 0.3° , represented an increment in angular acceleration of roughly 0.02 radian per second squared; or in other words, twisting of the stabilizer reduced the maximum angular accelerations by about 5 percent. The computed effect of elevator twist on angular acceleration was about half that due to stabilizer twist and was of an additive nature. These aeroelastic effects, of course, increase with dynamic pressure which is borne out by comparisons available in figure 31. The estimated (rigid airplane) maximum angular accelerations agreed quite well with the experimental values for the pull-up at $V_1 = 168$ miles per hour. A considerable discrepancy occurred for a similar comparison for the maneuver at $V_1 = 240$ miles per hour and this discrepancy is approximately that expected from calculations based on the measured structural deflections.

Thus it was concluded that, for the airplane as flown, the twisting of the stabilizer and elevator caused a moderate reduction in the maximum angular acceleration from that of a rigid airplane. Since the component of tail load associated with angular acceleration for this airplane is roughly one-third of the design load in the more severe pull-ups, the effect of tail flexibility will have a proportionately small effect on tail load.

Vertical-tail distortion.- The lateral bending deflections of the vertical stabilizer were measured in a manner similar to that used in the case of the horizontal stabilizer. The magnitude of these bending deflections may be judged by observing figures 42 and 52 which contain time histories of the tip deflection for a rudder-kick maneuver and for a rolling pull-out maneuver.

As previously pointed out, it is the twisting deflections which are of importance. The twist of the vertical stabilizer measured at the 64.5-percent-span station during the rudder kick (see fig. 42), and rolling pull-out (see fig. 52), were approximately half a degree. Because of the sizable angles of sideslip involved, 10° to 12° , it is apparent that the effect of this stabilizer twist upon the aerodynamic loading was relatively small. Because the induced flow angles due to the wing are smaller and also because of different plan form and structure, the vertical stabilizer suffered a relatively larger twist with angle of sideslip than did the horizontal stabilizer with angle of attack.

¹¹Abrupt motion is specified here since a change in angle of attack can cause stabilizer and elevator twist.

The twist of the rudder is defined as the twist with respect to the vertical stabilizer and was measured in the same manner as was the elevator twist. In figure 58(b) is shown the variation of rudder twist with incremental (abrupt) control force. Also shown is the variation of rudder twist with control force for the steady sideslip. The difference between these curves was caused by the stabilizer twist due to sideslip. The maximum twist measured, 1.4° , occurred when rudder deflections (at the root) were approximately 20° at 144 miles per hour and 12° at 208 miles per hour. This twist would, of course, become relatively larger at higher speeds.

CONCLUSIONS

The following conclusions were drawn as a result of the flight tests of the Navy XR60-1 airplane. Although certain restrictions were given to the pilots, it is believed that the pilots' actions gave an indication of maximums an experienced pilot would exert in this type of airplane.

Pitching Maneuvers

1. A noticeable time lag existed between the pilot's control force and the subsequent response of the airplane. For a rapid pull and release of the control this time lag was found to agree well with the values predicted using NACA TN 2078 (reference 9).
2. In performing rapid pull-ups the pilots caused the airplane to reach higher accelerations than desired. Pilots were more wary in regard to push-downs so little overshoot occurred in the negative direction.
3. The maximum rate of application of a pull force was about 275 pounds per second. However, the pilots did not apply abrupt control-force increments greater than about 90 pounds pull and 60 pounds push.
4. The maximum rates of elevator motion in pulling up were found to be about equal to the rates obtained in recovering from a pull-up. However, these latter rates were obtained with little or zero control force.
5. The maximum angular accelerations measured during the pull-up push-down maneuvers were (1) in very good agreement with values specified by ICAO; (2) greater negatively than those specified by CAA; (3) greater than those computed by the methods of NACA TN 2103; and (4) less than those specified by the Navy and the method of reference 5.
6. The motion of the airplane as computed using stability derivatives as obtained from wind-tunnel results and the experimental elevator

motion agreed closely with the measured motion, provided the equations of motion were not overly simplified. For a large airplane the direct effect of tail load upon the airplane load factor was found to affect the shape of the load factor curve quite markedly.

Yawing Maneuvers

7. The response of the airplane in sideslip was much slower than in pitch. The pilot was able to apply large forces and rudder-angle changes before the airplane could respond..

8. The maximum rates of change of rudder angle obtained in releasing the rudder were nearly twice the maximums obtained in deflecting the rudder.

9. The maximum rate of change of rudder-pedal force was approximately 300 pounds per second. The maximum value of abrupt control-force change was 125 pounds.

10. The largest vertical-tail loads were found to occur when the pilot released the rudder-pedal force during a sideslip. Pilots are normally not acquainted with this critical condition.

Rolling-Pull-Out Maneuver

11. The rolling pull-out was found to produce large loads on the vertical tail. Although the rolling pull-out constitutes an uncoordinated maneuver, several pilots expressed the opinion that such a maneuver may be encountered in flying through turbulent air.

Structural Deflections

12. Bending deflections of the fuselage due to horizontal-tail loads during various maneuvers were small.

13. The twists of the horizontal stabilizer, vertical stabilizer, elevator, and rudder, measured during the maneuvers, were found to be moderately small.

Ames Aeronautical Laboratory,
National Advisory Committee for Aeronautics,
Moffett Field, Calif., Jan. 10, 1951.

APPENDIX

EQUATIONS OF MOTION

The equations of motion used in computing the airplane motions of figure 31 were:

$$mV\dot{\gamma} - \left(\frac{dC_L}{d\alpha} + \frac{C_D}{57.3} \right) \Delta\alpha \, qS = + \frac{dC_L}{d\delta_e} qS \, \Delta\delta_e \quad (1)$$

$$\frac{I_y}{qSc} \ddot{\theta} + \frac{dC_m}{d\dot{\theta}} \dot{\theta} + \frac{dC_m}{d\dot{\alpha}} \dot{\alpha} + \frac{dC_m}{d\alpha} \Delta\alpha = - \frac{dC_m}{d\delta_e} \Delta\delta_e \quad (2)$$

$$\left. \begin{aligned} \dot{\gamma} &= \dot{\theta} - \dot{\alpha} \\ n &= \frac{V\dot{\gamma}}{g} \end{aligned} \right\} \quad (3)$$

where

$$\frac{dC_m}{d\dot{\theta}} = -K \frac{l_H^2}{Vc} \frac{S_H}{S} \frac{dC_{L_H}}{d\alpha_H}$$

$$\frac{dC_m}{d\dot{\alpha}} = - \frac{l_H^2}{Vc} \frac{d\epsilon}{d\alpha} \frac{S_H}{S} \frac{dC_{L_H}}{d\alpha_H}$$

REFERENCES

1. Stevens, W. P.: Lockheed 89 Aerodynamic Structural Data. Lockheed Aircraft Corp. Rep. 4046, 1943.
2. Matheny, Cloyce E.: Comparison Between Calculated and Measured Loads on Wing and Horizontal Tail in Pull-Up Maneuvers. NACA ARR No. L5H11, 1945.
3. Sadoff, Melvin, and Clousing, Lawrence A.: Measurements of the Pressure Distribution on the Horizontal-Tail Surface of a Typical Propeller-Driven Pursuit Airplane in Flight. III - Tail Loads in Abrupt Pull-Up Push-Down Maneuvers. NACA TN 1539, 1948.
4. Carrillo, J. G.: Navy Demonstration Tests for the XR60-1 Airplane. Lockheed Aircraft Corp. Rep. 6535, 1948.
5. Bouton, Innes: Maneuvering Horizontal Tail Loads. Jour. of the Aero. Sciences, Vol. 16, No. 7, July 1949, pp. 440-441.
6. Matheny, Cloyce E.: Maximum Pitching Angular Accelerations of Airplanes Measured in Flight. NACA TN 2103, 1950.
7. Civil Air Regulations, Part 4b, Airplane Airworthiness. Transport Categories, Effective July 20, 1950. Civil Aeronautics Board, Wash., D. C.
8. International Civil Aviation Organization: Standards and Recommended Practices, Airworthiness of Aircraft, Annex 8 to the Convention on International Civil Aviation, 2d ed., March 1951. (Available through Secretary, ICAO, International Aviation Bldg., 1080 University Street, Montreal, Canada)
9. Pearson, Henry A., McGowan, William A., and Donegan, James J.: Horizontal Tail Loads in Maneuvering Flight. NACA TN 2078, 1950.
10. White, Maurice D., Lomax, Harvard, and Turner, Howard L.: Sideslip Angles and Vertical-Tail Loads in Rolling Pull-Out Maneuvers. NACA TN 1122, 1947.

TABLE I.- PERTINENT DIMENSIONS, LOCKHEED XR60-1 AIRPLANE

Item	Wing	Horizontal tail	Vertical tail	Elevator	Aileron (each)	Rudder
Airfoil section, root	Lockheed D-20%	NACA 64,2-013	NACA 65,2-012	---	---	---
Airfoil section, tip	Lockheed D-12%	NACA 64,2-013	NACA 65,2-010	---	---	---
Span, feet	189.1	69.5	28	---	---	---
Area, square feet	3610	908.4	381.9	236	109	94
Mean aerodynamic chord, feet	21.08	14.5	15.8	4.08	3.33	3.44
Aspect ratio	9.9	5.35	2.06	---	---	---
Taper ratio	0.30	0.32	0.173	---	---	---
Twist, wash-in positive	-1.5°	0	0	---	---	---
Tail length, feet	---	77*	74*	---	---	---
Deflection limits, degrees	---	---	---	+20 -40	+10 -25	±30
Tab area, square feet	---	---	---	10.2 (each)	7.2	7

*Distance from 25-percent wing M.A.C. to 20-percent tail M.A.C.



TABLE II.- POWER AND TAB SETTINGS FOR TRIM AT $n = 1.0$ (a) $h_p = 5,000$ feet

Engine				Tab	
V_i	rpm	Torque (lb-ft)	Cowl flaps	Elevator tab	Rudder tab
145	1900	135	0°	5° nose up	1° left
166	1900	160	0°	1° nose up	1° left
204	2150	196	20°	0° nose up	1° left
239	2550	220	25°	2° nose down	1° left
290	2550	230	25° - 40°	4° nose down	1° left

(b) $h_p = 20,000$ feet

Engine					Tab	
V_i	rpm	Torque (lb-ft)	Turbo rpm (approx.)	Cowl flaps	Elevator tab	Rudder tab
145	2150	150	12,500	25°-50°	$\frac{1}{2}$ ° nose up	0°
166	2150	175	14,000	25°	2° nose up	0°
204	2550	230	18,500	60°	1° nose down	0°
239	2550	230	18,500	75°	2° nose down	0°



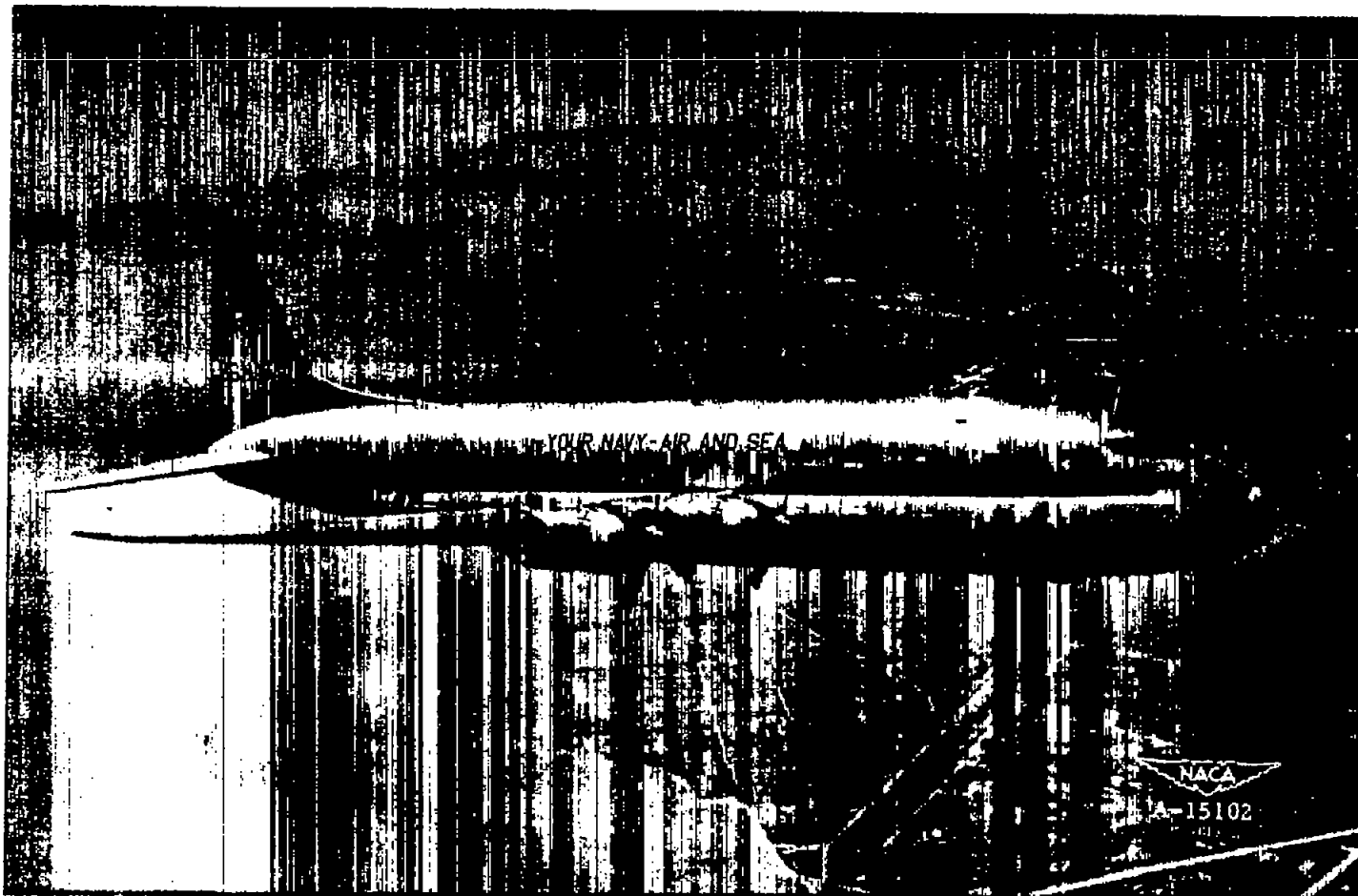


Figure 1.— Side view of Lockheed XR 60-1 Constitution in flight.

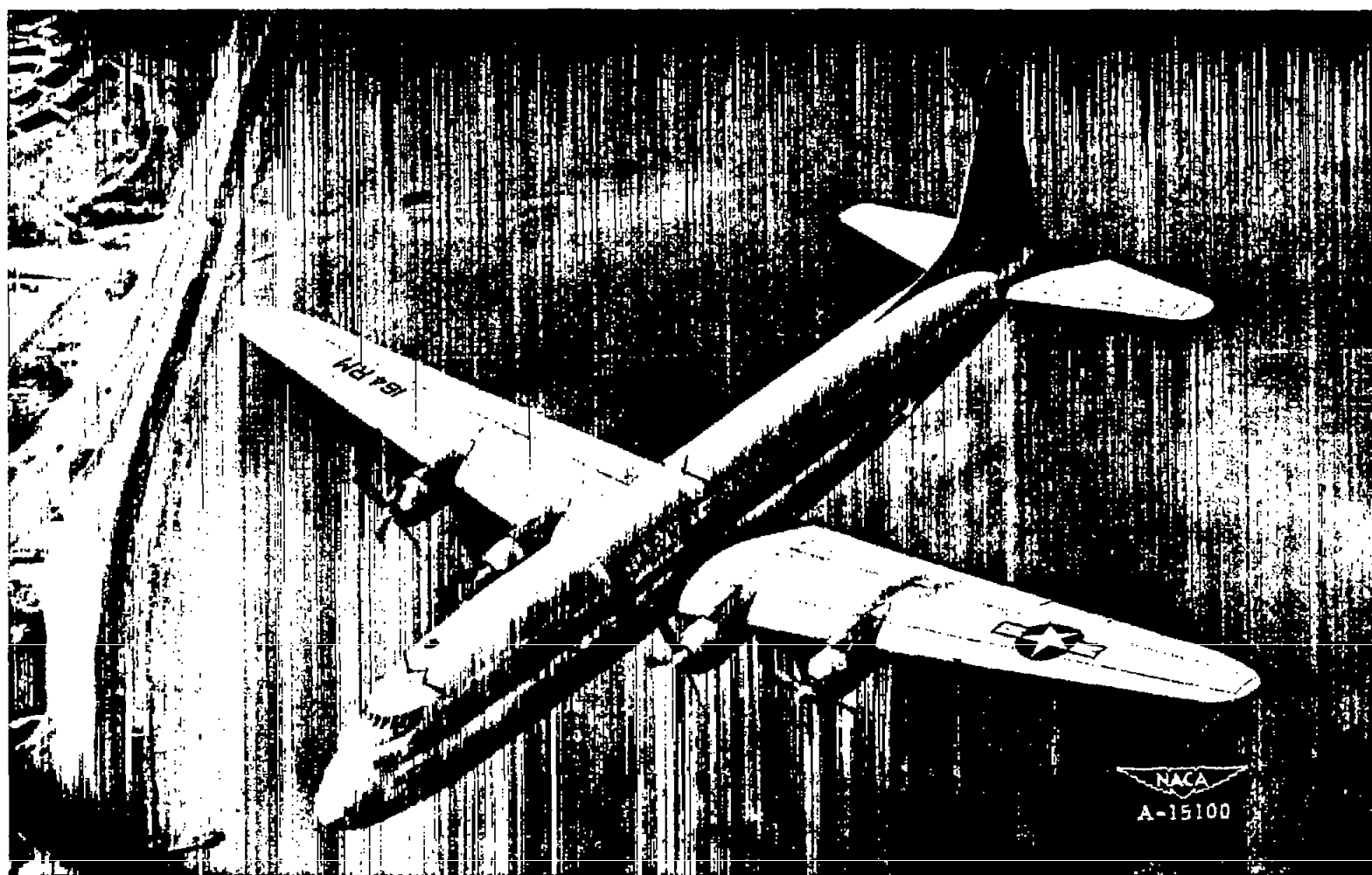


Figure 2.- View of Lockheed XR 60-1 Constitution from above.

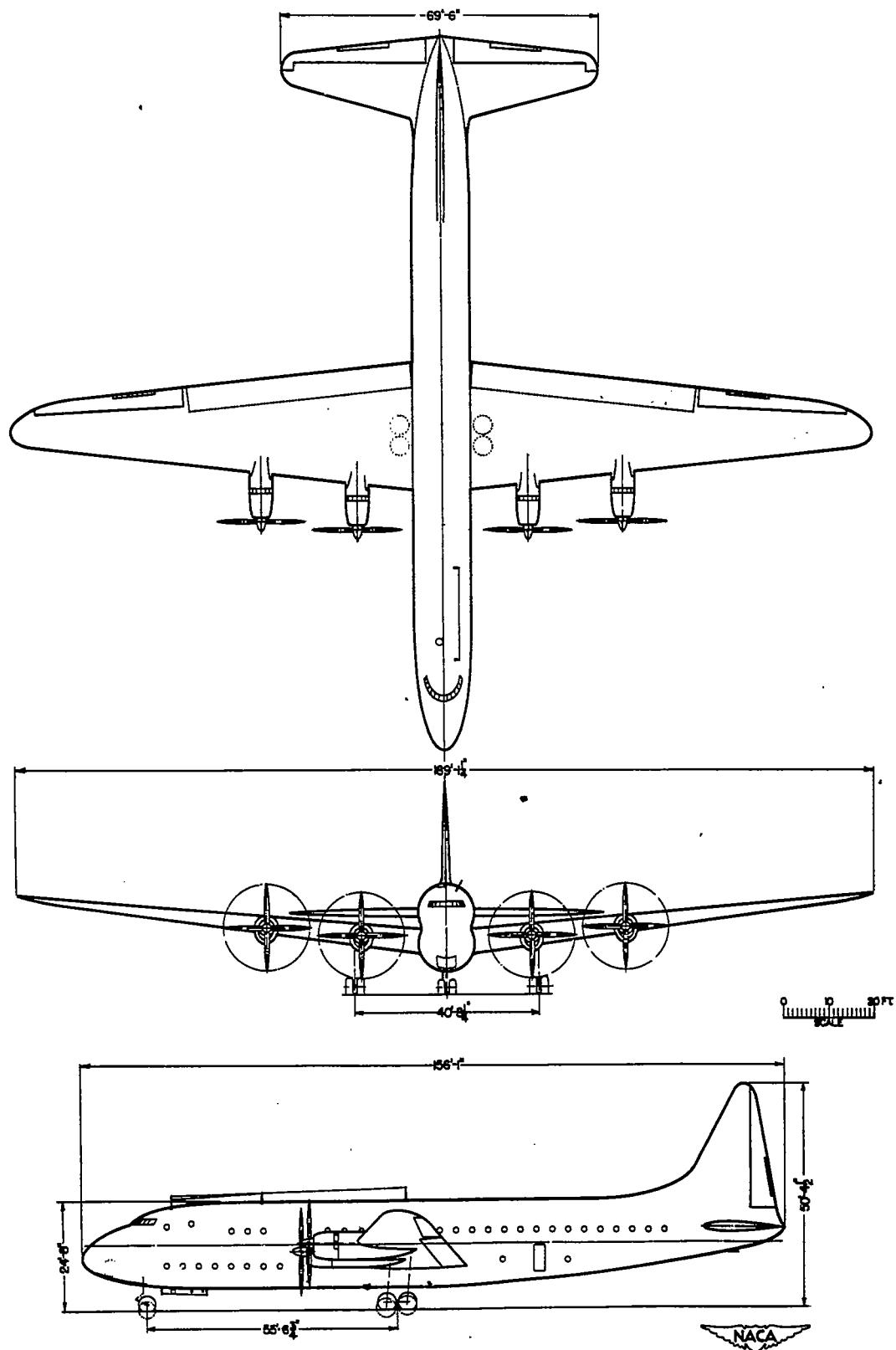
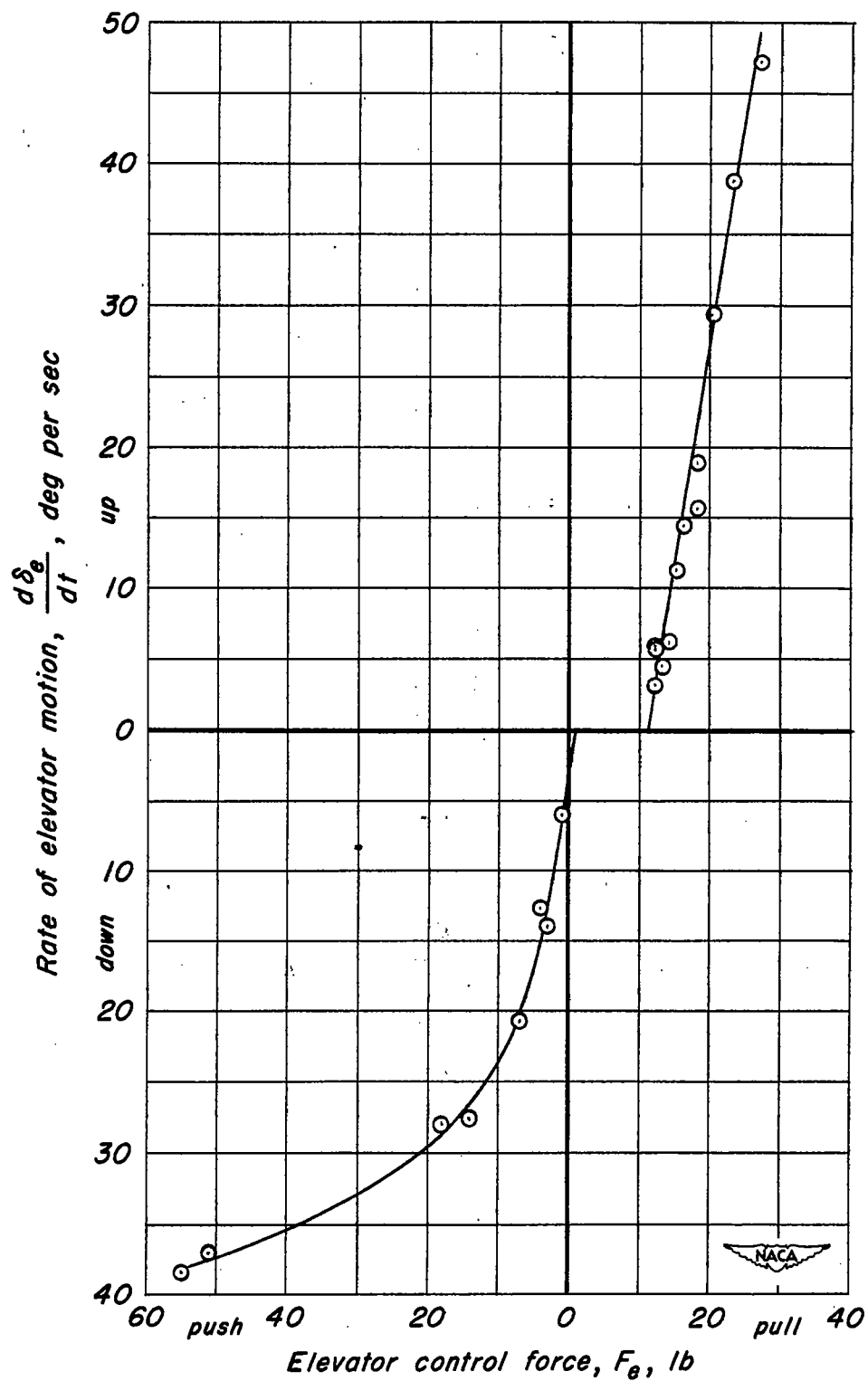
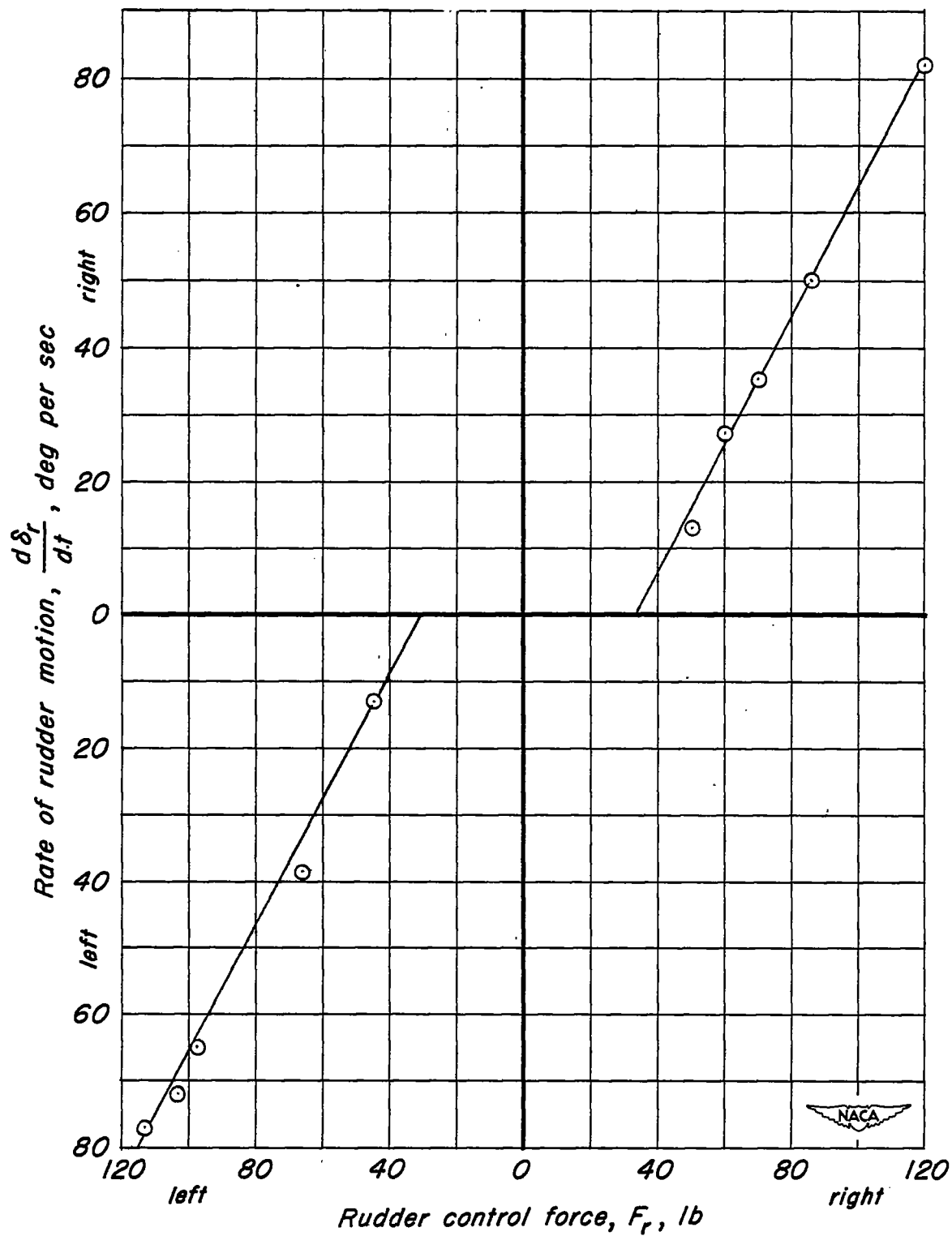


Figure 3.- Three-view drawing of Lockheed XR 60-1 airplane.



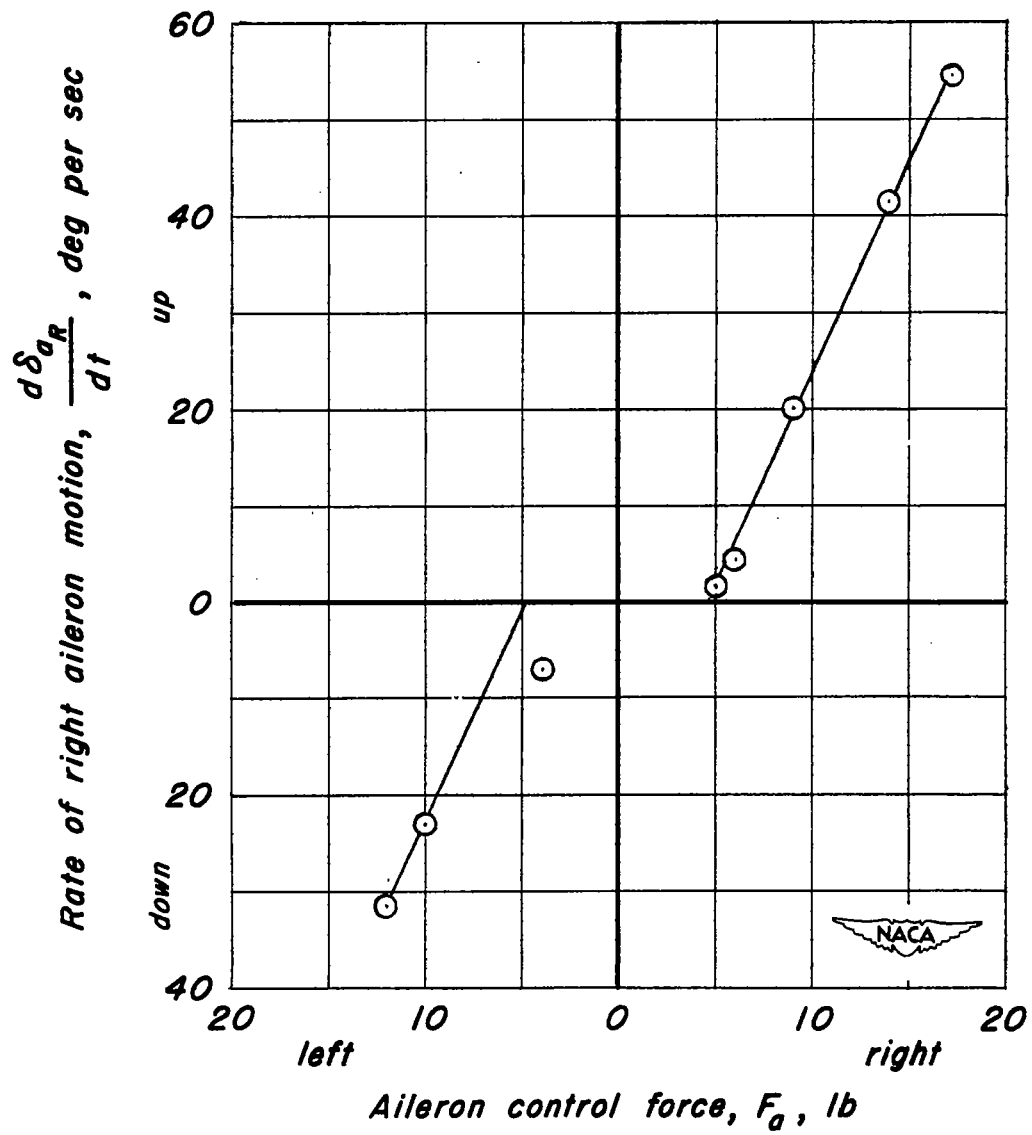
(a) Elevator.

Figure 4.—Rates of control-surface motion obtained during ground tests.



(b) Rudder.

Figure 4.- Continued.



(c) Ailerons.

Figure 4.-Concluded.

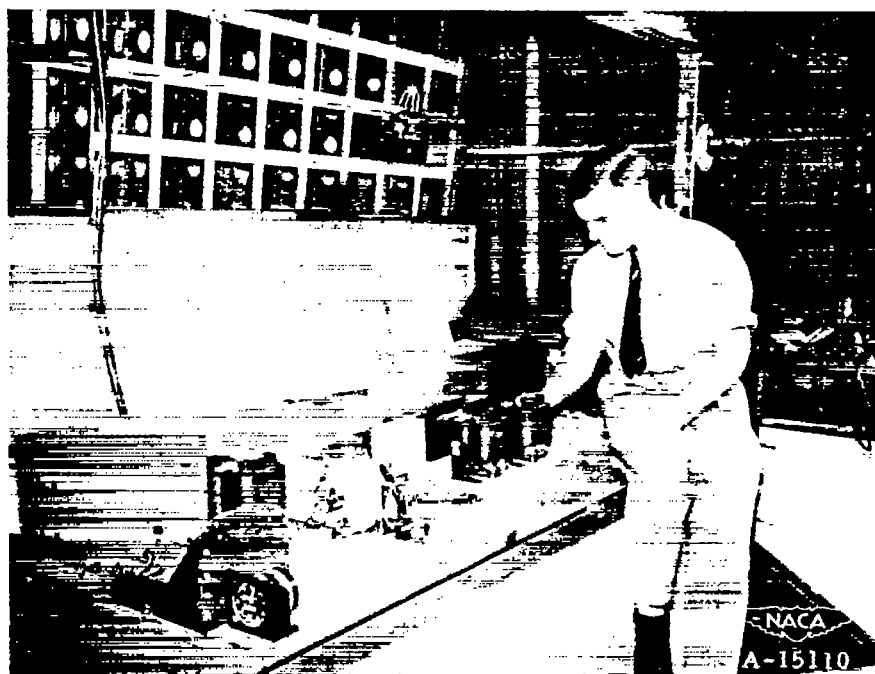
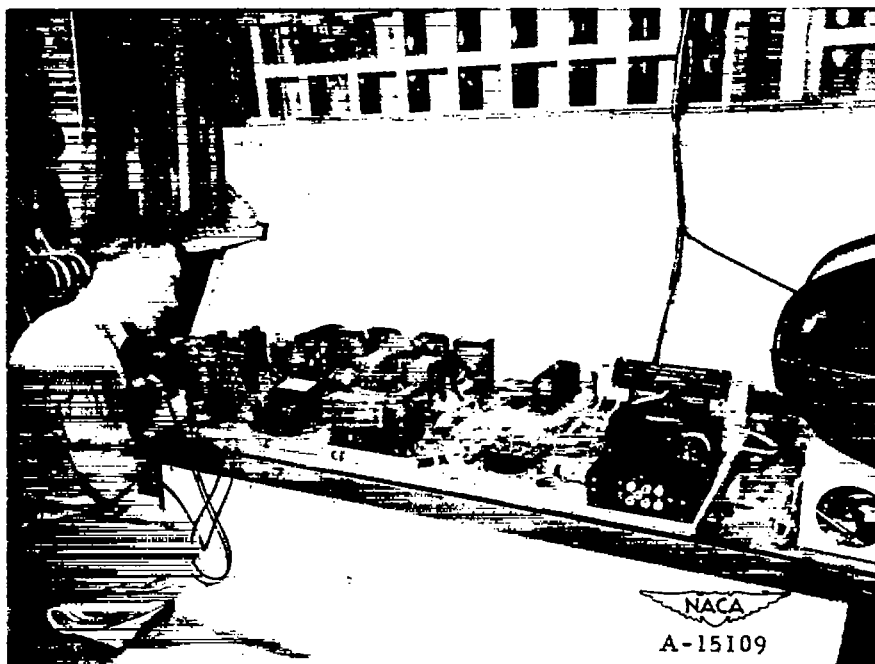


Figure 5.- Views showing some of the instrumentation.

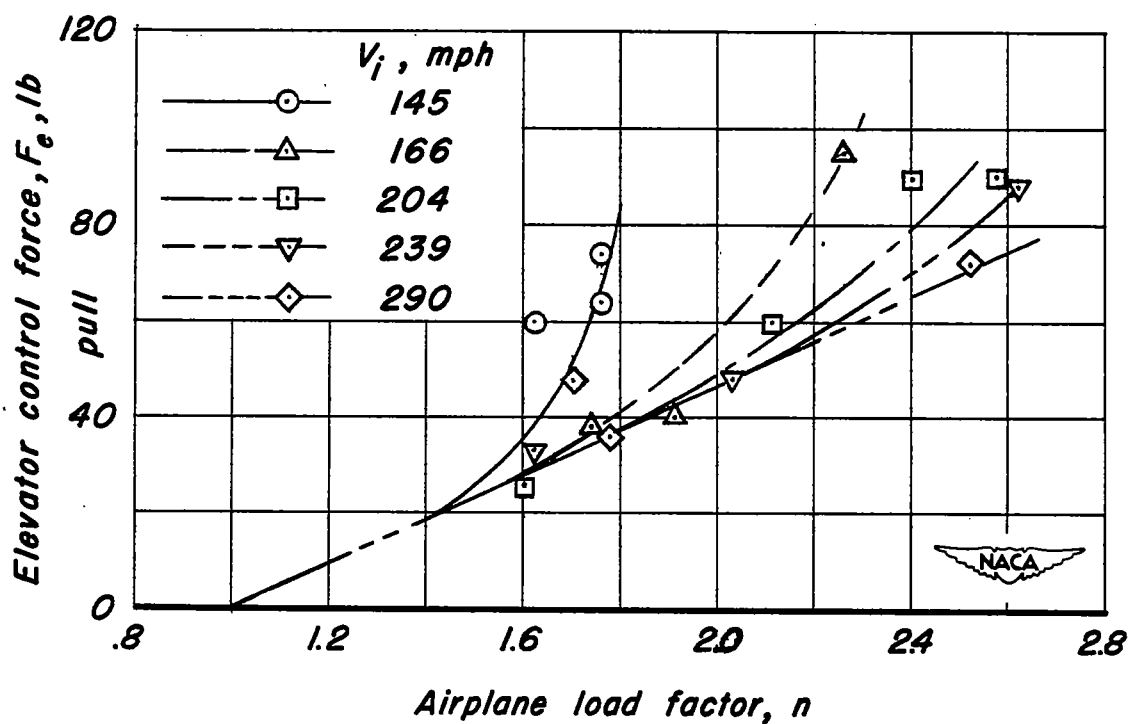


Figure 6.- Variation of elevator control force with airplane load factor in turning flight at 5,000 feet.

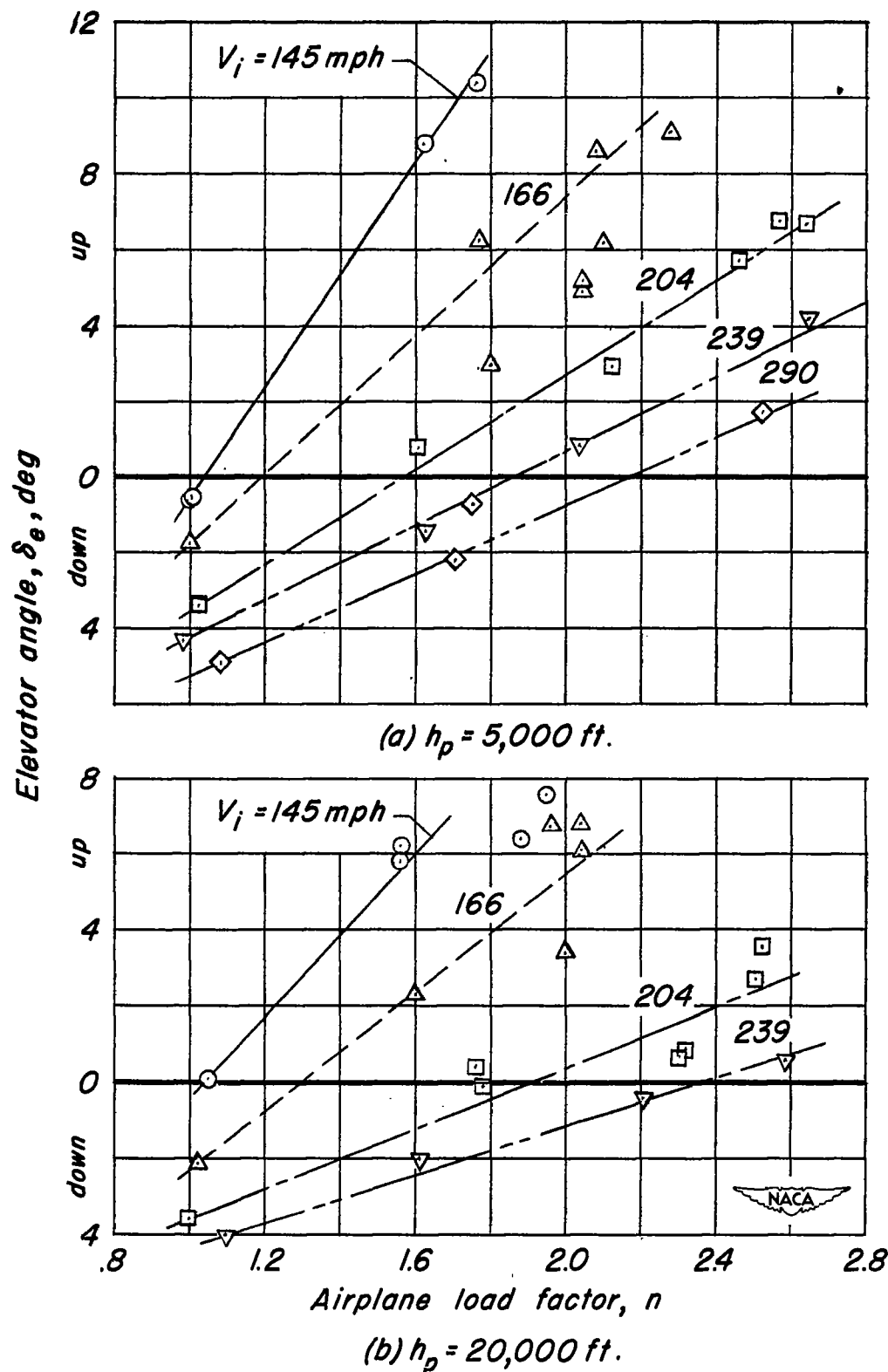


Figure 7.— Variation of elevator angle with airplane load factor in turning flight.

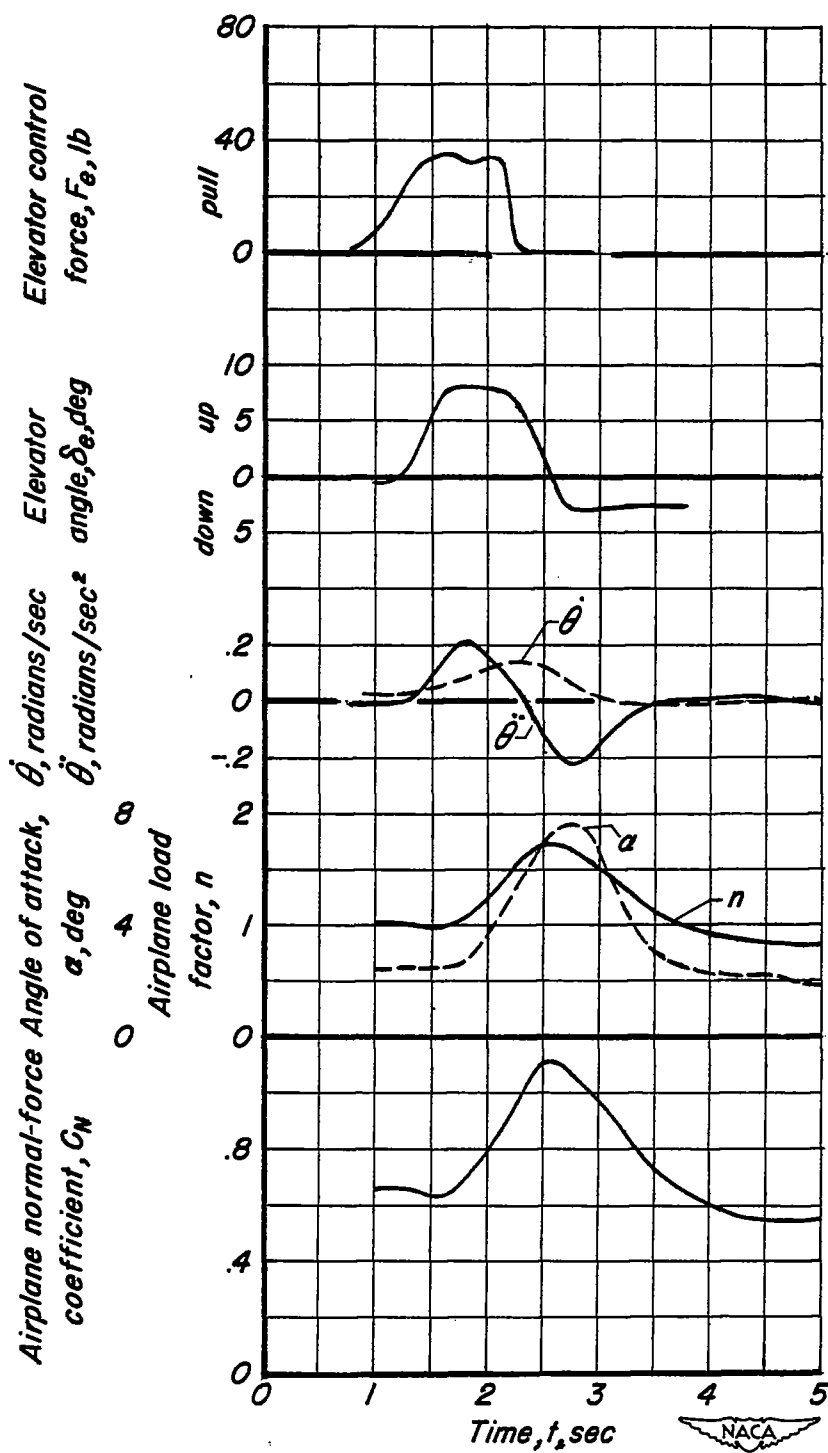
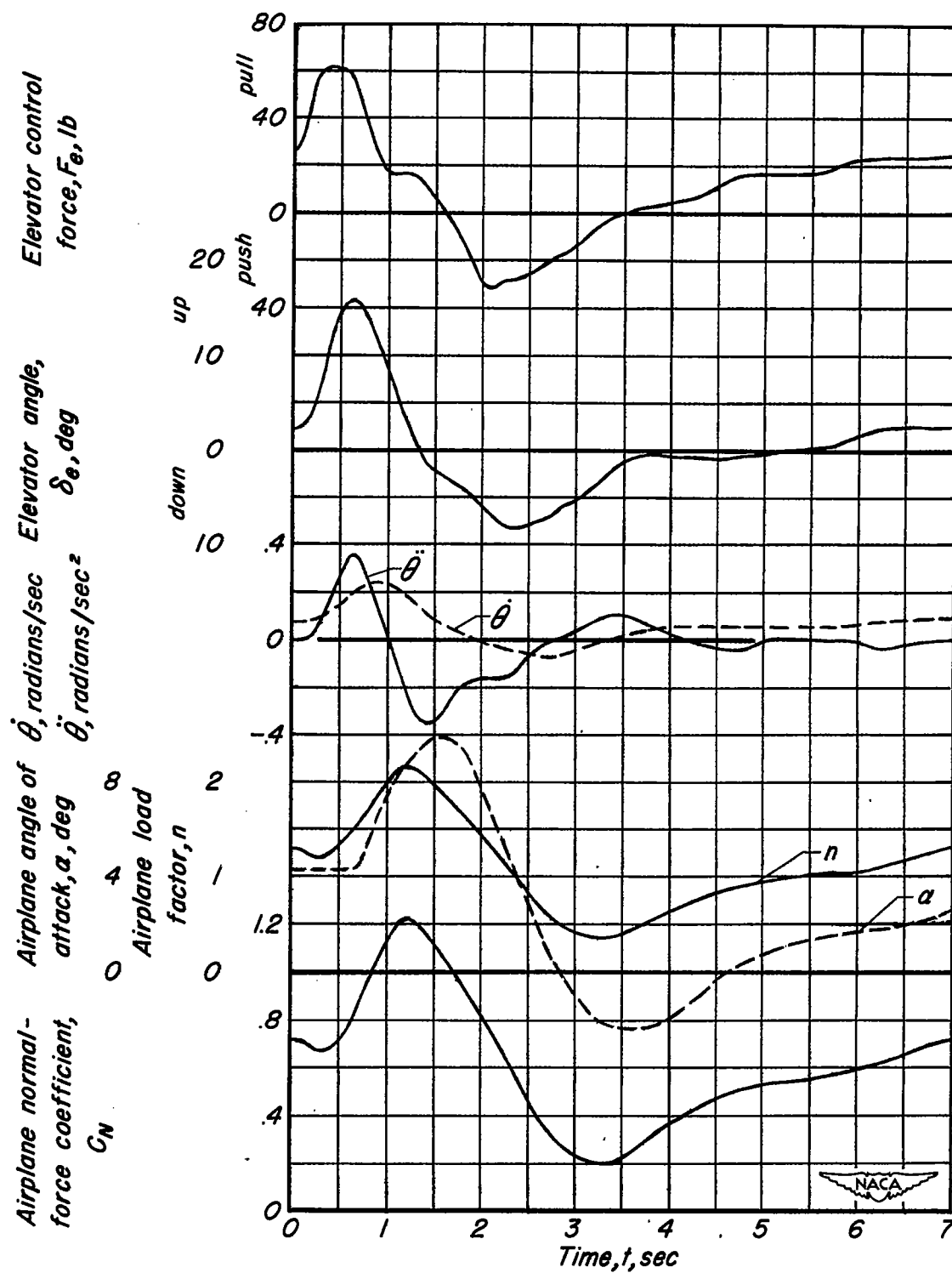
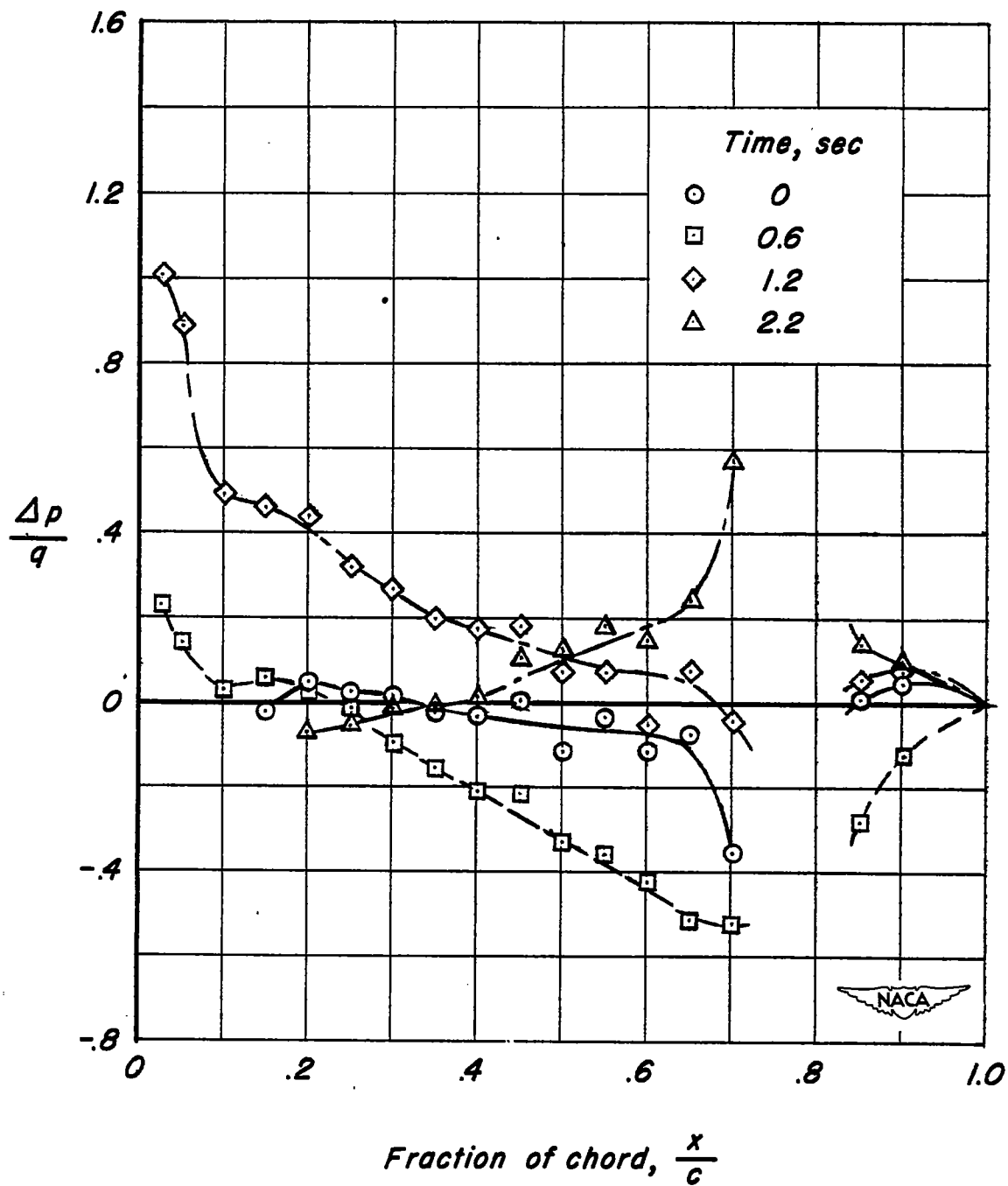


Figure 8.—Time history of pertinent quantities measured during pull-up maneuver; airspeed, 155 miles per hour; altitude, 5300 feet.



(a) Time history.

Figure 9.- Pertinent quantities measured during pull-up push-down maneuvers; airspeed, 168 miles per hour; altitude, 5,100 feet.



(b) Chordwise distribution of load coefficient at 30.6 % span on horizontal stabilizer.

Figure 9.- Concluded.

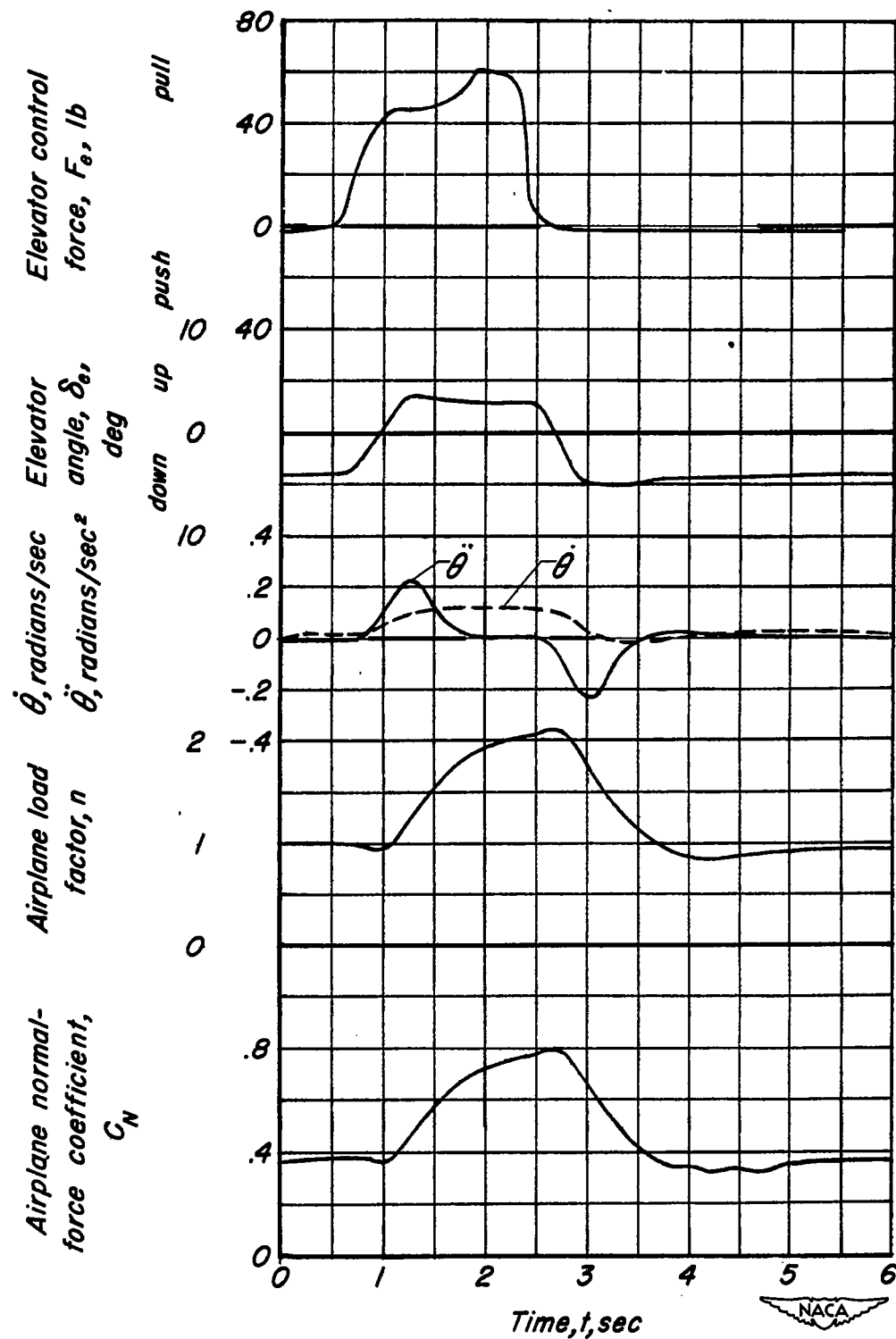


Figure 10.- Time history of pertinent quantities during pull-up maneuver; airspeed, 206 miles per hour; altitude, 5,000 feet.

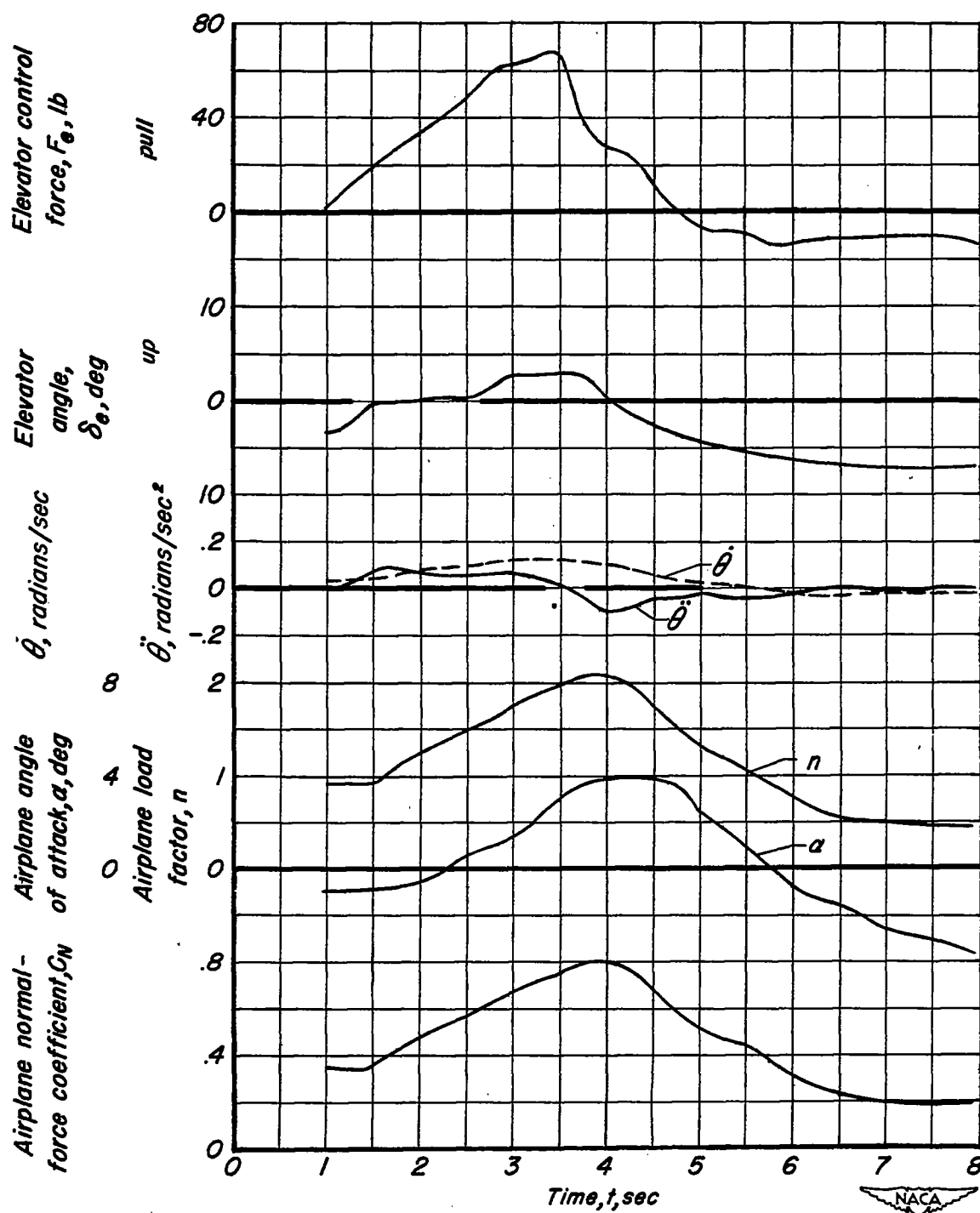


Figure 11.—Time histories of pertinent quantities during pull-up push-down maneuvers; airspeed, 204 miles per hour; altitude, 5000 feet.

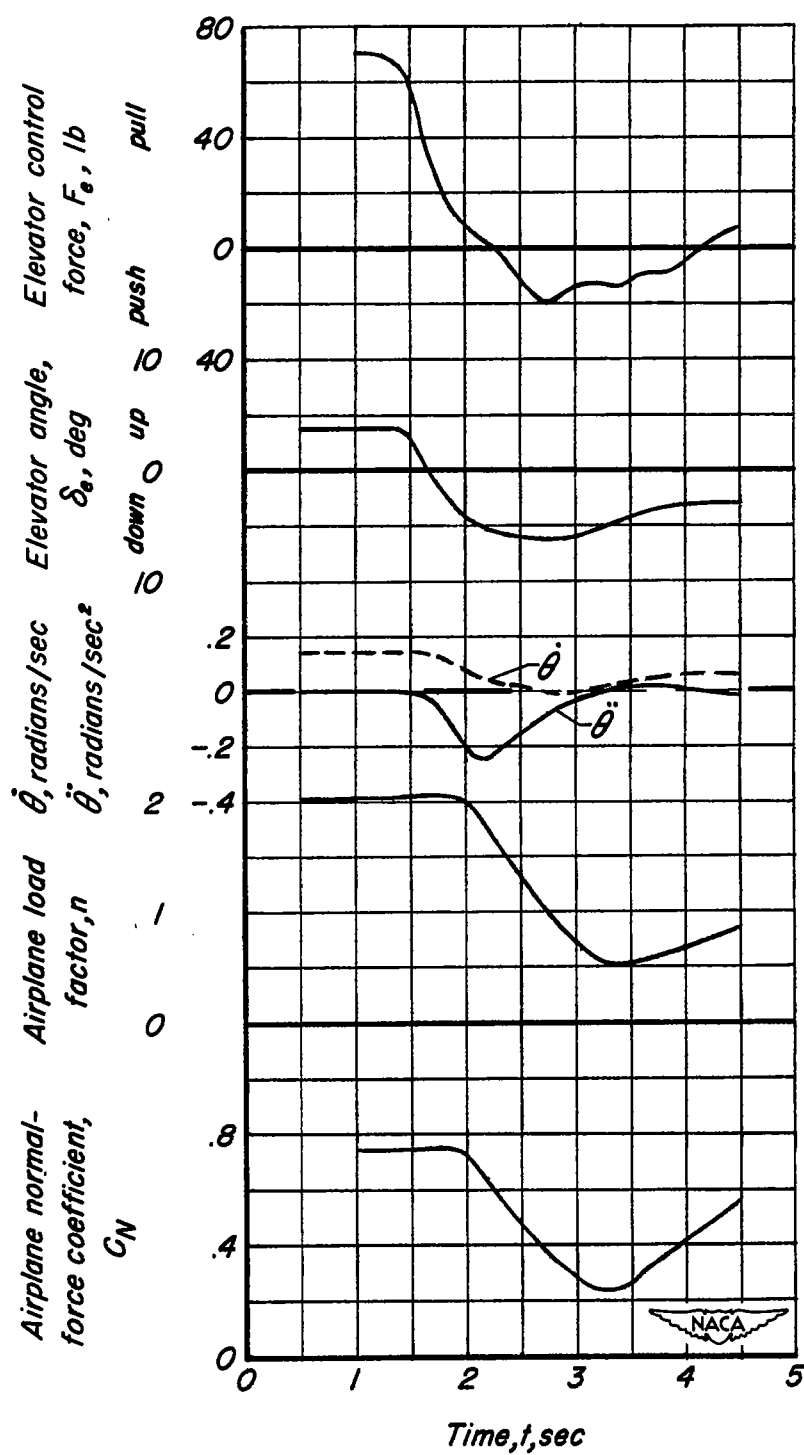


Figure 12.—Time history of pertinent quantities during push-down from steady turn; airspeed, 208 miles per hour; altitude, 5000 feet.

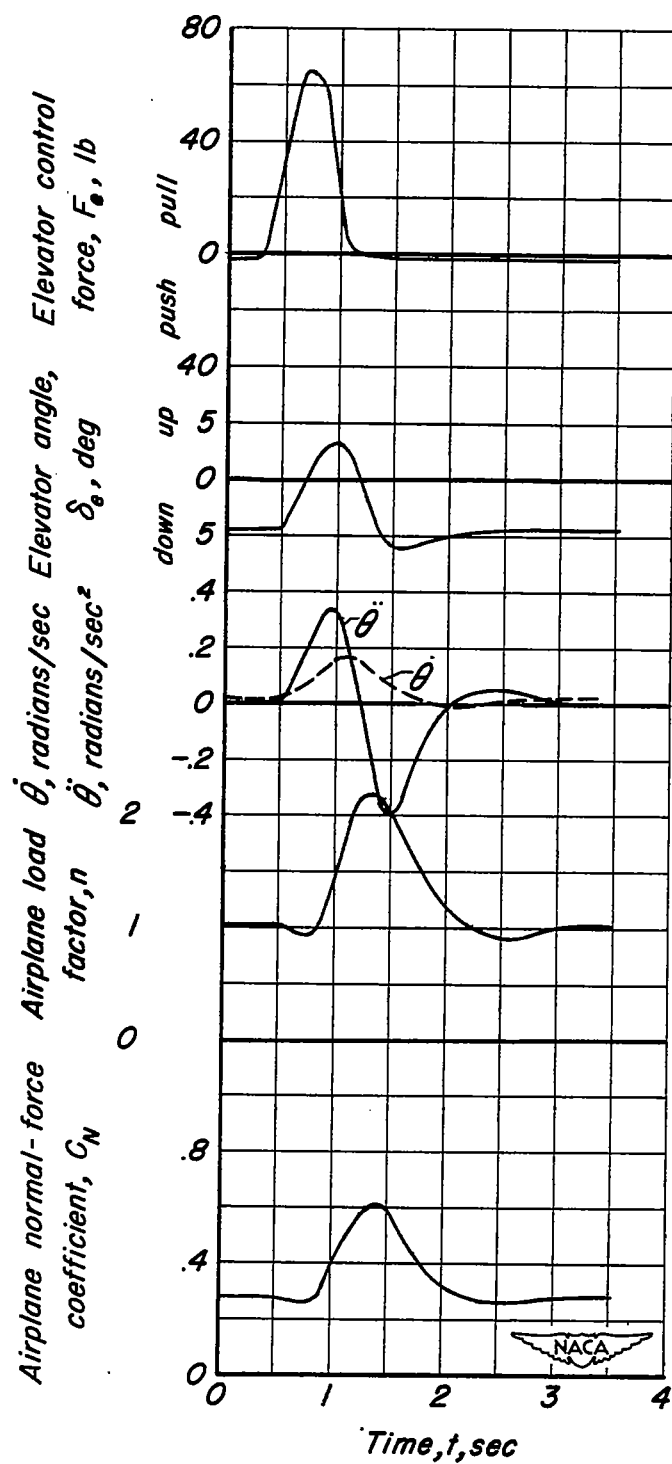


Figure 13.— Time history of pertinent quantities during pull-up maneuver; airspeed, 240 miles per hour; altitude, 4,600 feet.

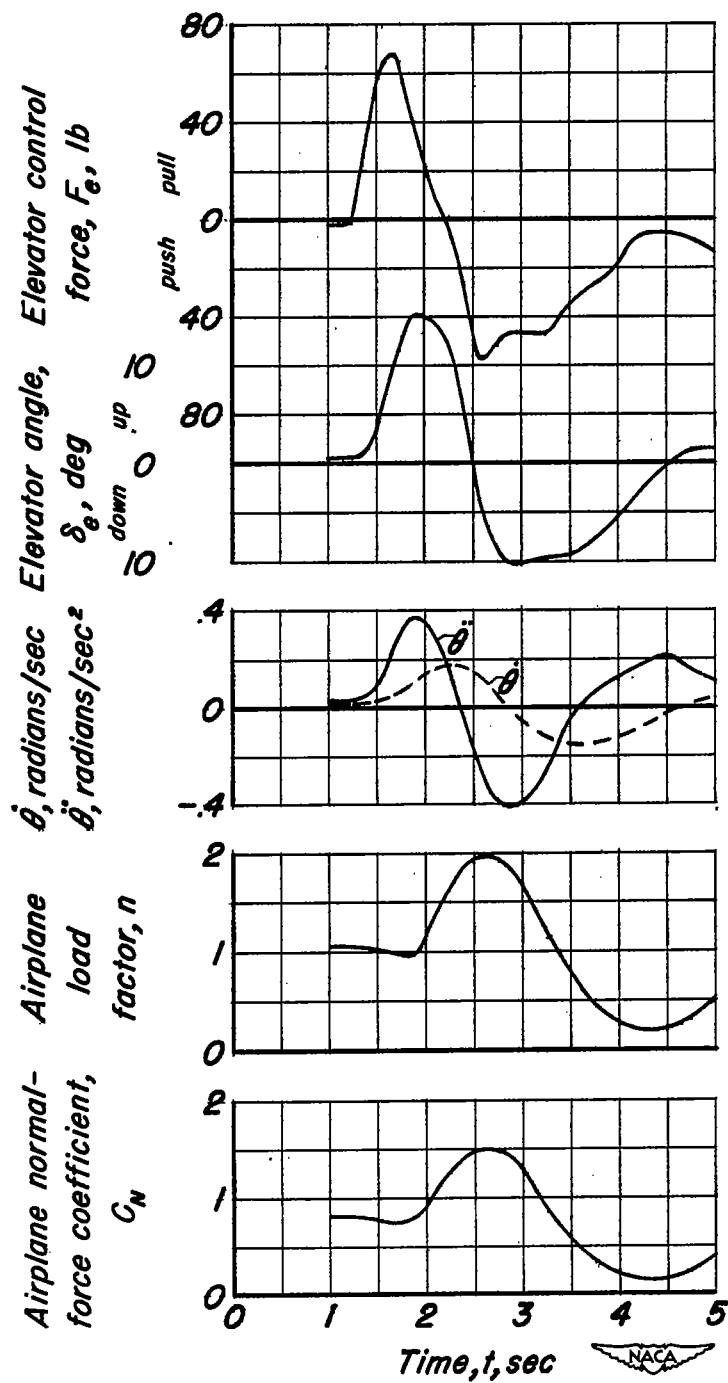


Figure 14.-Time history of pertinent quantities during pull-up push-down maneuver; airspeed, 144 miles per hour; altitude, 20,300 feet.

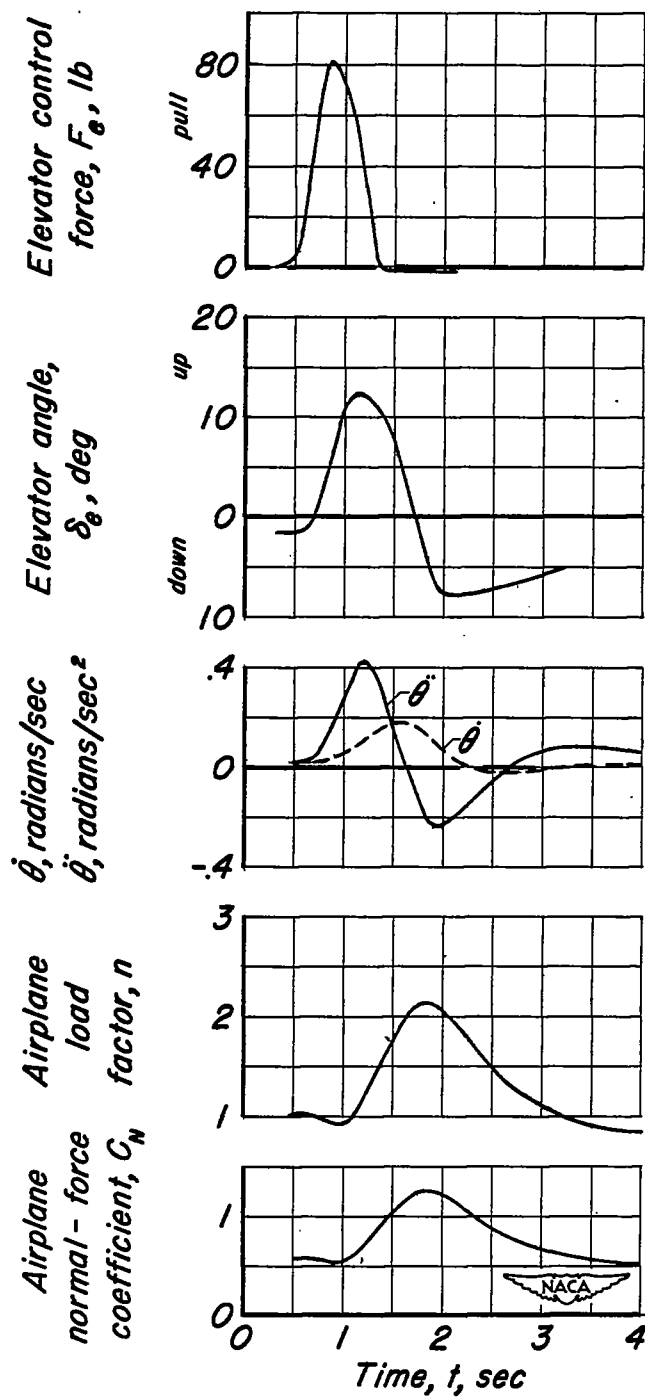


Figure 15.— Time history of pertinent quantities during pull-up maneuver; airspeed, 164 miles per hour; altitude, 20,400 feet.

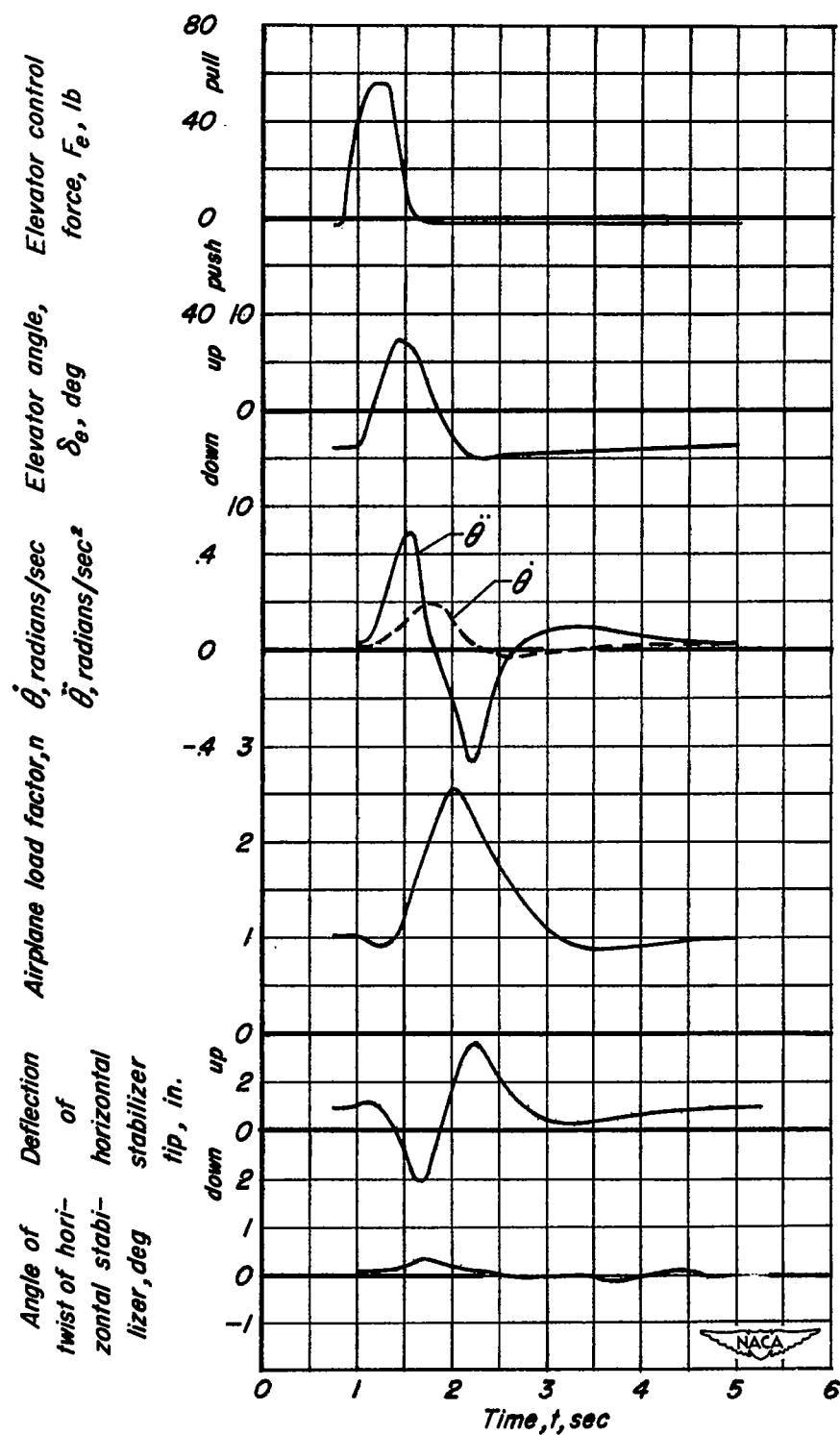


Figure 16.—Time histories of pertinent quantities during pull-up maneuvers, airspeed, 204 miles per hour; altitude, 20,200 feet.

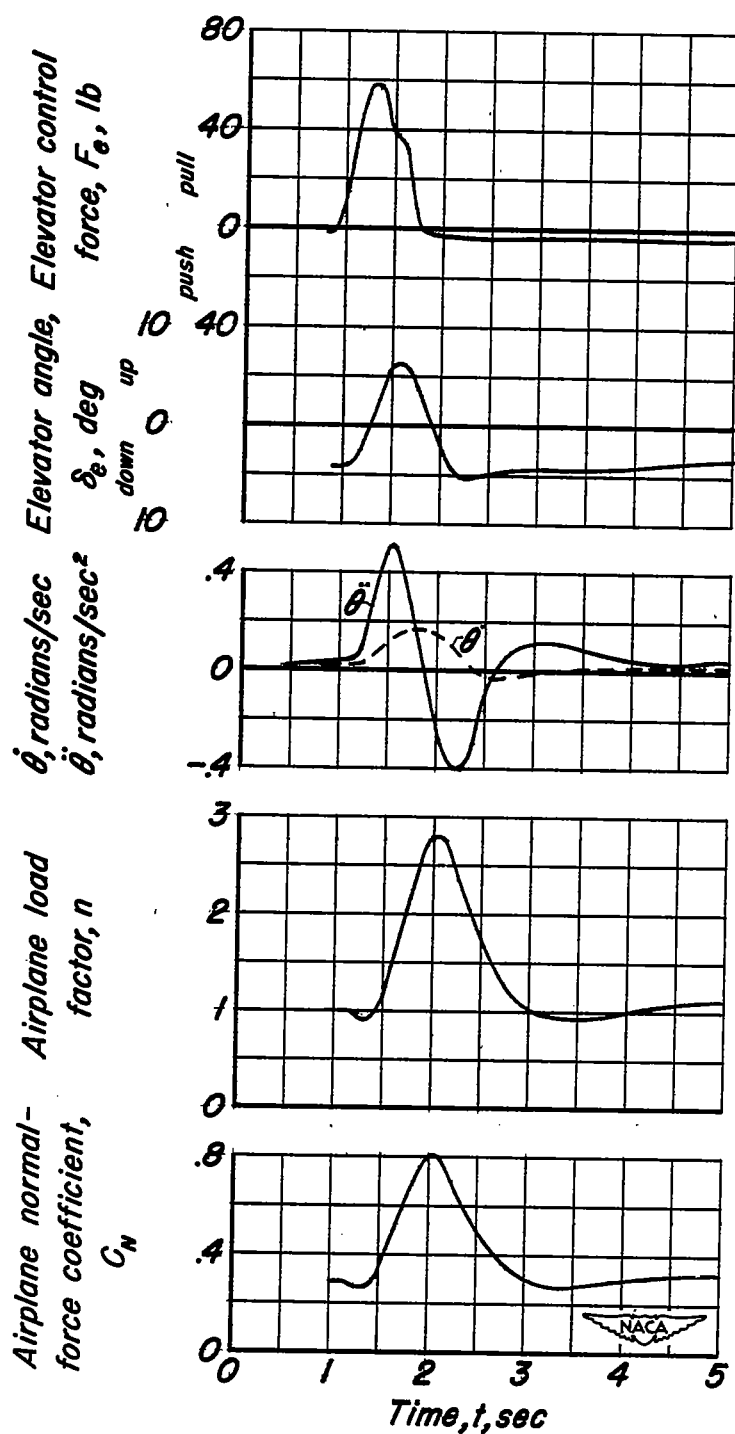


Figure 17.-Time history of pertinent quantities during pull-up maneuver; airspeed, 240 miles per hour; altitude, 19,800 feet.

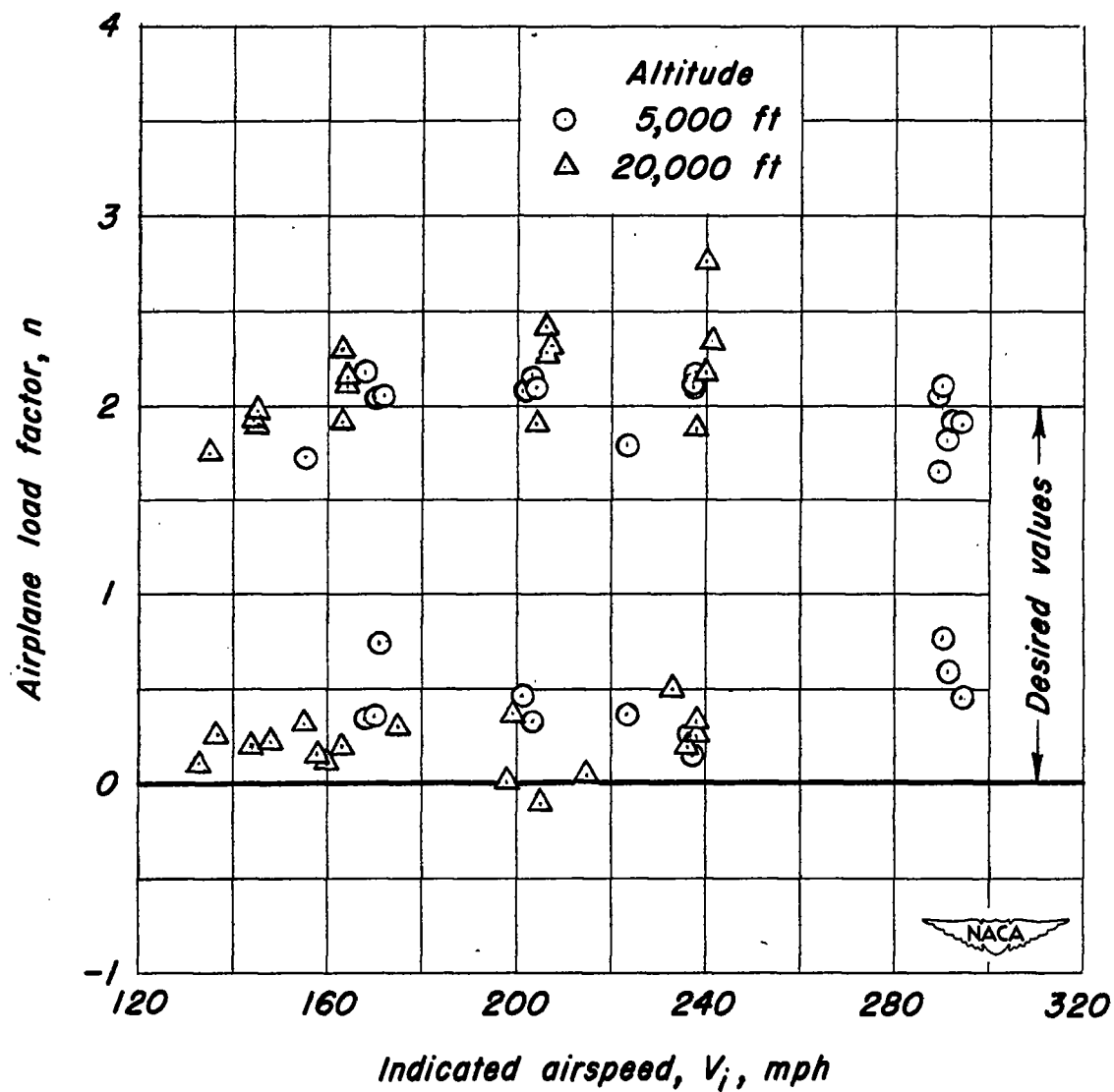


Figure 18.- Maximum and minimum airplane load factors attained in pitching maneuvers.

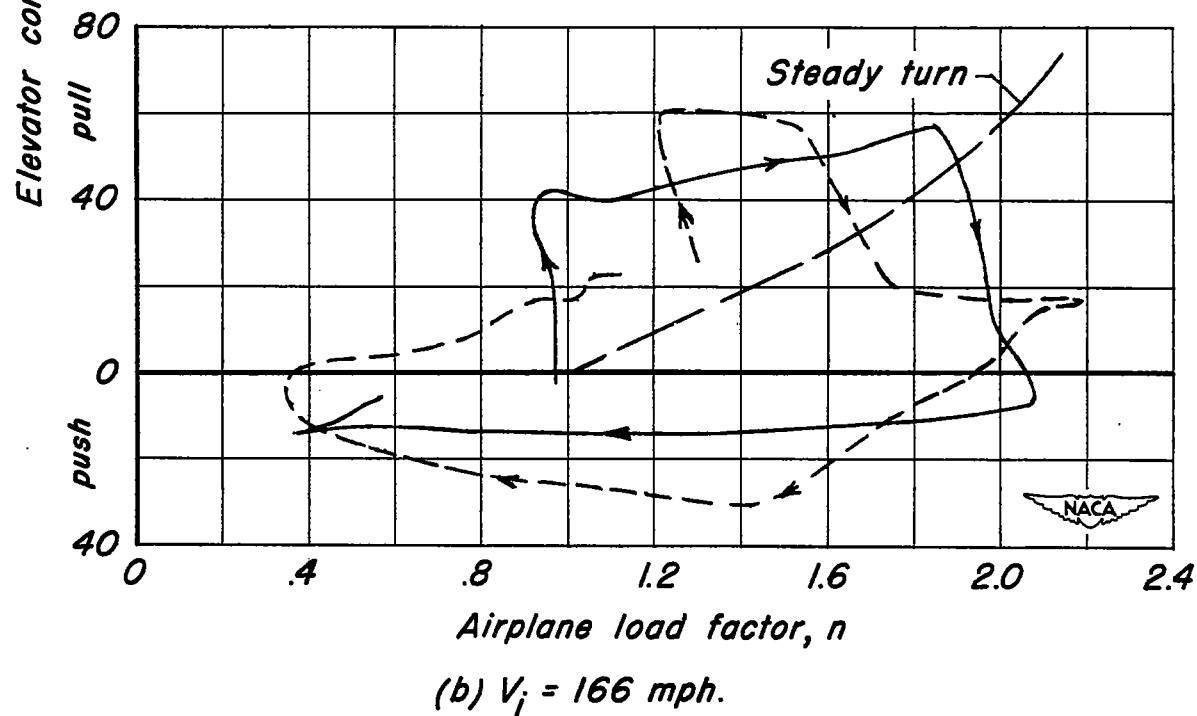
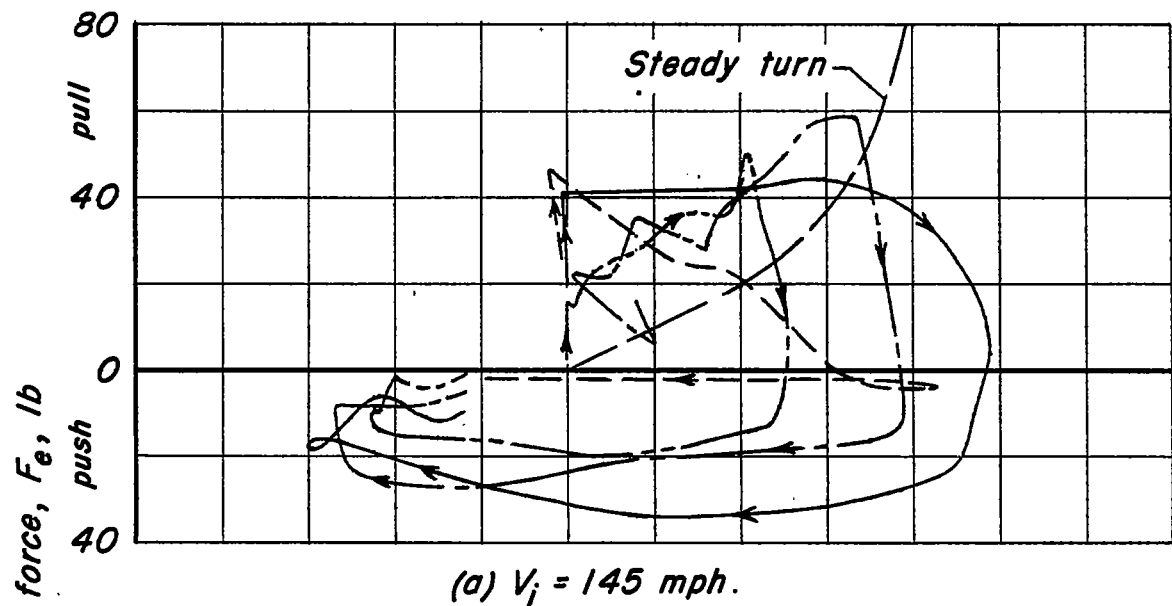


Figure 19.— Concurrent variation of elevator control force and airplane load factor during pitching maneuvers, 5,000 feet altitude.

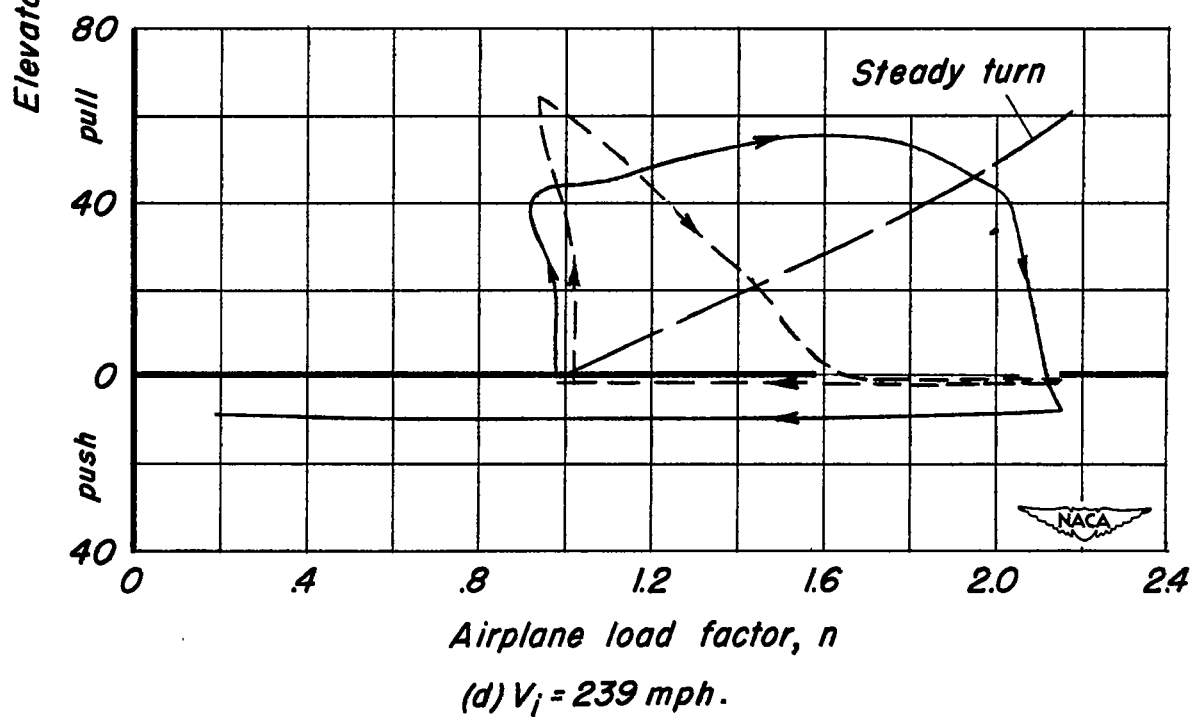
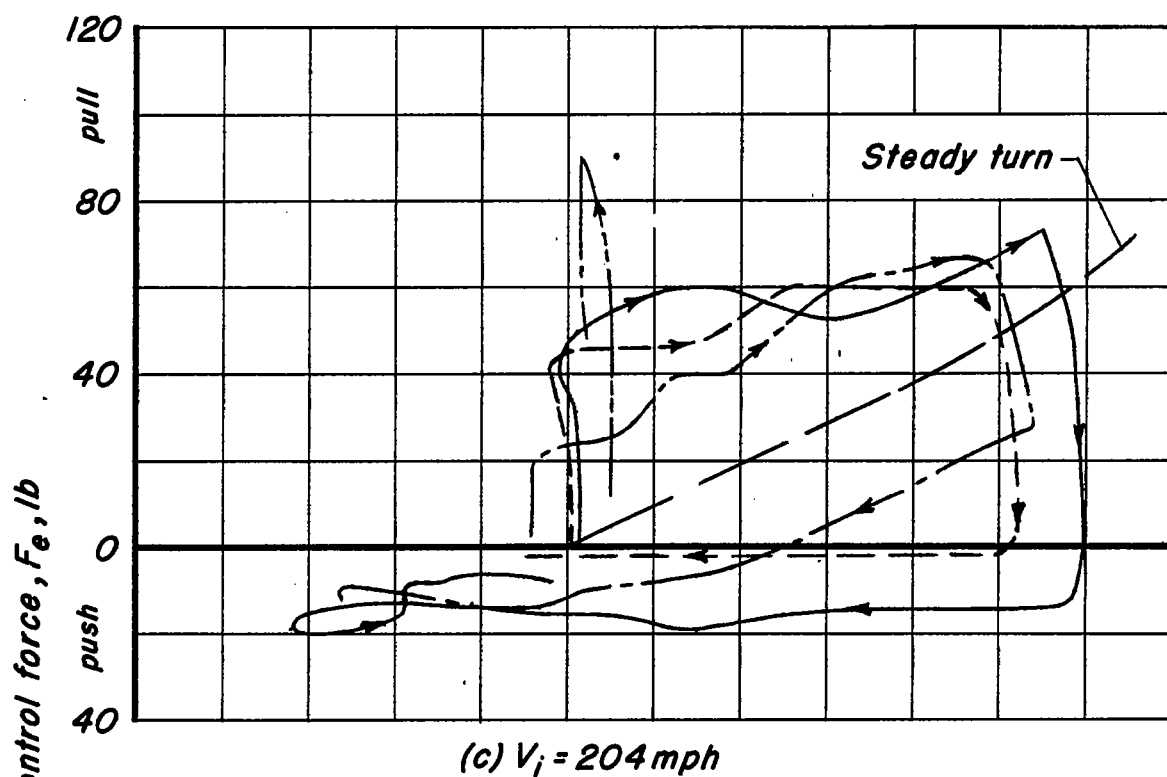
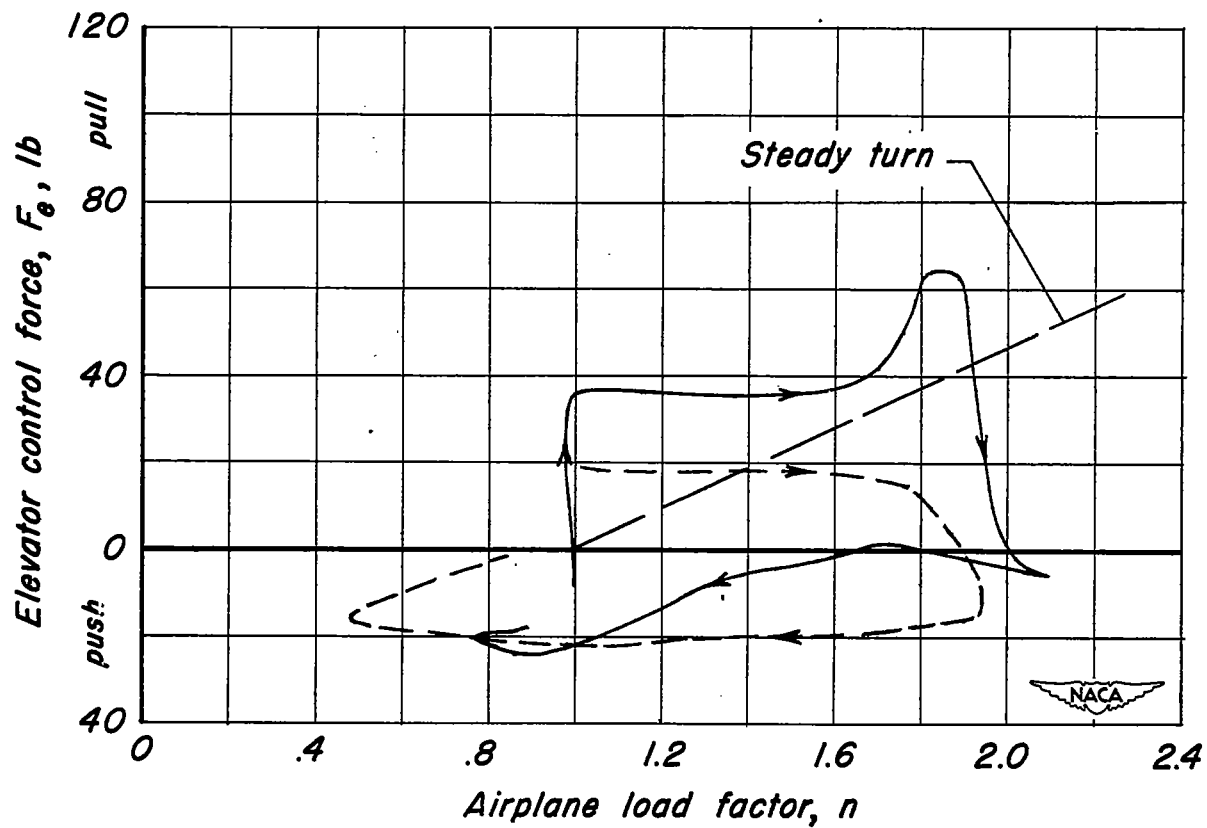


Figure 19.- Continued.



(e) $V_i = 290$ mph.

Figure 19.— Concluded.

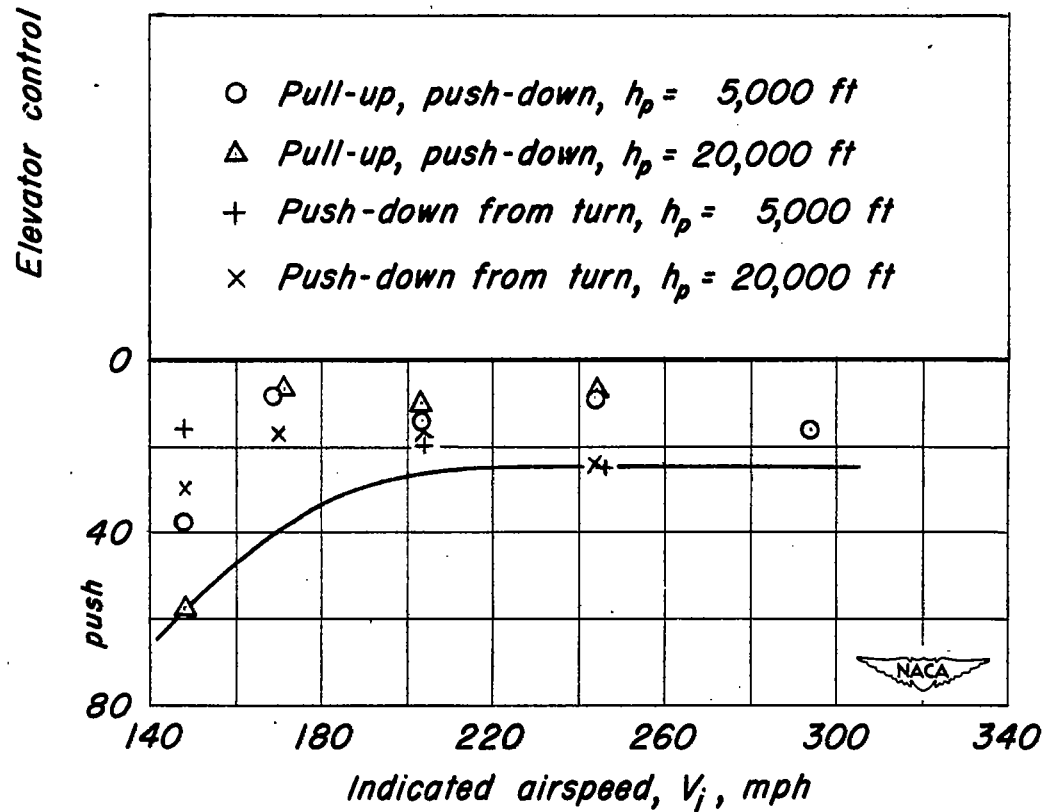
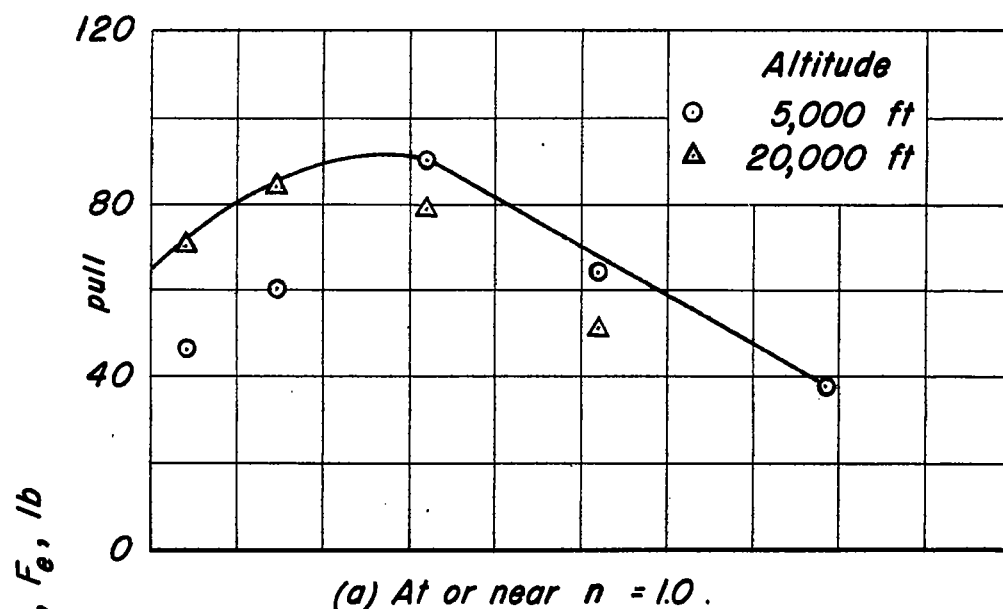


Figure 20.- Maximum elevator control forces exerted during pitching maneuvers.

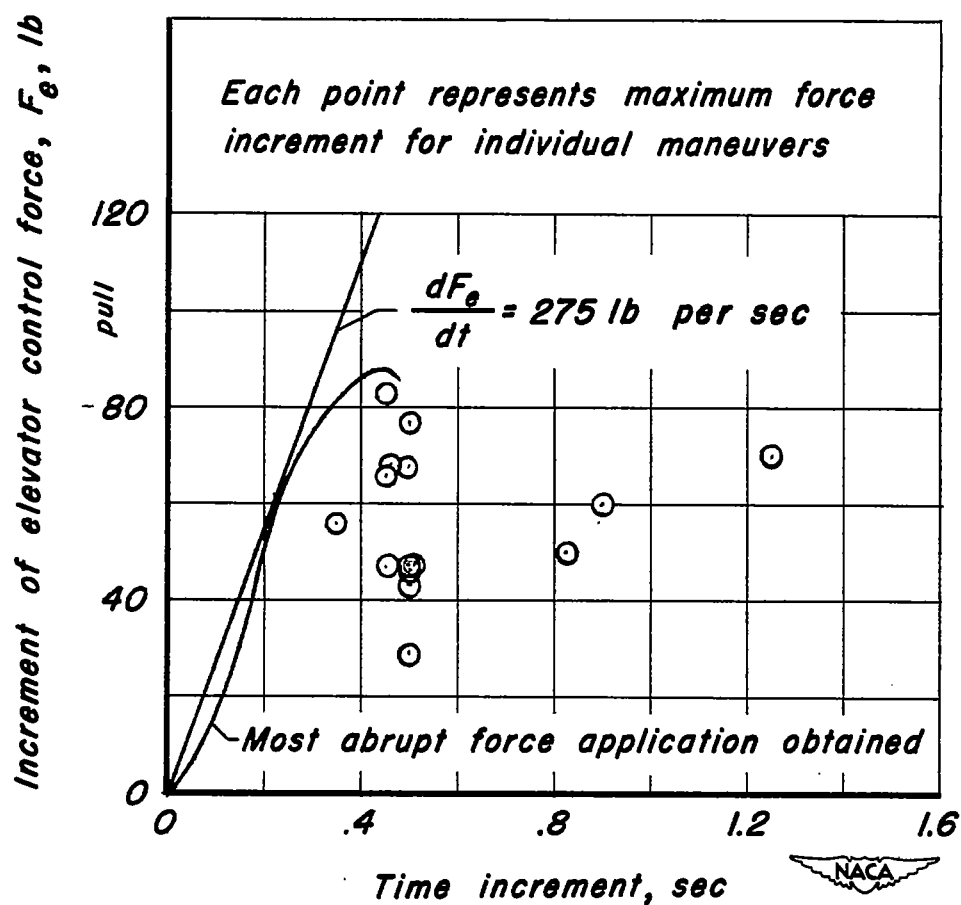
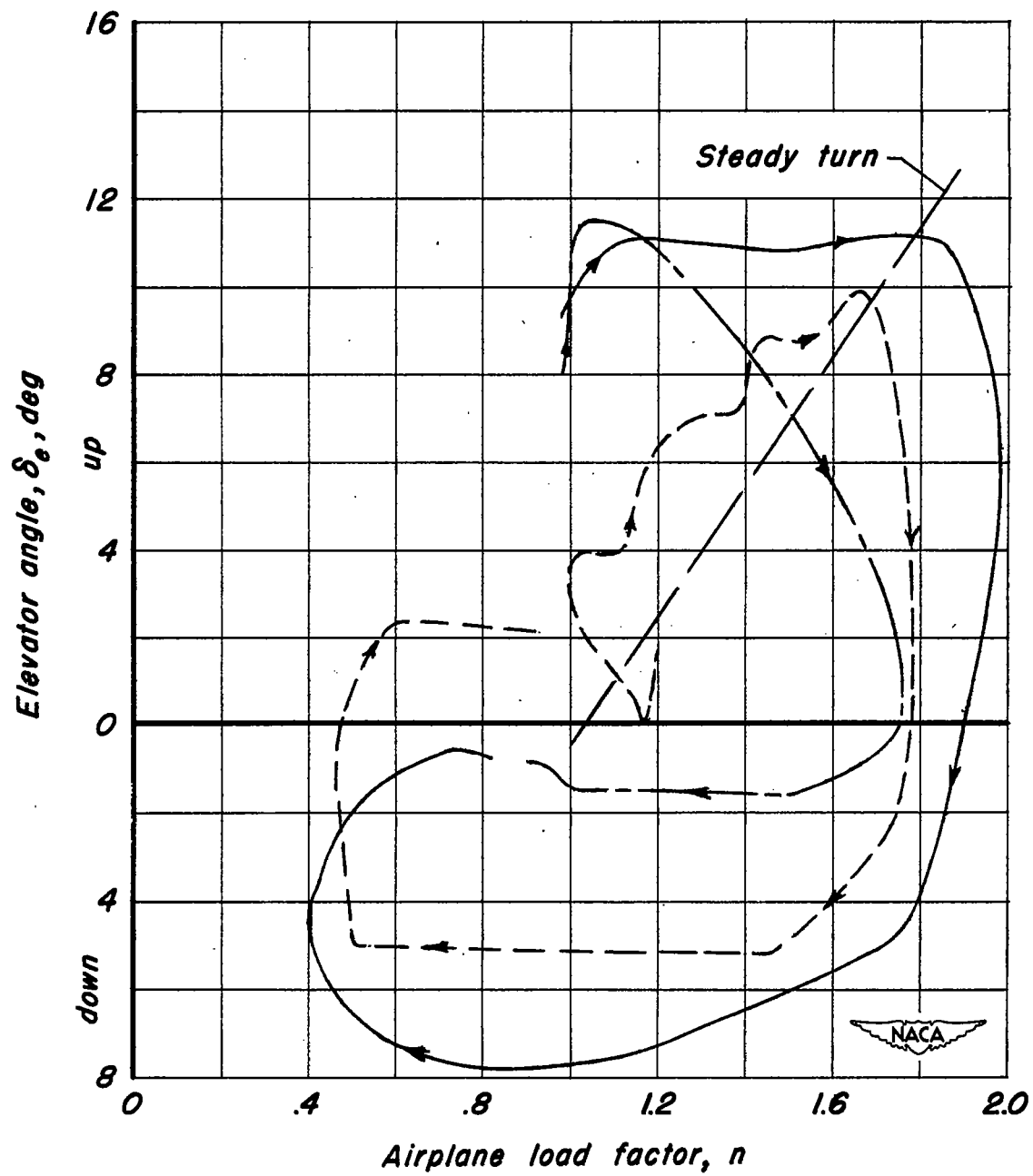
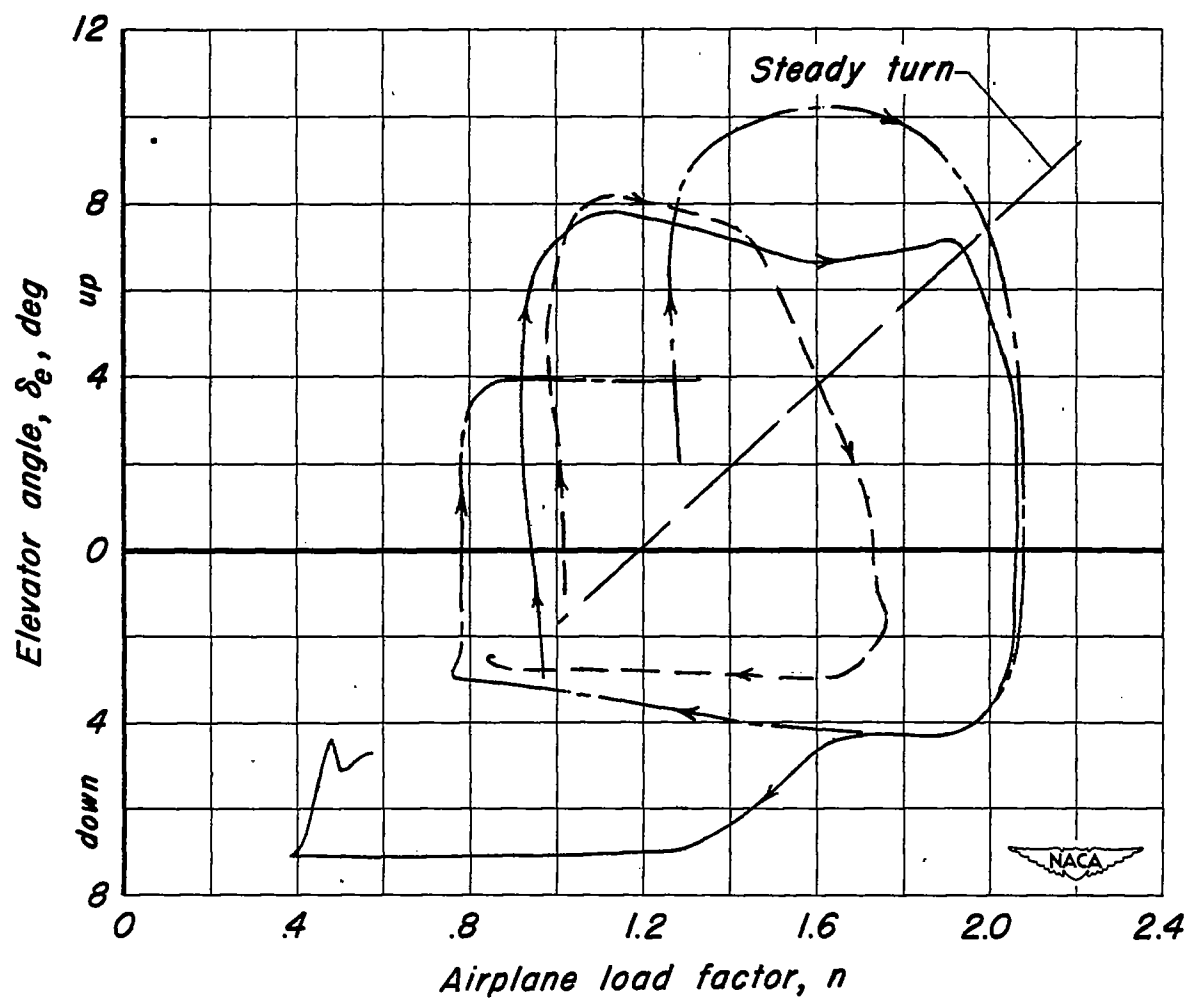


Figure 21.— Time required to apply elevator control forces during pull-up maneuvers .



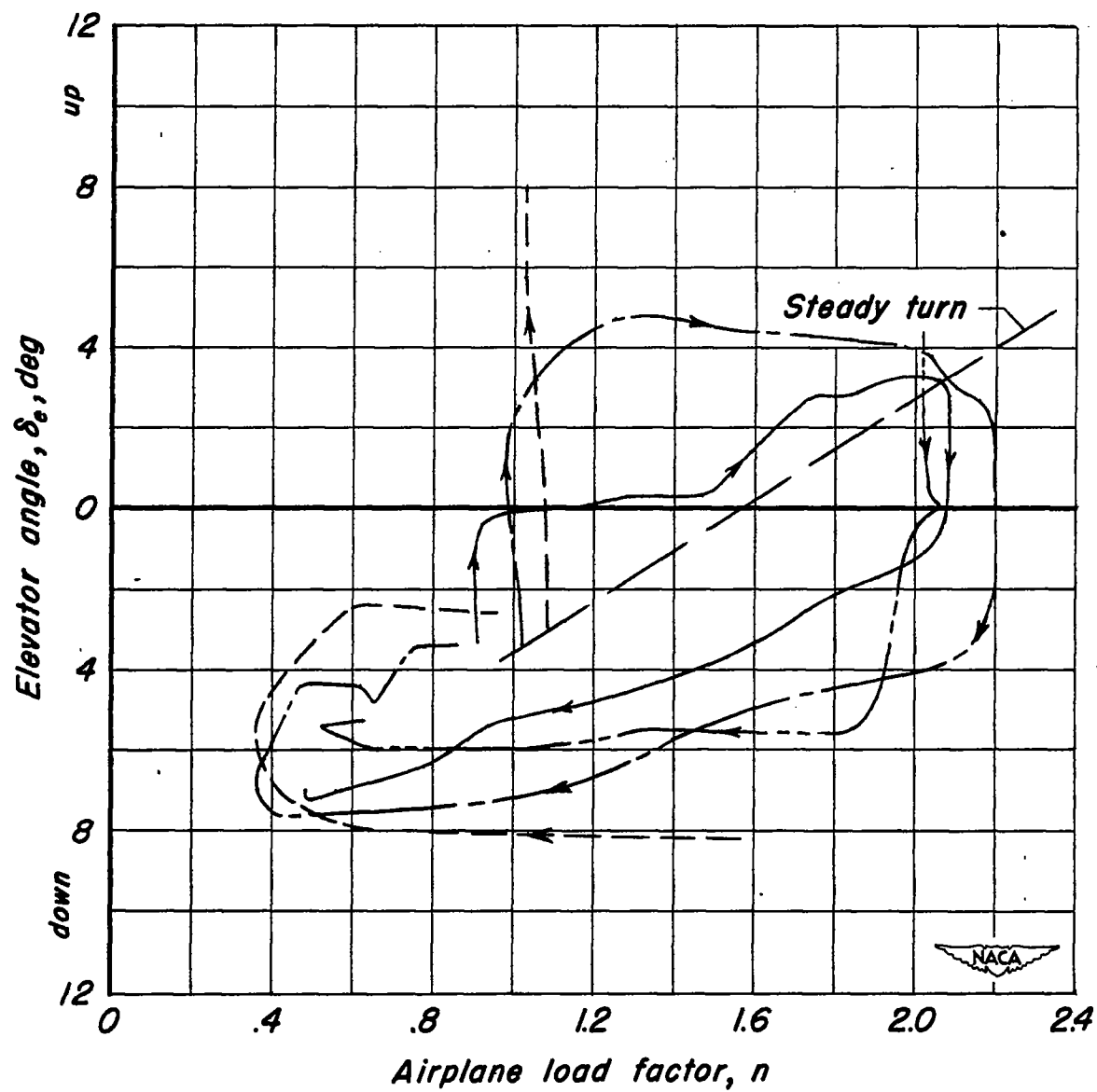
(a) $V_i = 145$ mph.

Figure 22.- Concurrent variation of elevator angle and airplane load factor during pitching maneuvers, 5,000 feet altitude.



(b) $V_i = 166$ mph.

Figure 22.- Continued.



(c) $V_i = 204$ mph.

Figure 22.- Continued.

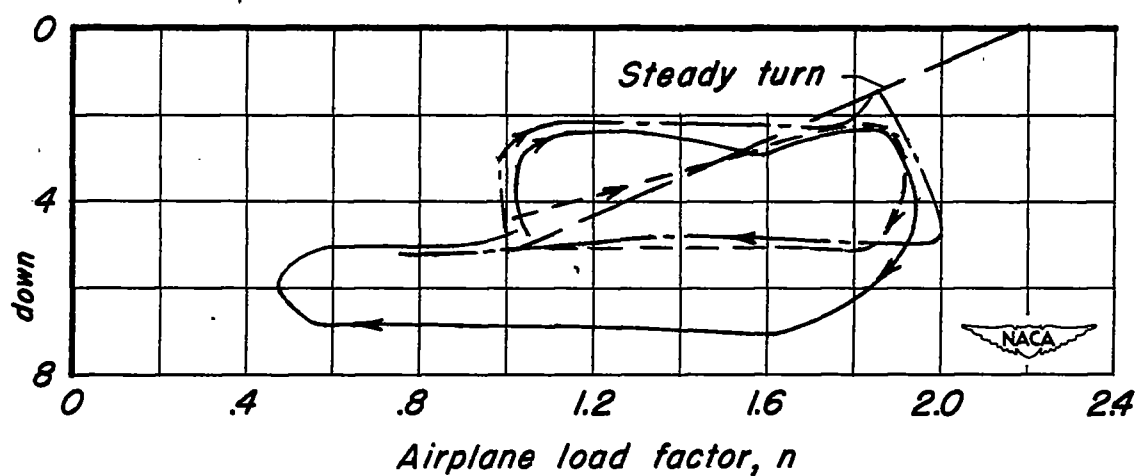
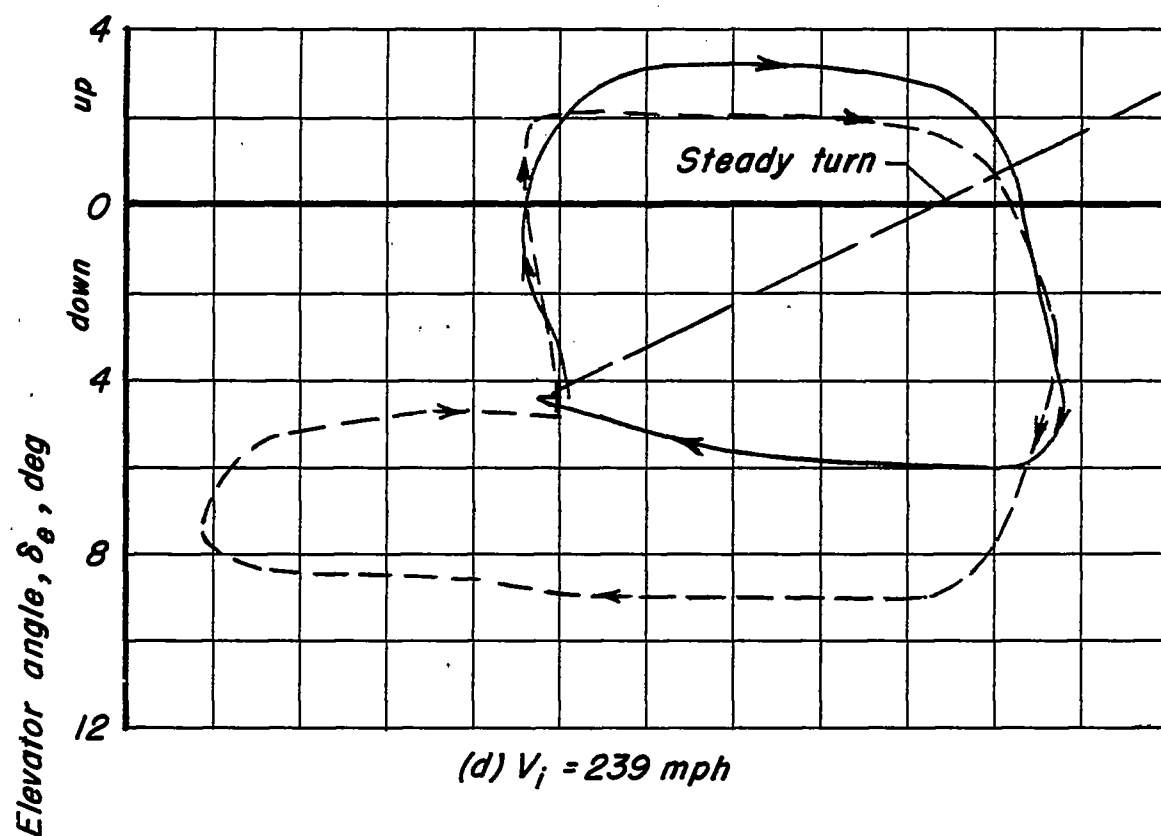


Figure 22.- Concluded.

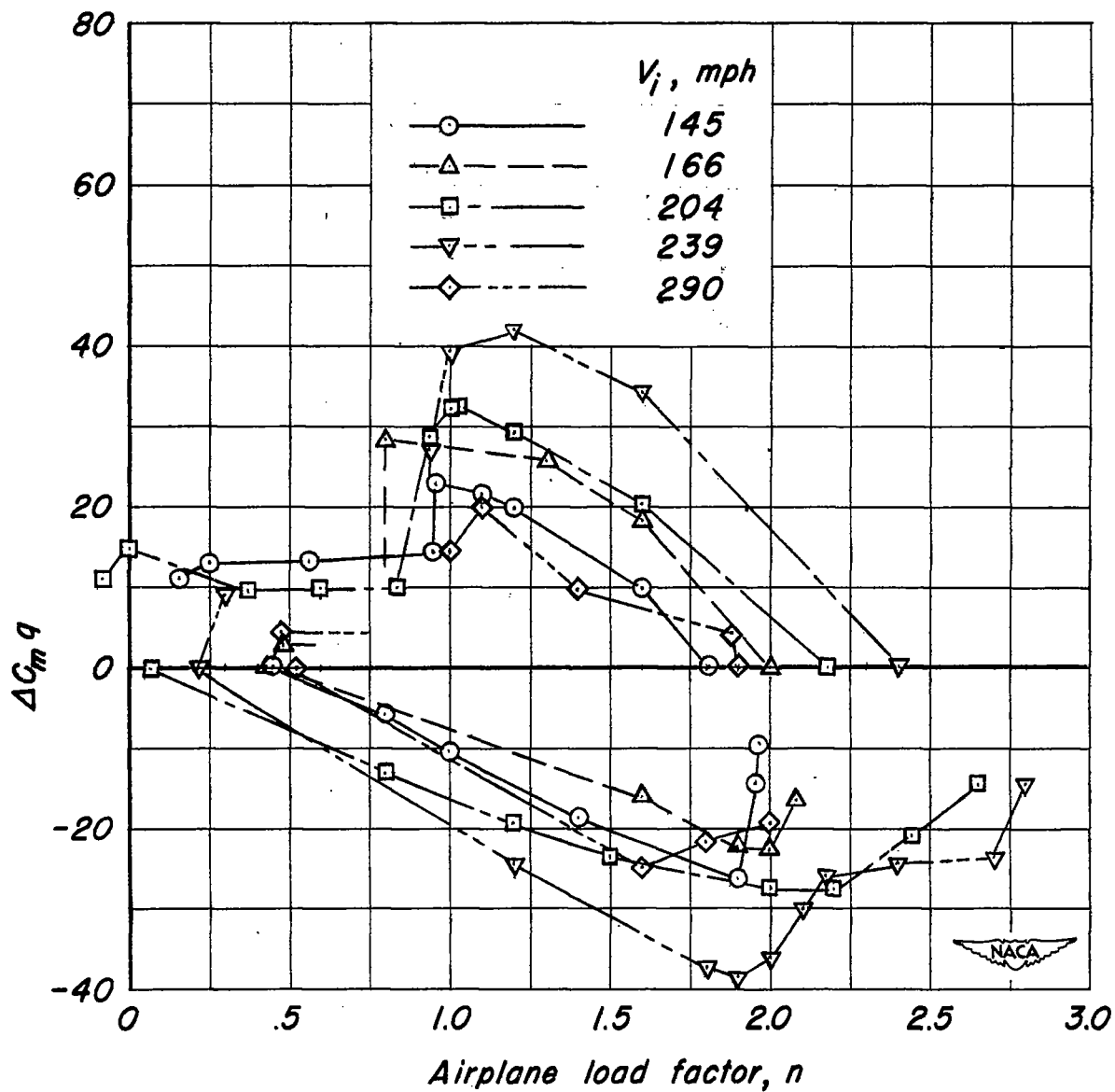


Figure 23.- Maximum out-of-balance pitching-moment parameter $\Delta C_m q$ derived from elevator angles employed during pitching maneuvers.

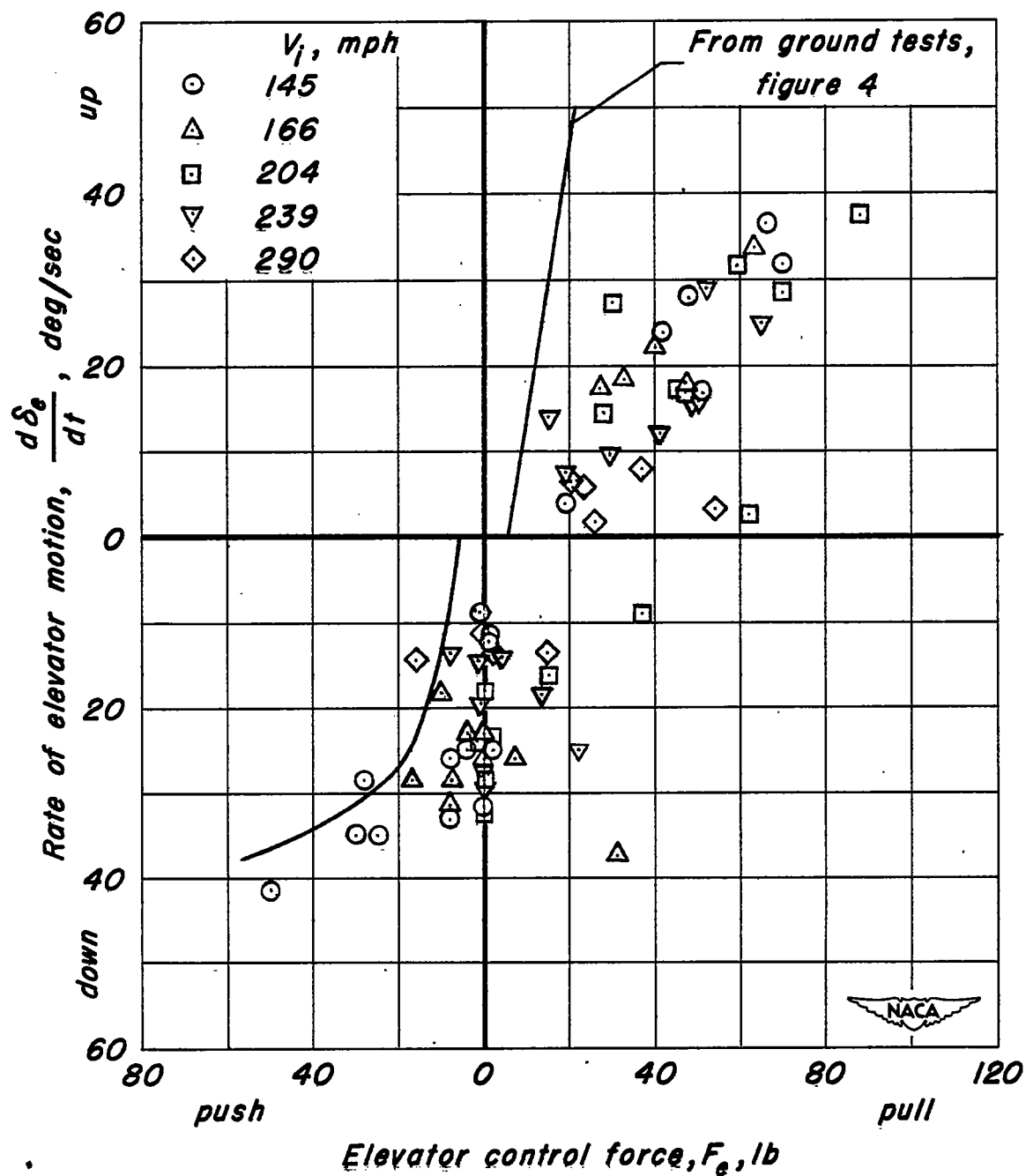


Figure 24.- Maximum rates of elevator motion attained in flight tests.

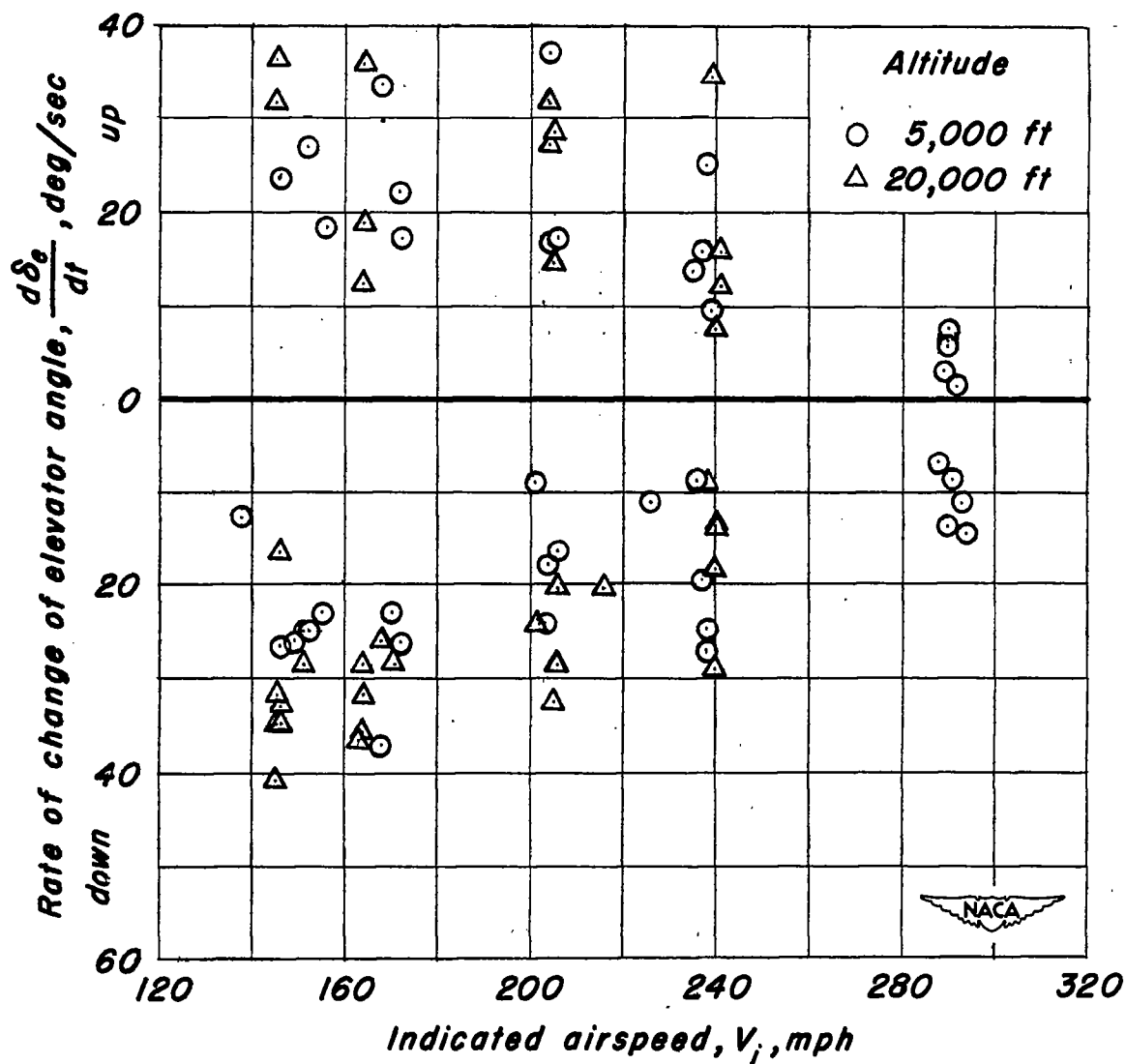


Figure 25.— Maximum rates of elevator motion shown as a function of airspeed.

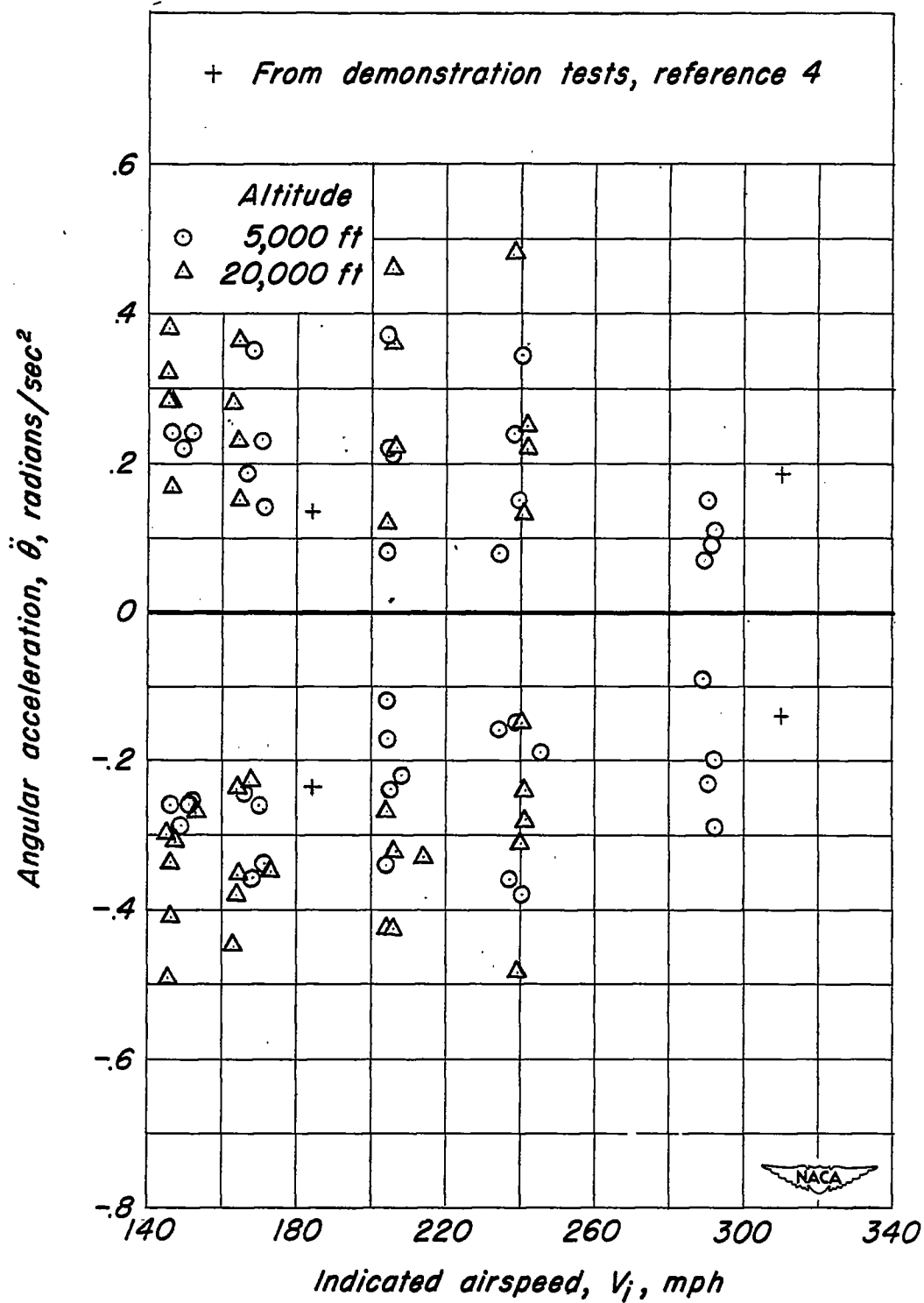


Figure 26.—Variation with indicated airspeed of maximum angular acceleration measured during pitching maneuvers.

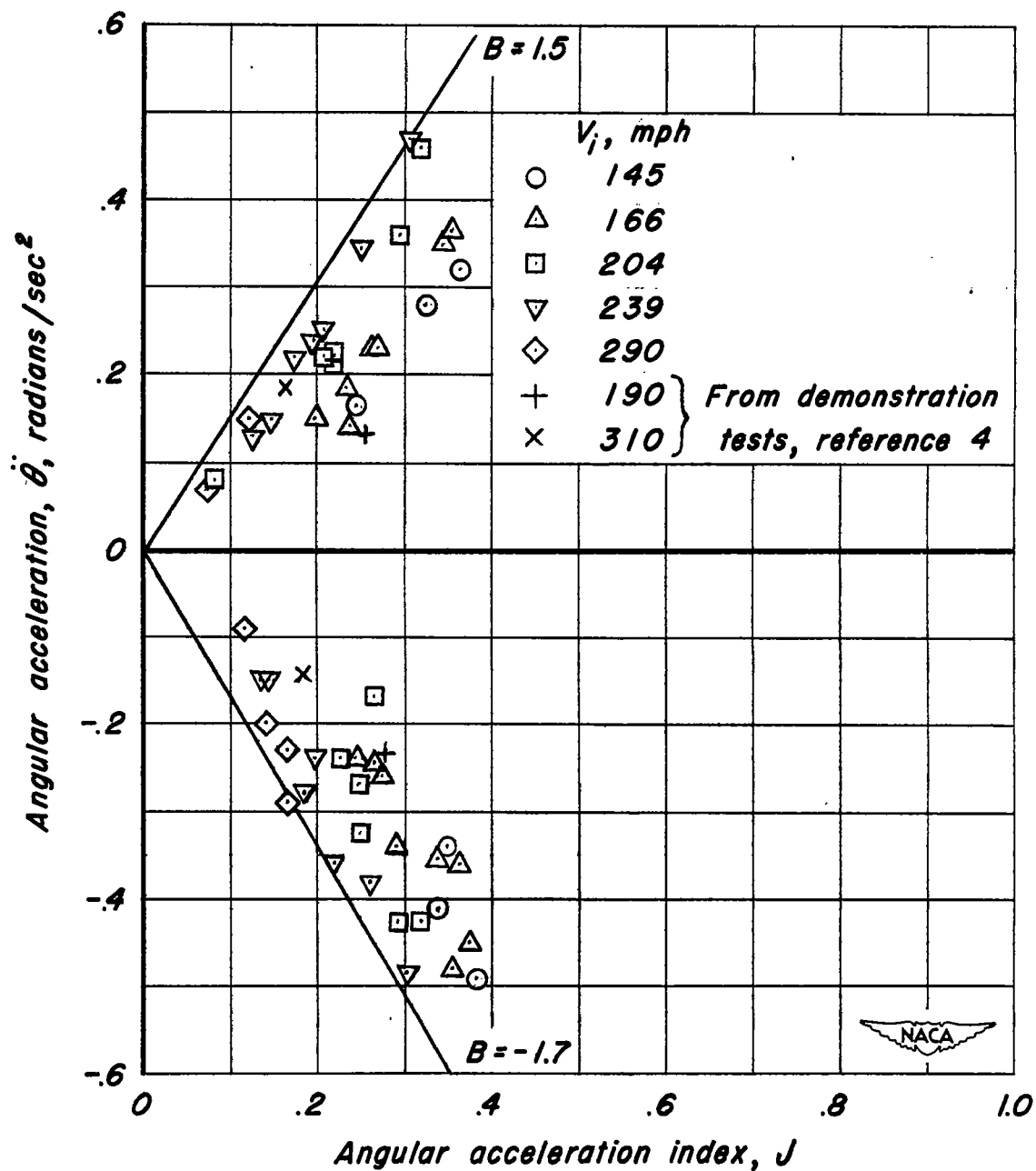


Figure 27.— Evaluation of method of reference 5 for estimating maximum angular accelerations.

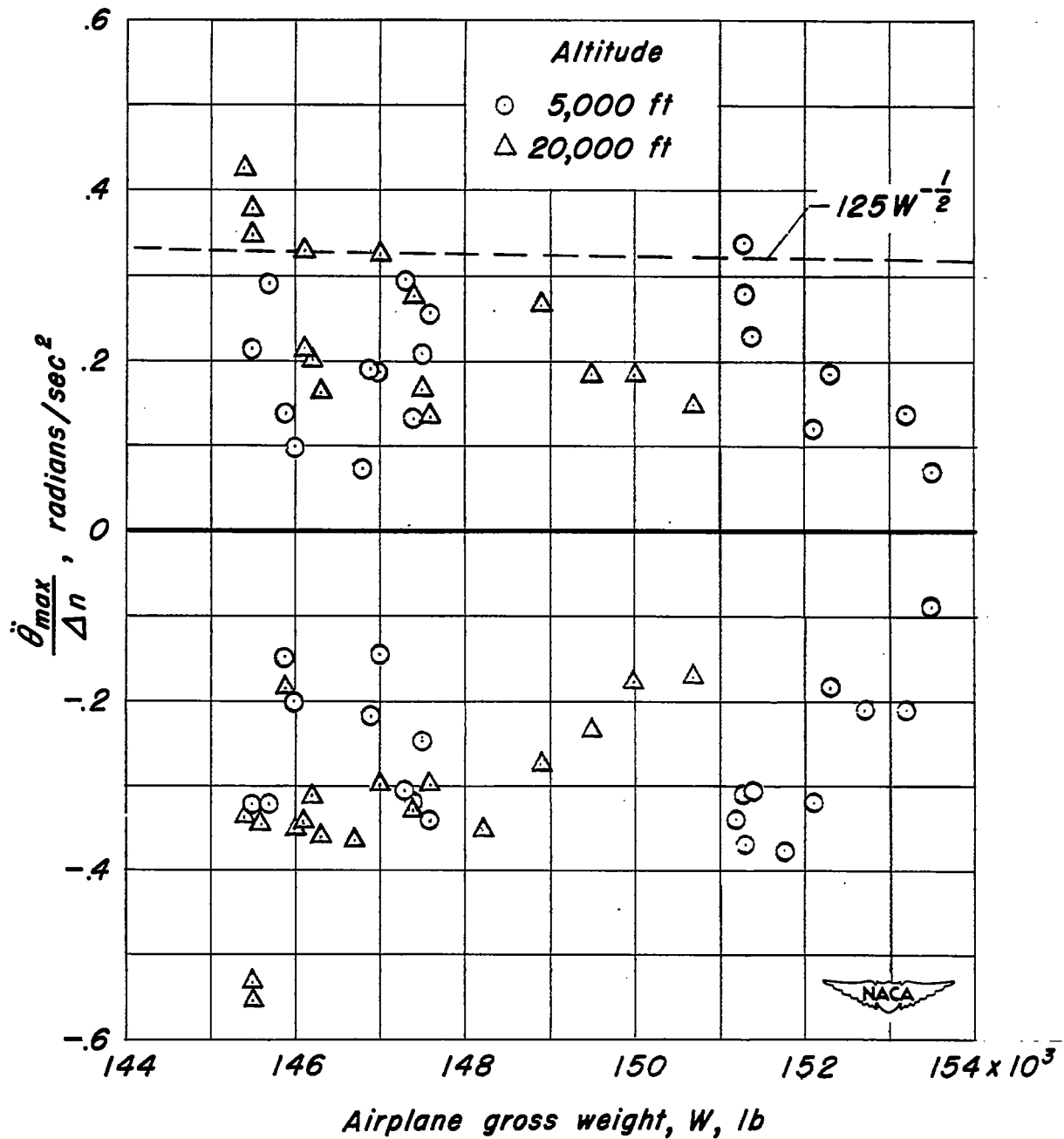
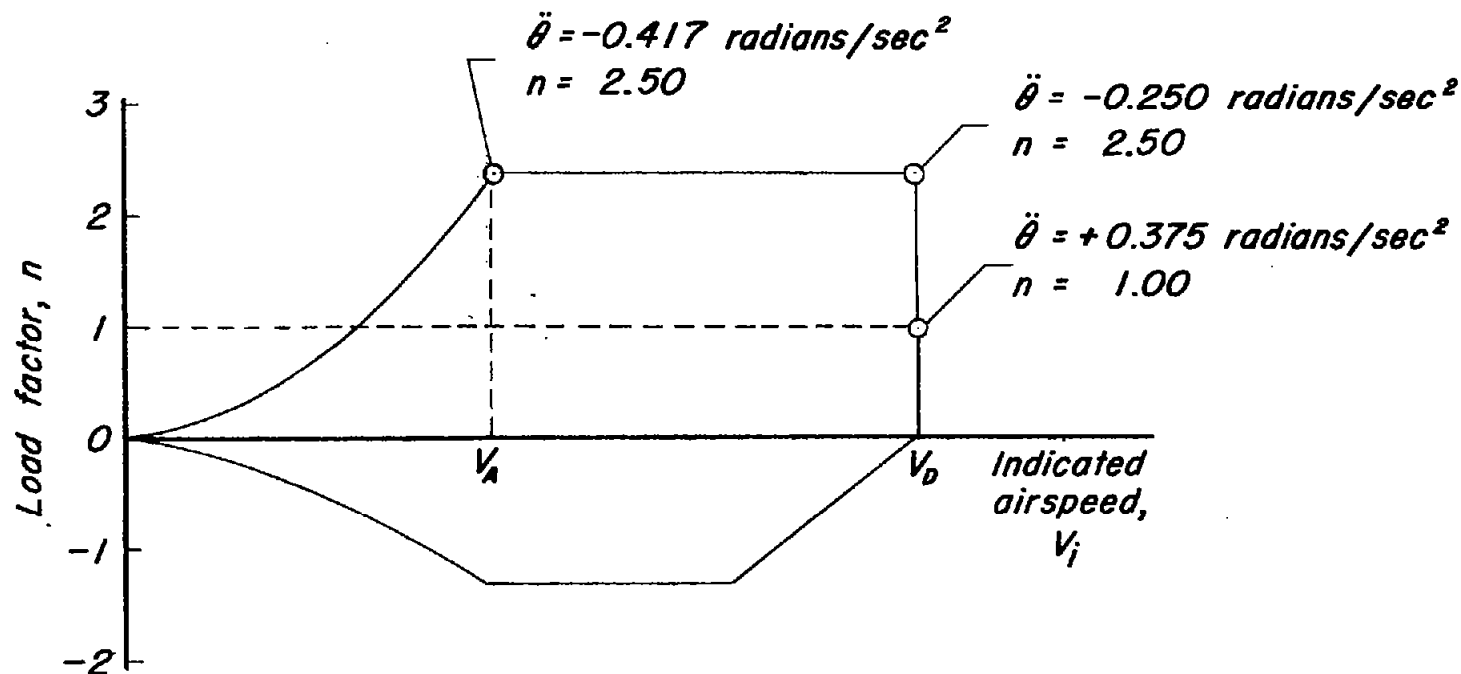


Figure 28.- Evaluation of equation of reference 6 for estimating maximum angular accelerations attainable in flight.

Note:

(1) The values of n shown are based on a design gross weight for the test airplane of 184,000 lbs.

(2) For the test airplane; $V_A \approx 180$ mph
 $V_D \approx 300$ mph



(a) Reference 7.

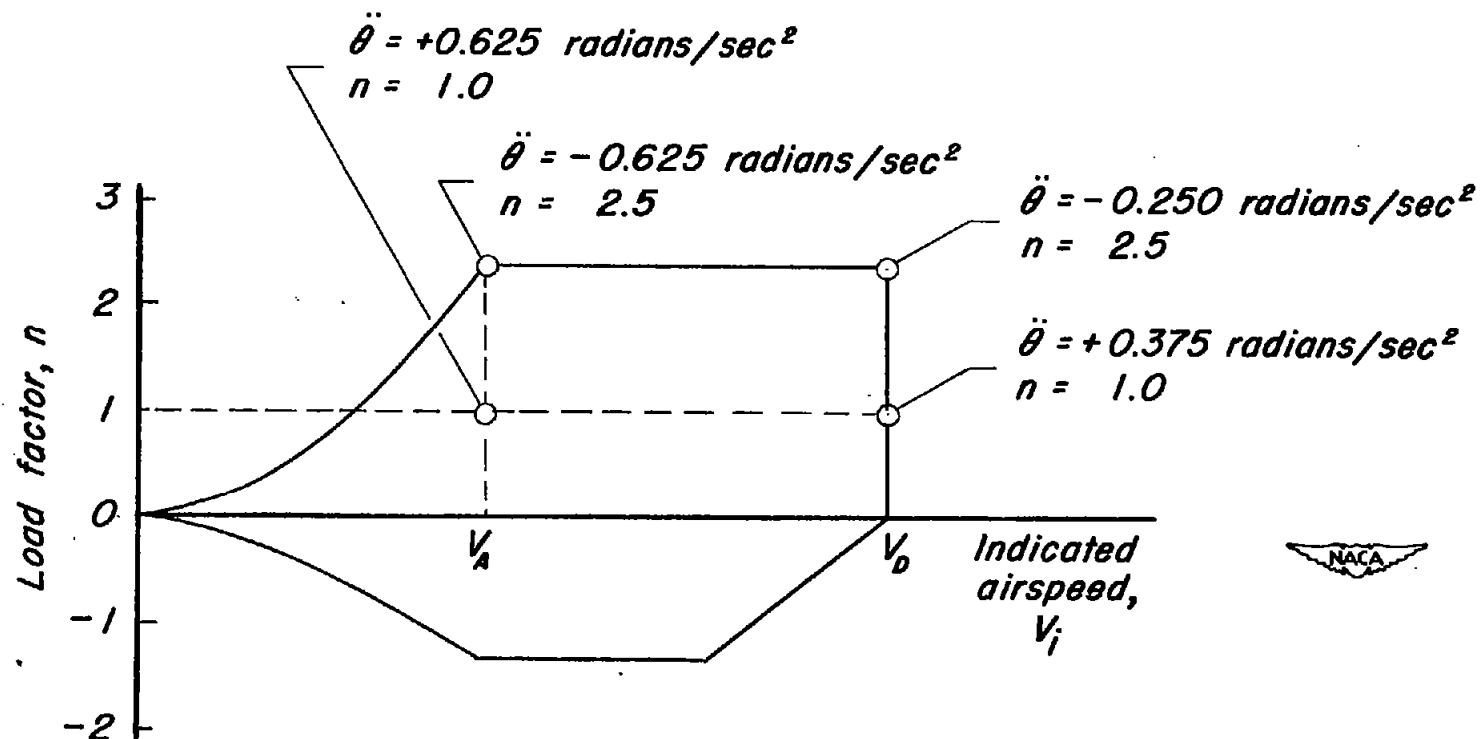


Figure 29.- Qualitative V - n diagrams showing the values of angular acceleration specified for design of the test airplane by various references.

Note:

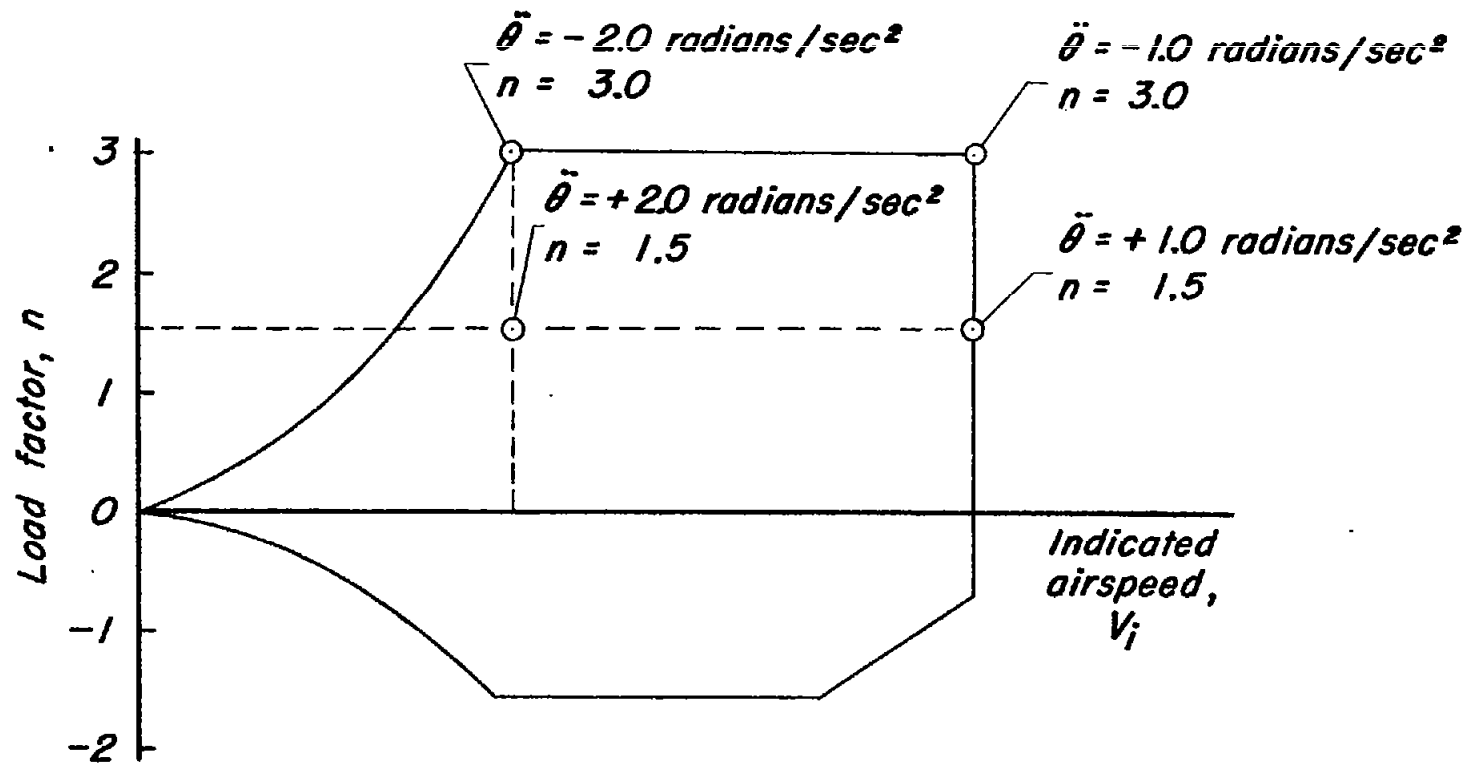
(1) The values of n shown are based on a design gross weight for the test airplane of 184,000 lbs.

(2) For the test airplane; $V_A \approx 180$ mph
 $V_D \approx 300$ mph



(b) Reference 8.

Figure 29.- Continued.



(c) Navy.



Figure 29.- Concluded.

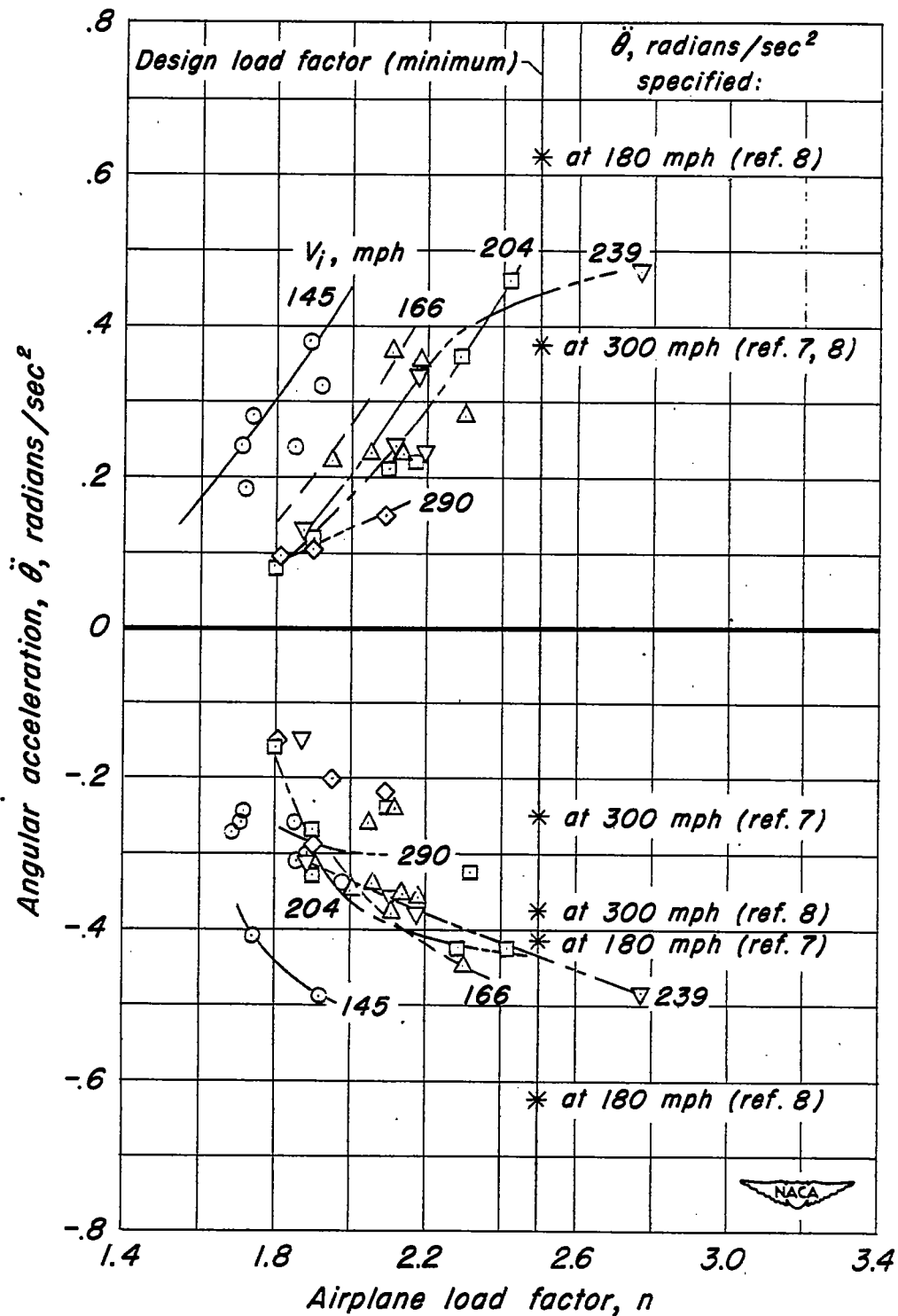


Figure 30.- Evaluation of specifications of references 7 and 8 for angular acceleration.

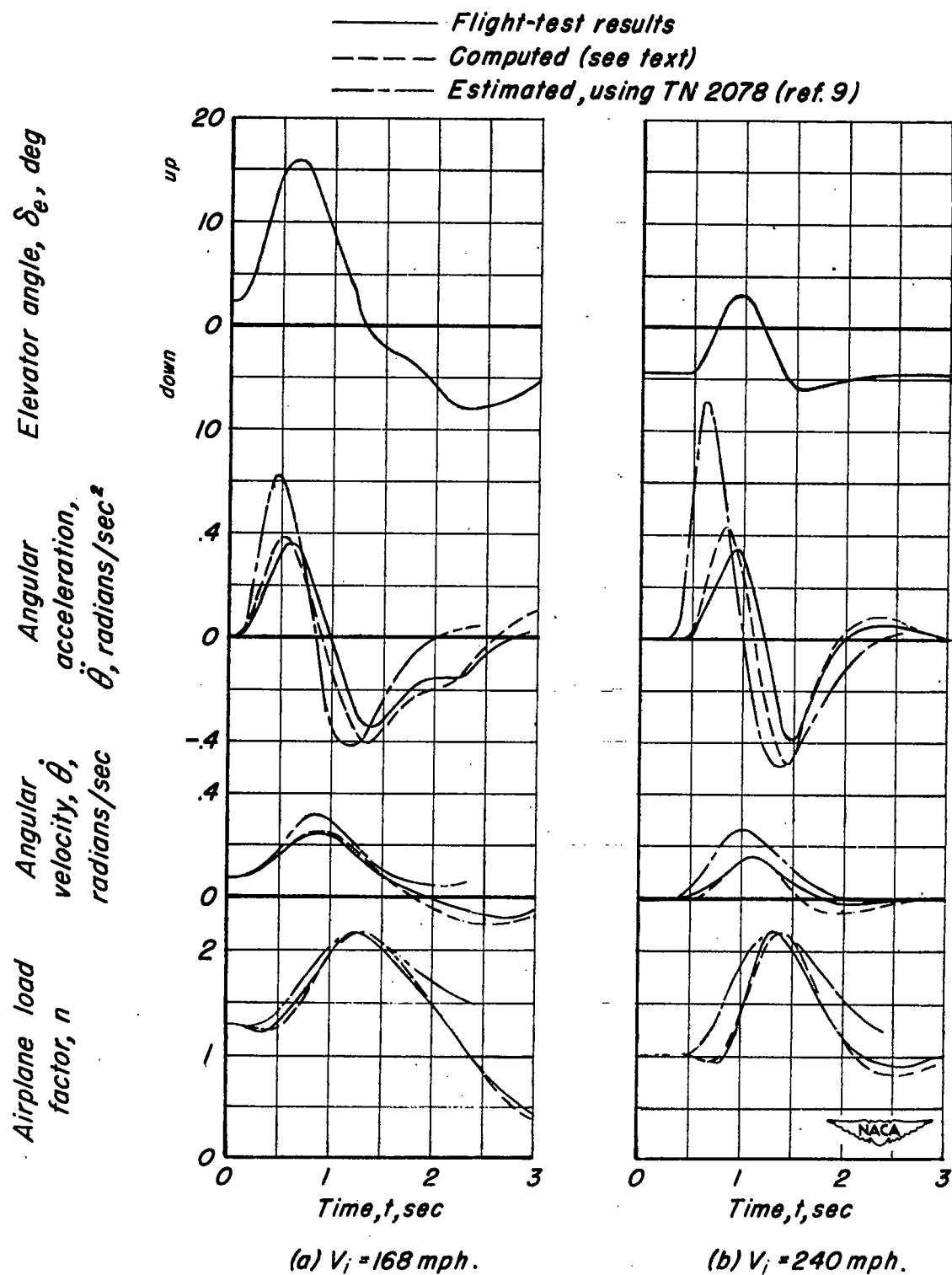


Figure 31.— Comparison between quantities measured during pitching maneuvers and estimated values.

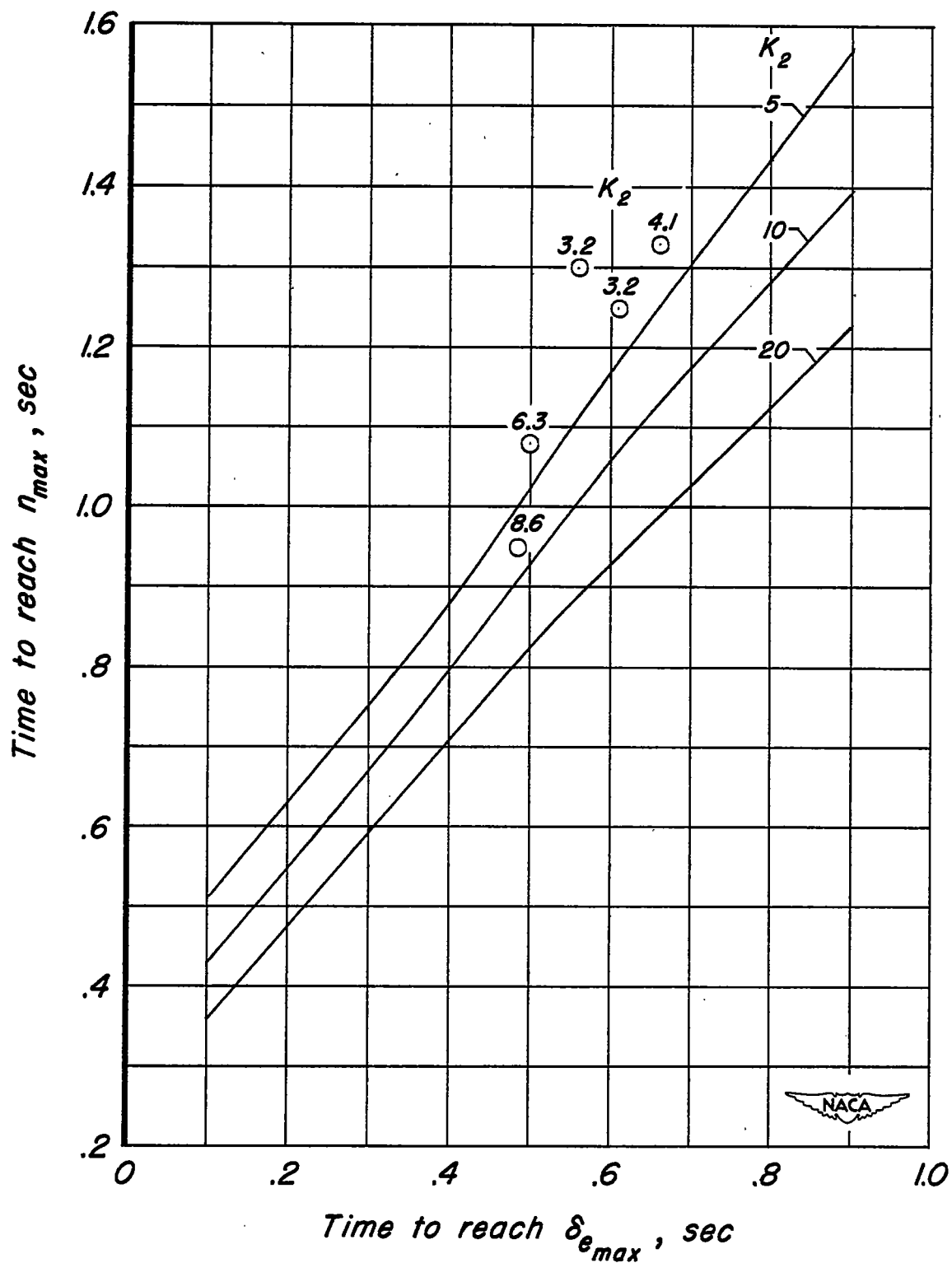
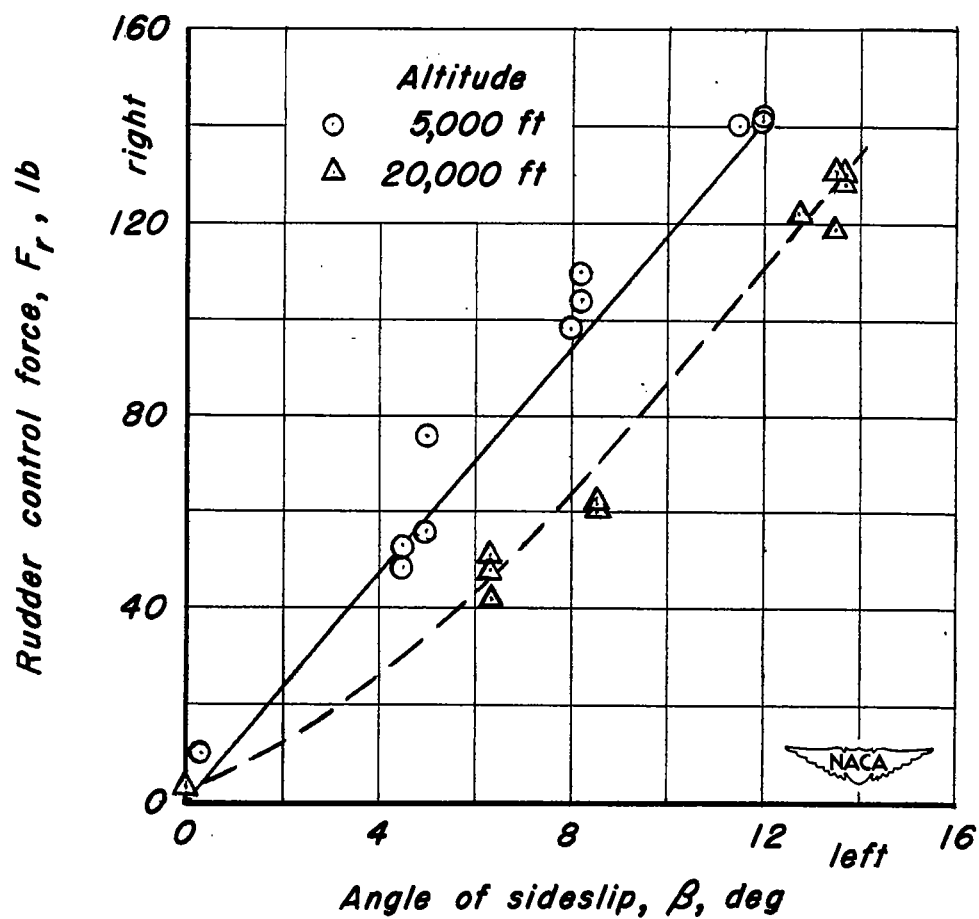
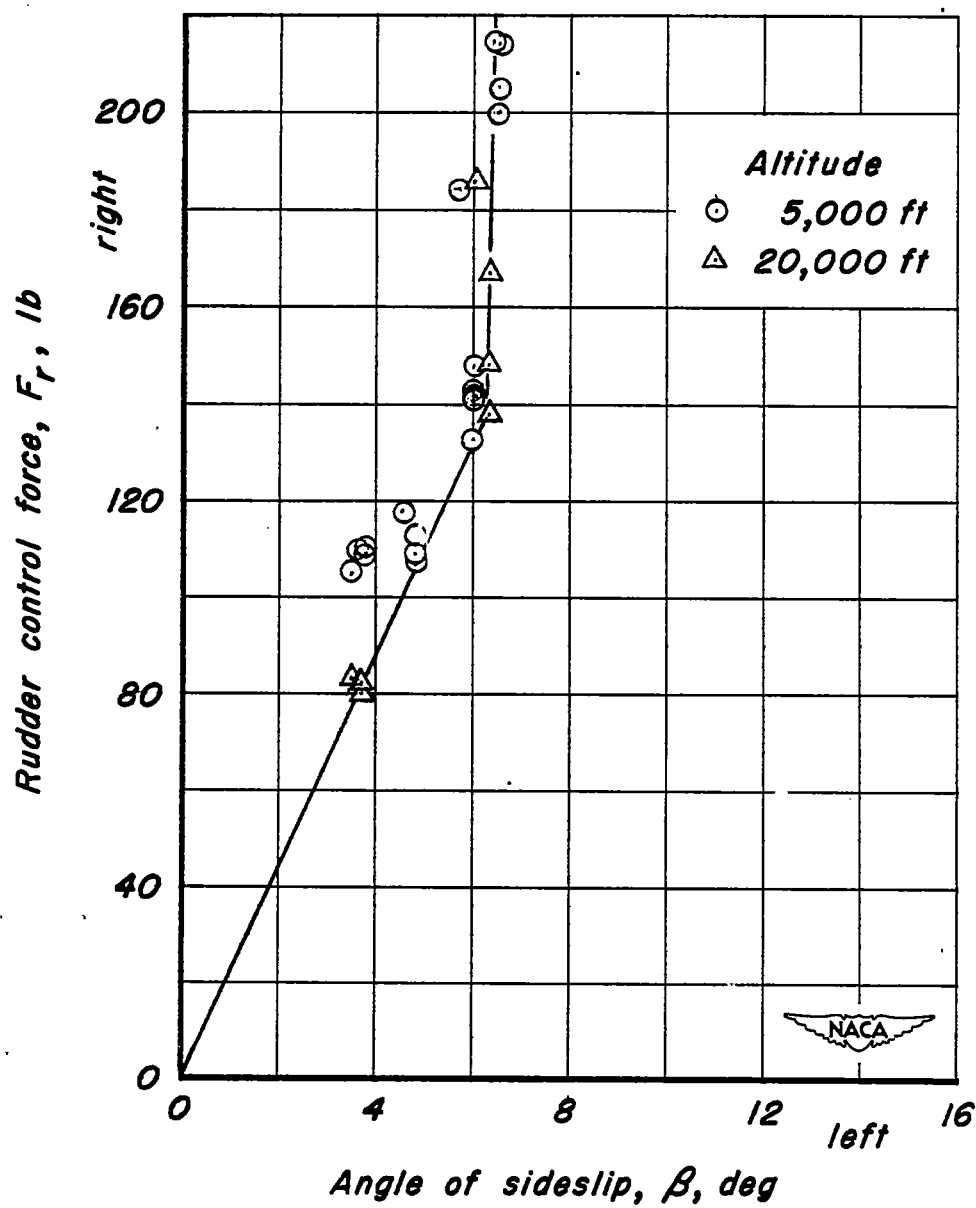


Figure 32.— Variation of time to reach maximum load factor as a function of time to attain maximum elevator deflection.



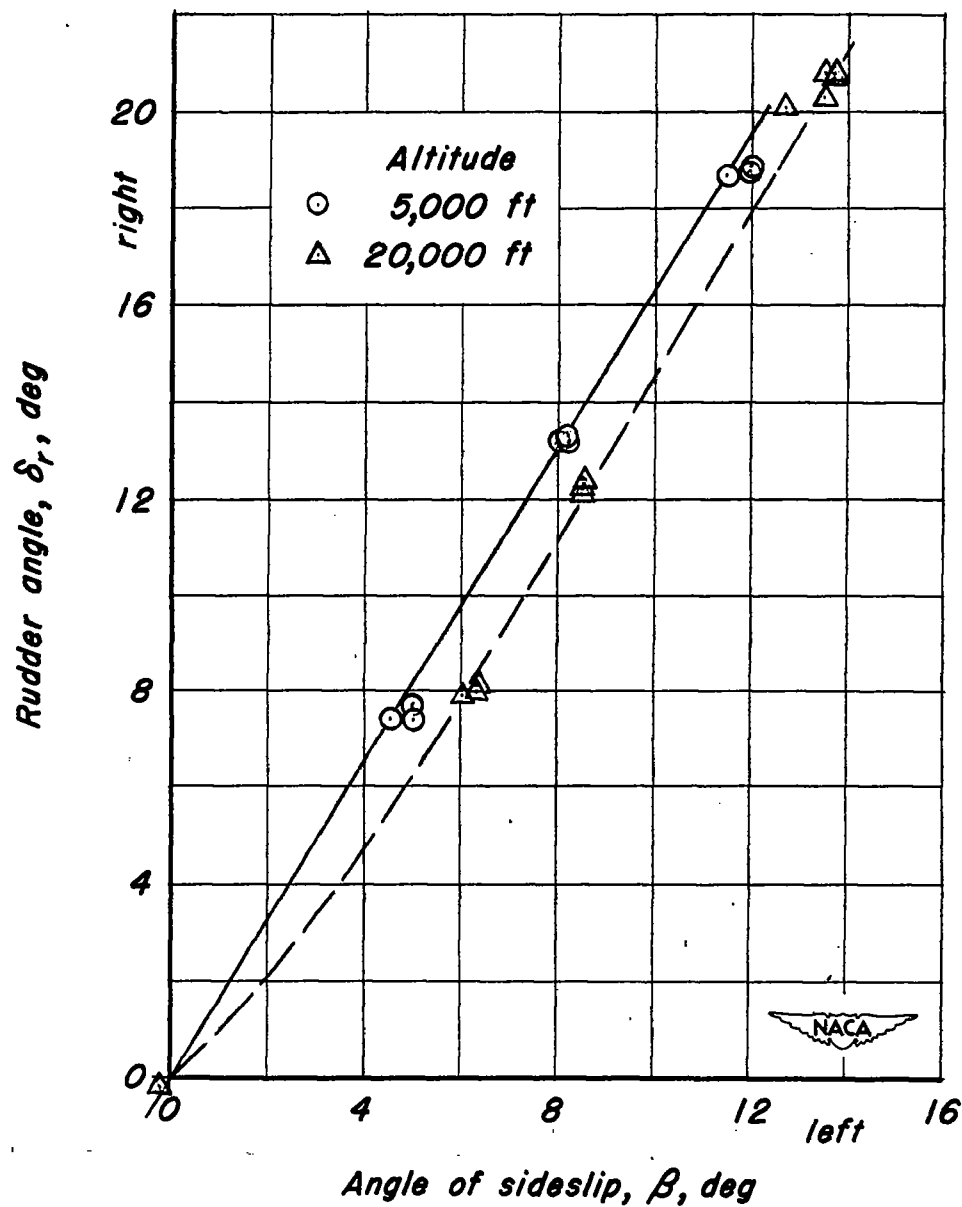
(a) $V_i = 145$ mph.

Figure 33.—Variation of rudder control force to maintain sideslip as a function of angle of sideslip.



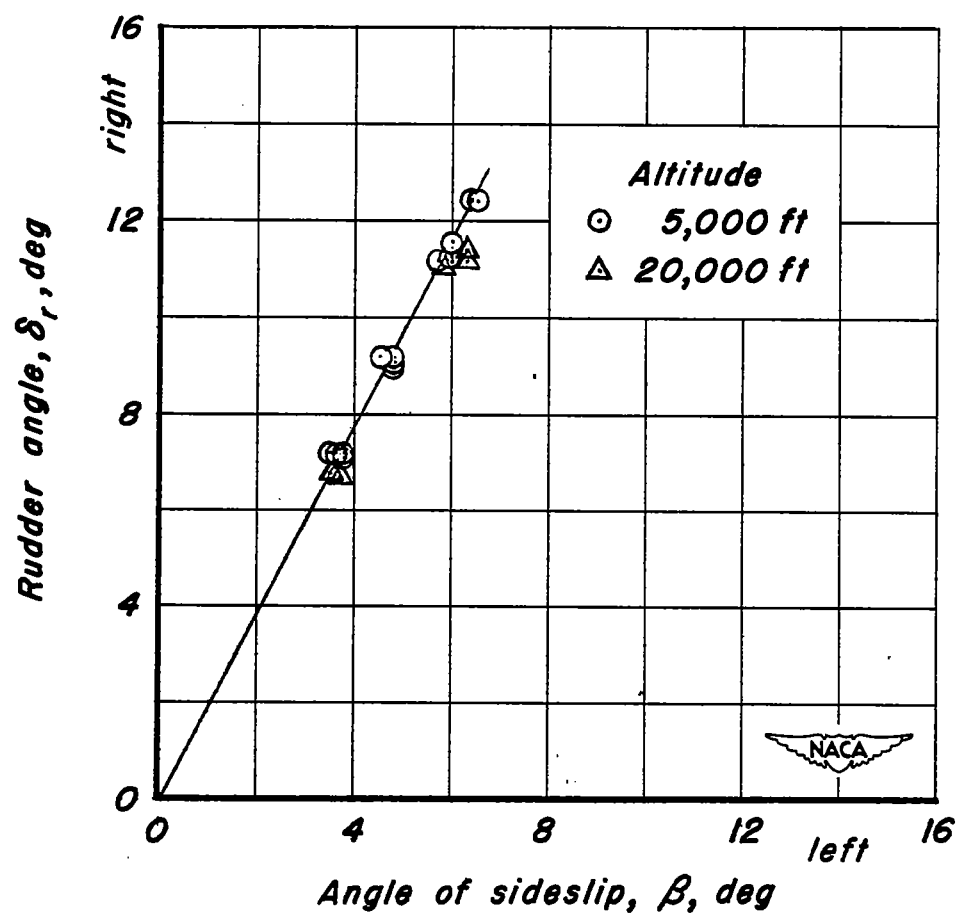
(b) $V_i = 204$ mph.

Figure 33.- Concluded.



(a) $V_i = 145$ mph.

Figure 34.— Variation of rudder angle to maintain sideslip as a function of angle of sideslip.



(b) $V_i = 204 \text{ mph}$.

Figure 34.-Concluded.

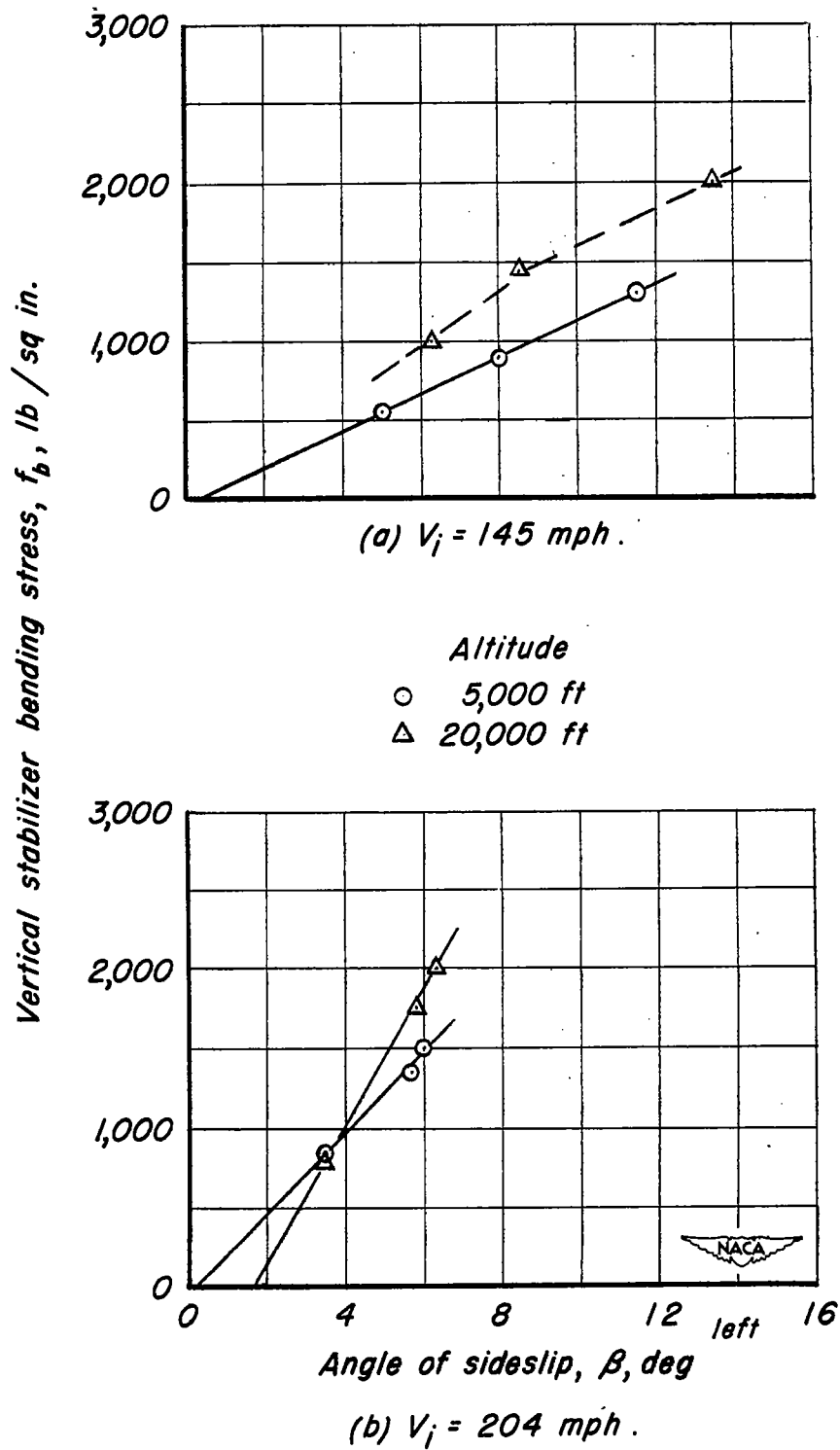
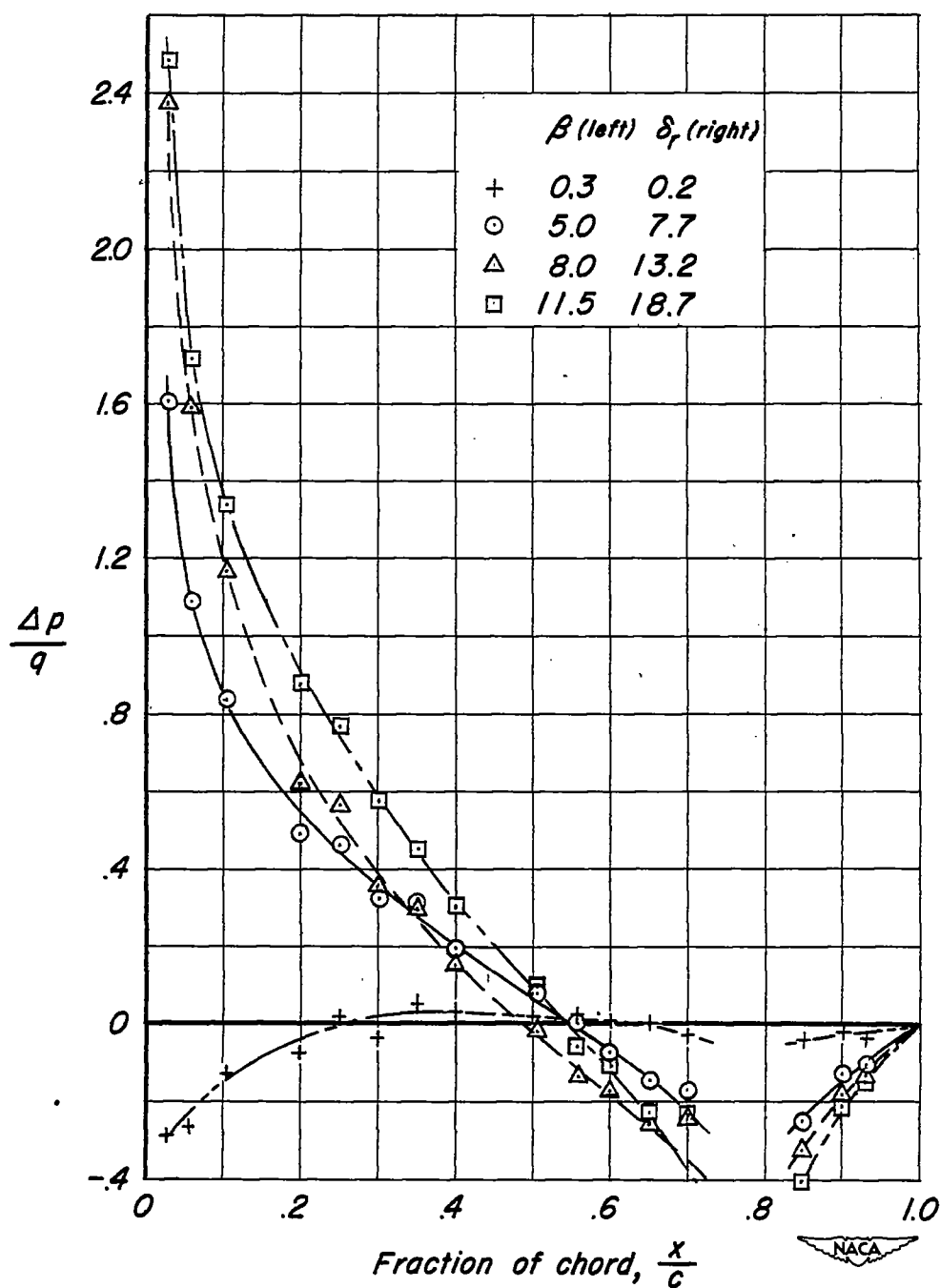
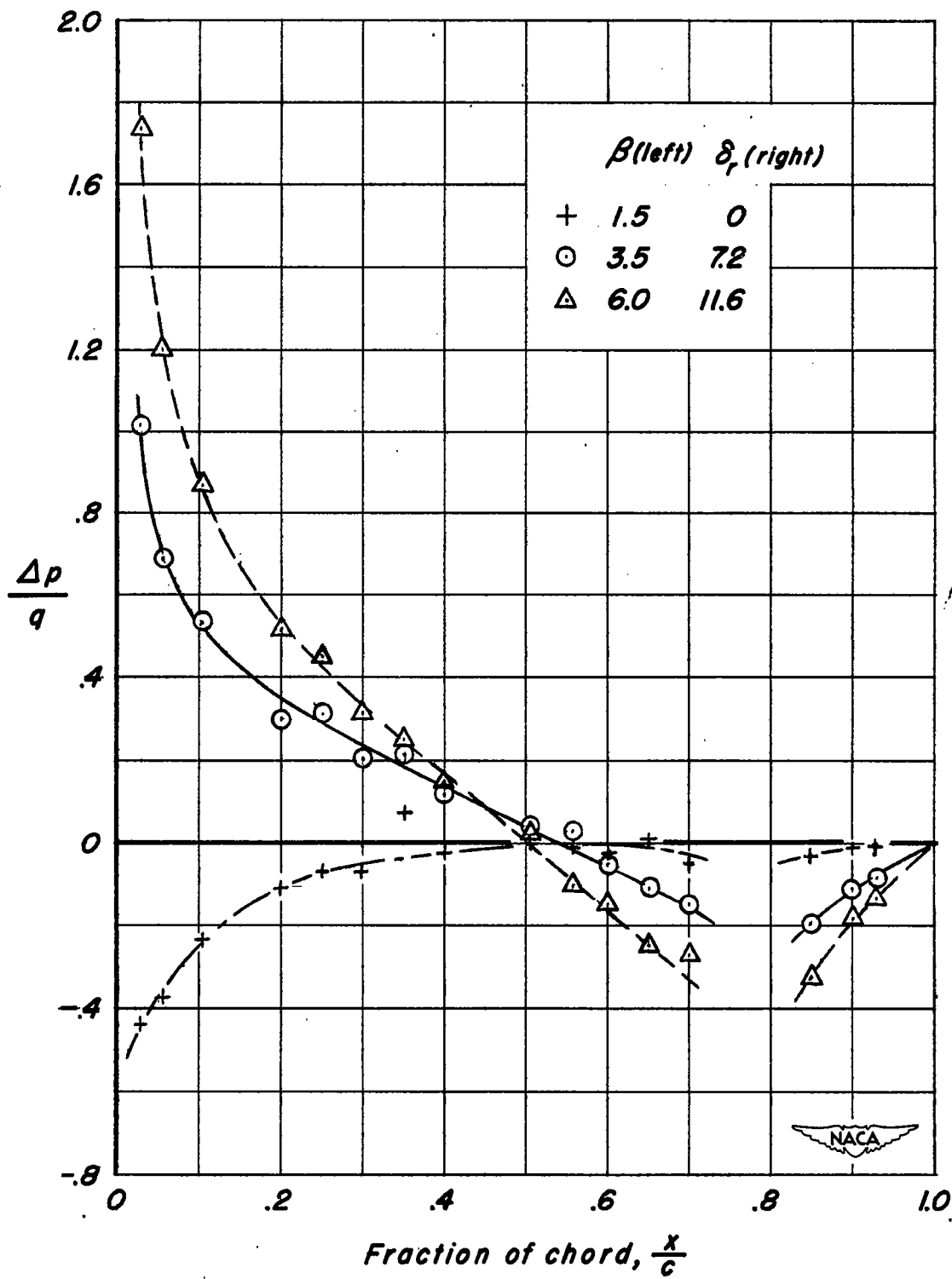


Figure 35.—Effect of angle of sideslip on bending stress in main beam of vertical stabilizer, steady sideslip conditions.



(a) $V_i = 145$ mph.

Figure 36.- Chordwise distribution of load coefficient at 42.2-percent span on vertical stabilizer at various angles of sideslip; steady sideslip conditions, 5,000 feet.



(b) $V_i = 204$ mph.

Figure 36.- Concluded.

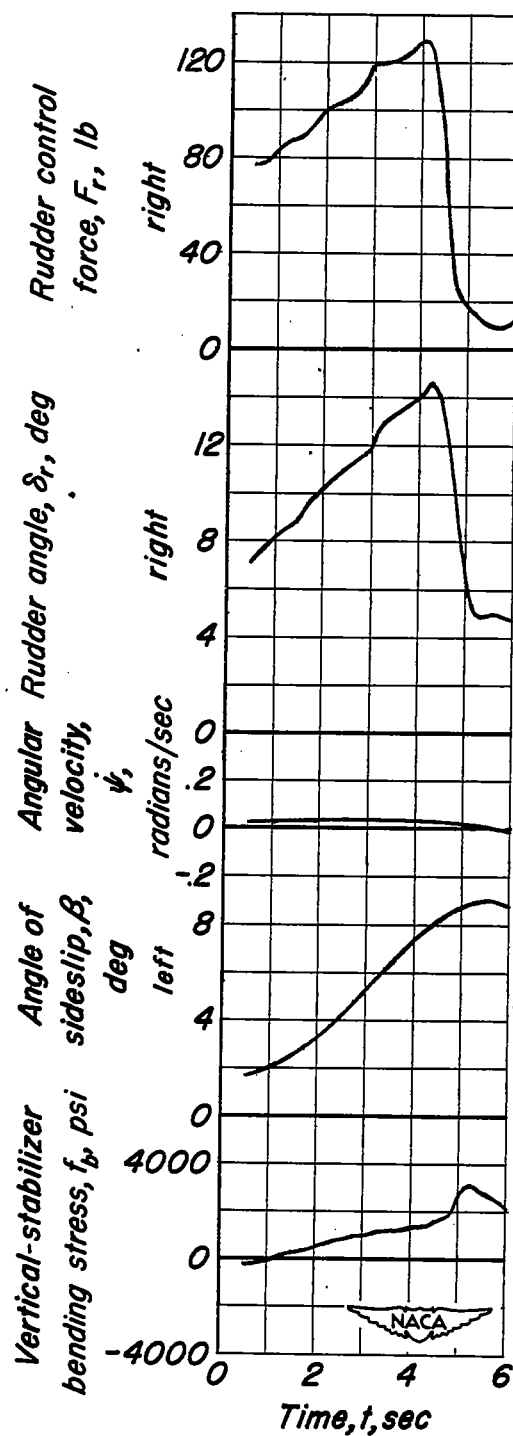


Figure 37.- Pertinent quantities measured during rudder-kick maneuver; airspeed, 150 miles per hour; altitude, 5,000 feet.

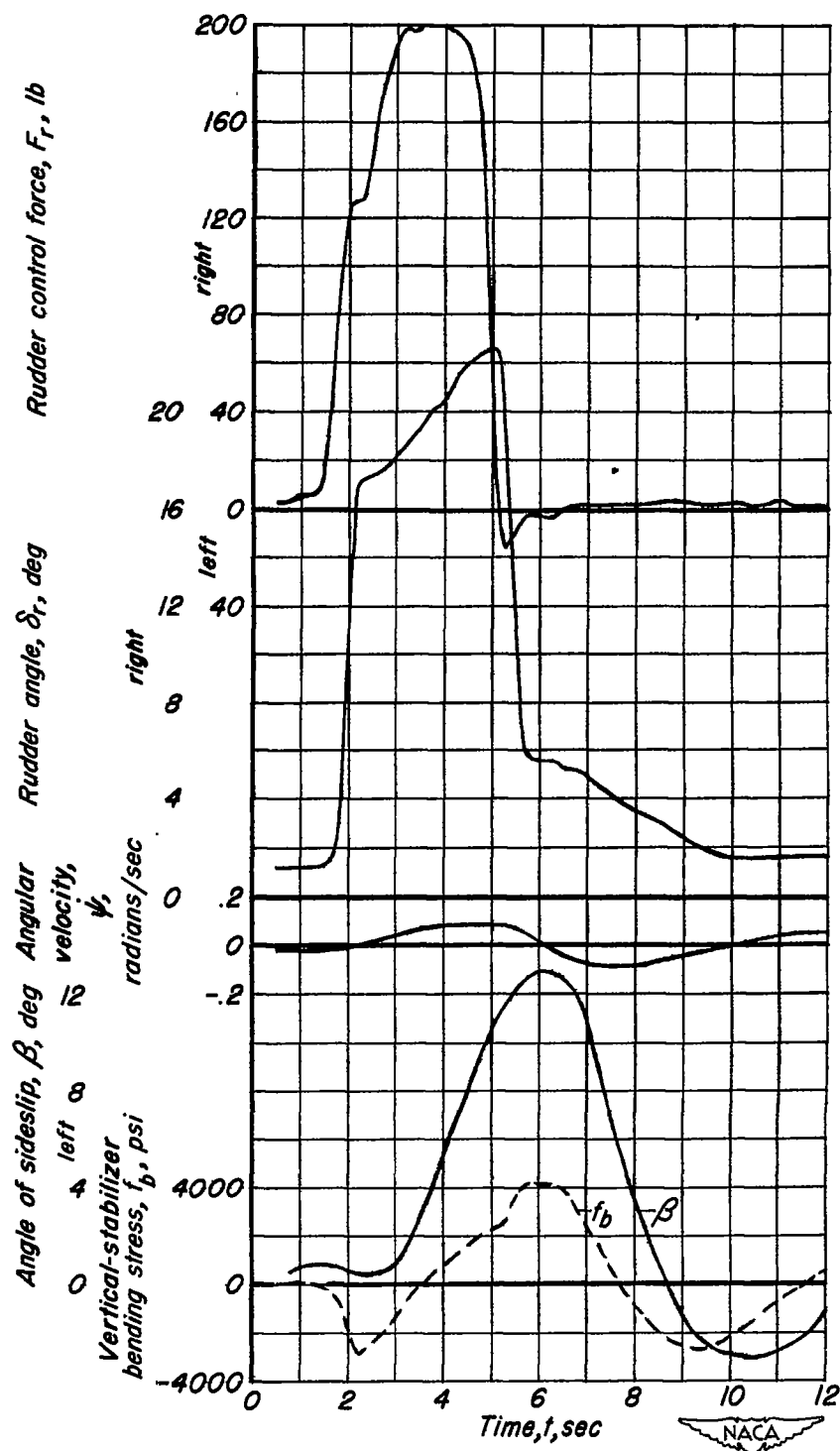
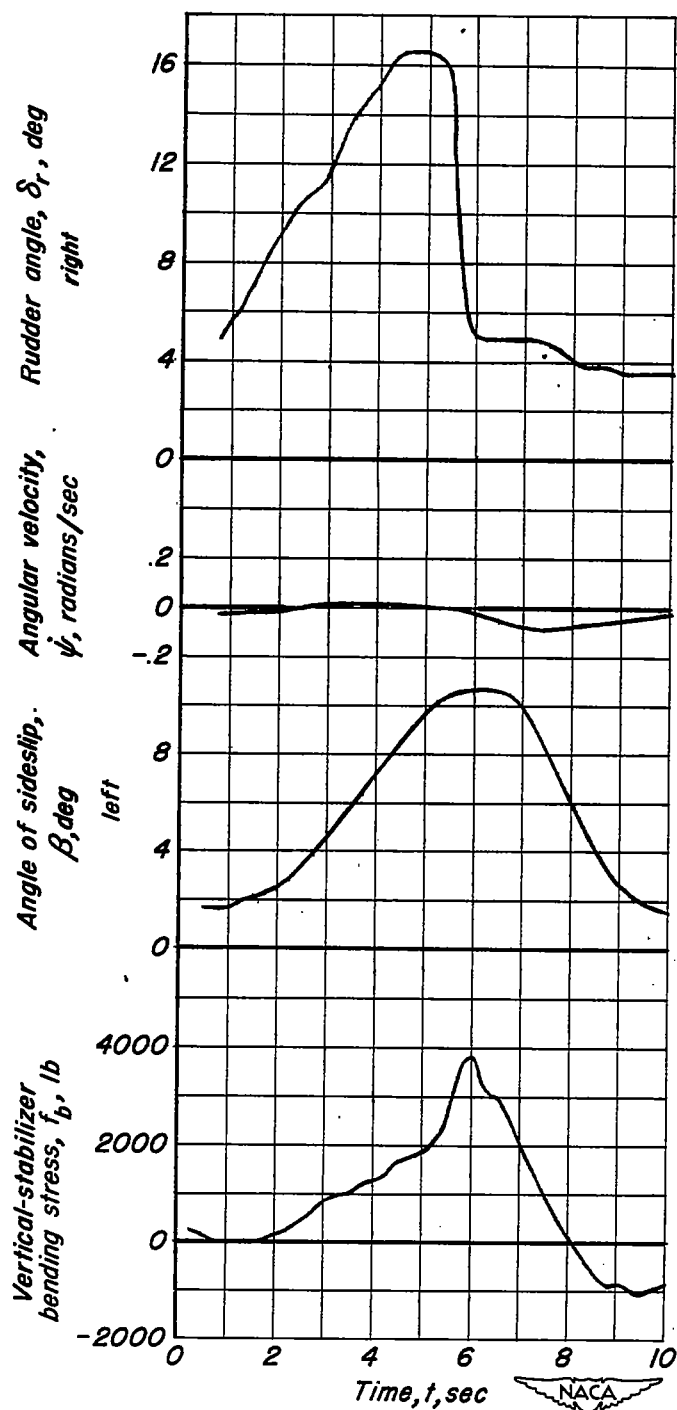
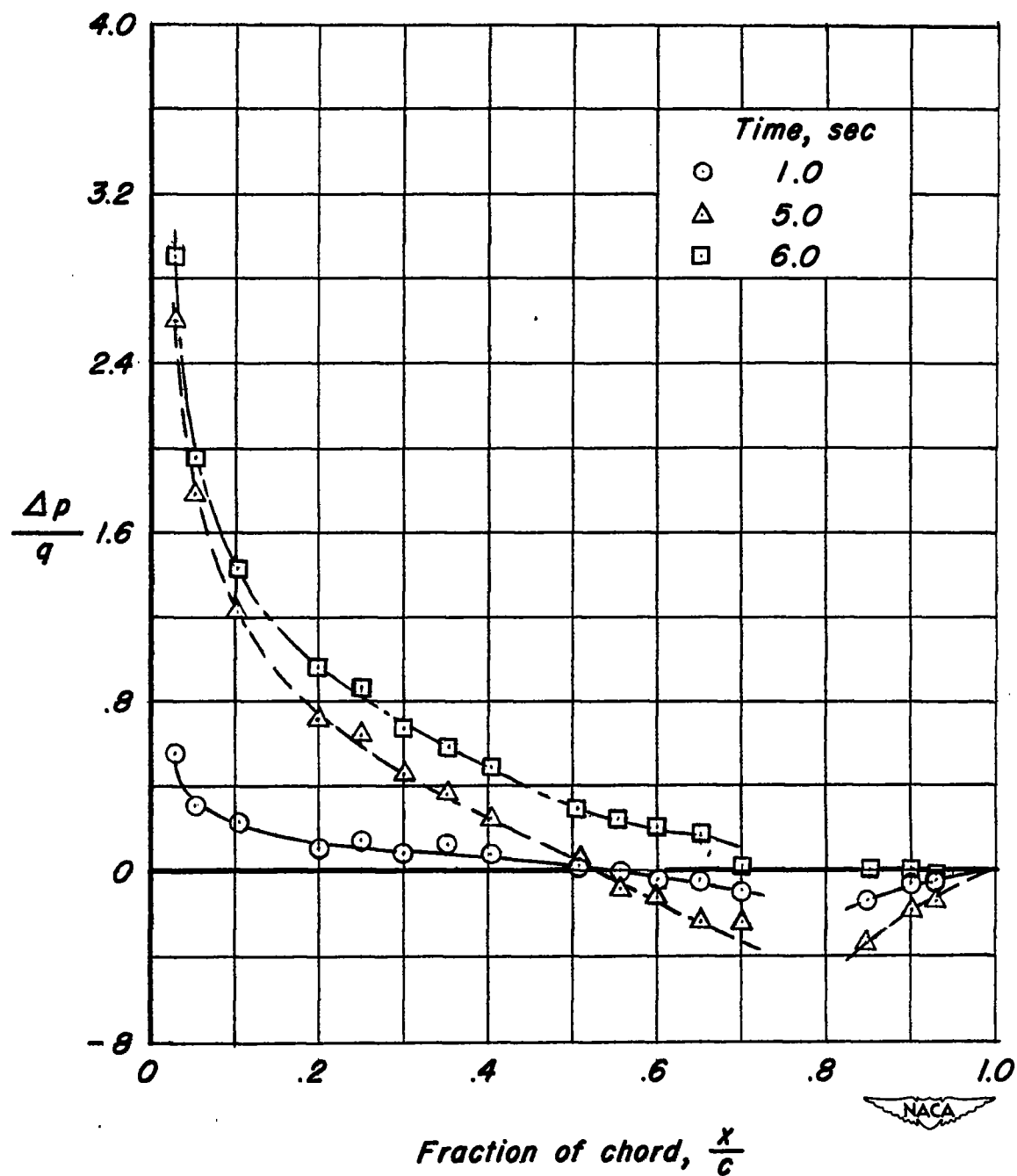


Figure 38.—Pertinent quantities measured during rudder-kick maneuver; airspeed, 145 miles per hour; altitude, 5000 feet.



(a) Time history.

Figure 39.—Pertinent quantities measured during rudder-kick maneuver; airspeed, 141 miles per hour; altitude, 5,300 feet.



(b) Chordwise distribution of load coefficient at 42.2 % span on vertical stabilizer.

Figure 39.— Concluded.

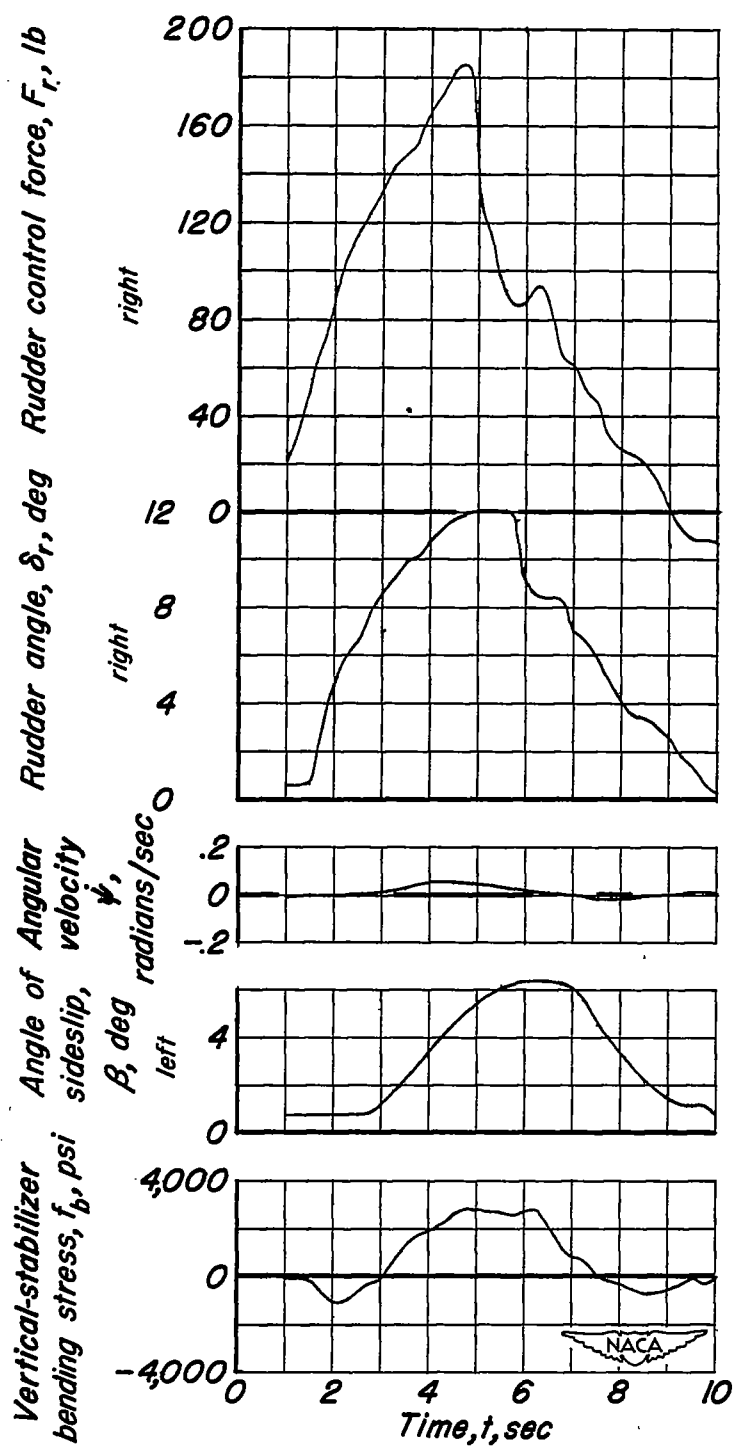


Figure 40.-Pertinent quantities measured during rudder-kick maneuver; airspeed, 204 miles per hour; altitude, 5,000 feet.

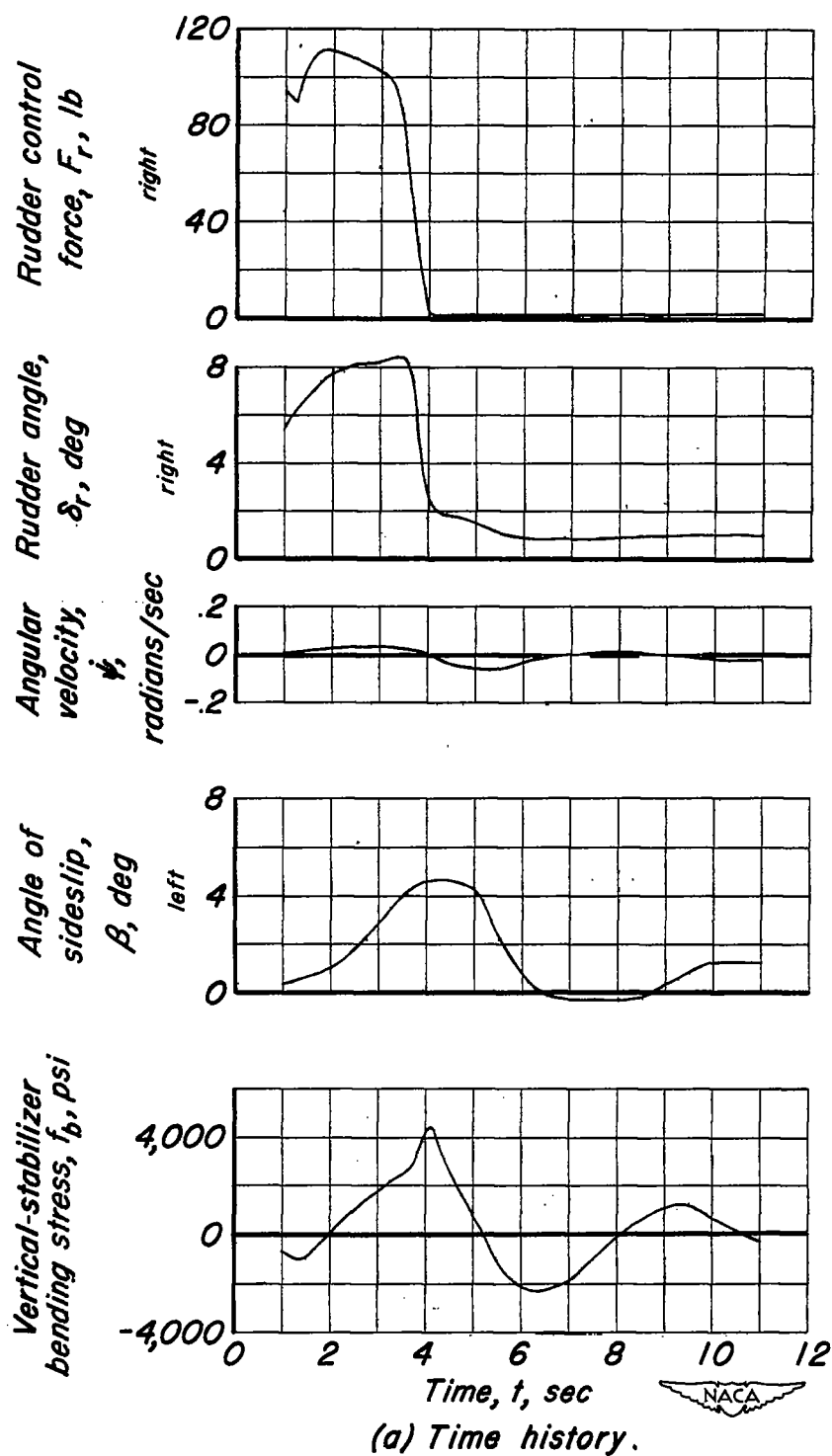
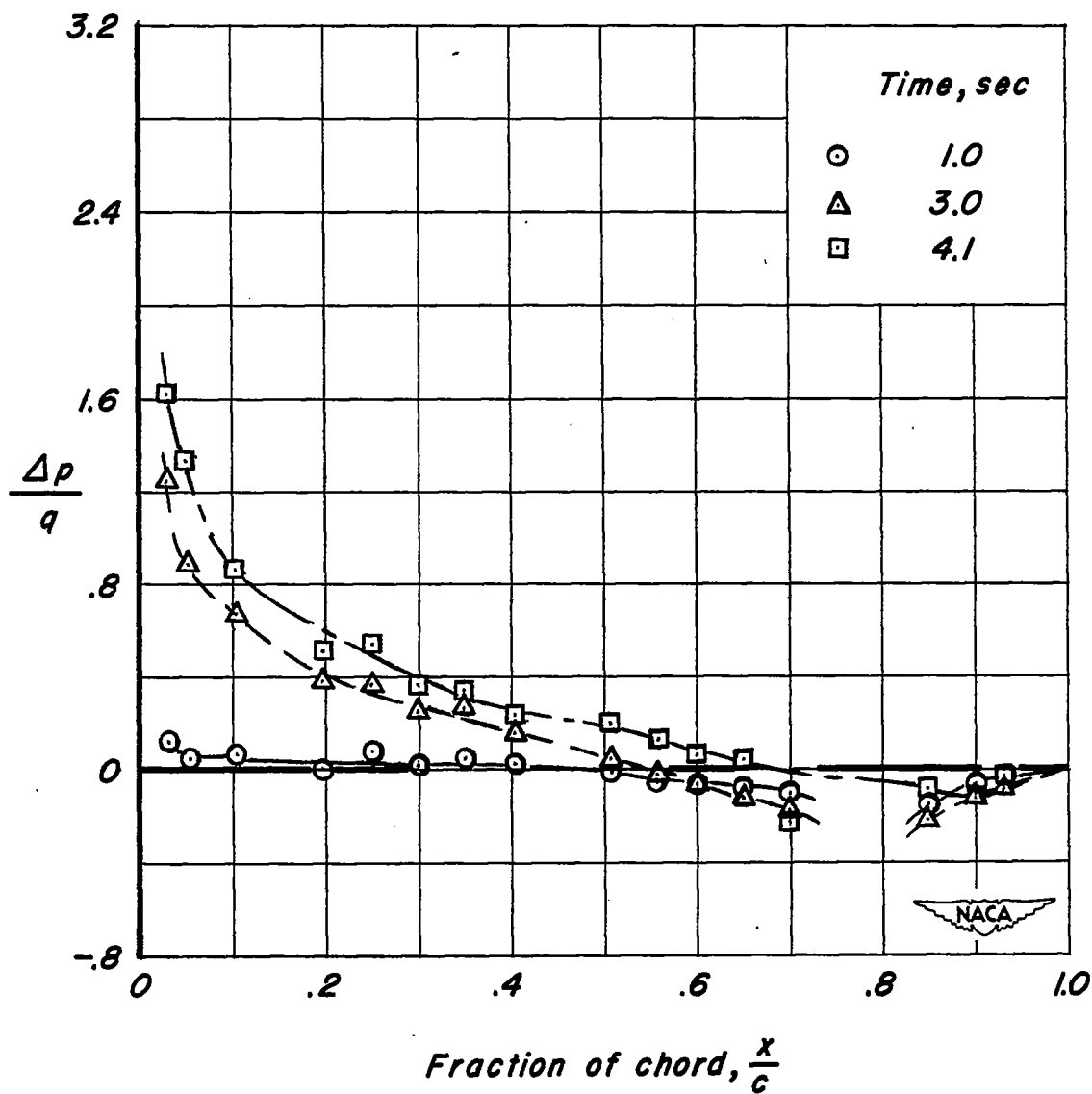
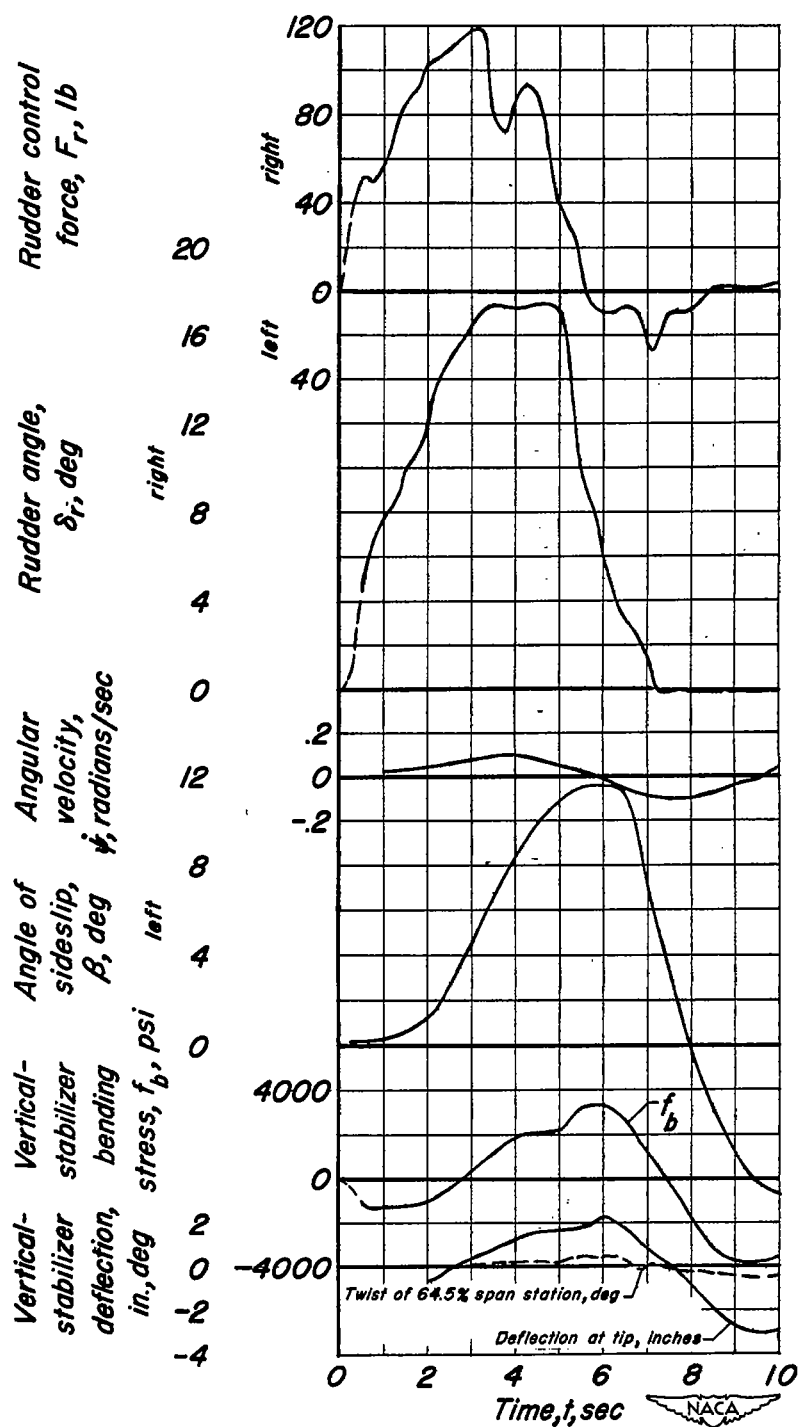


Figure 41.- Pertinent quantities measured during rudder-kick maneuver; airspeed, 197 miles per hour; altitude, 5,000 feet.



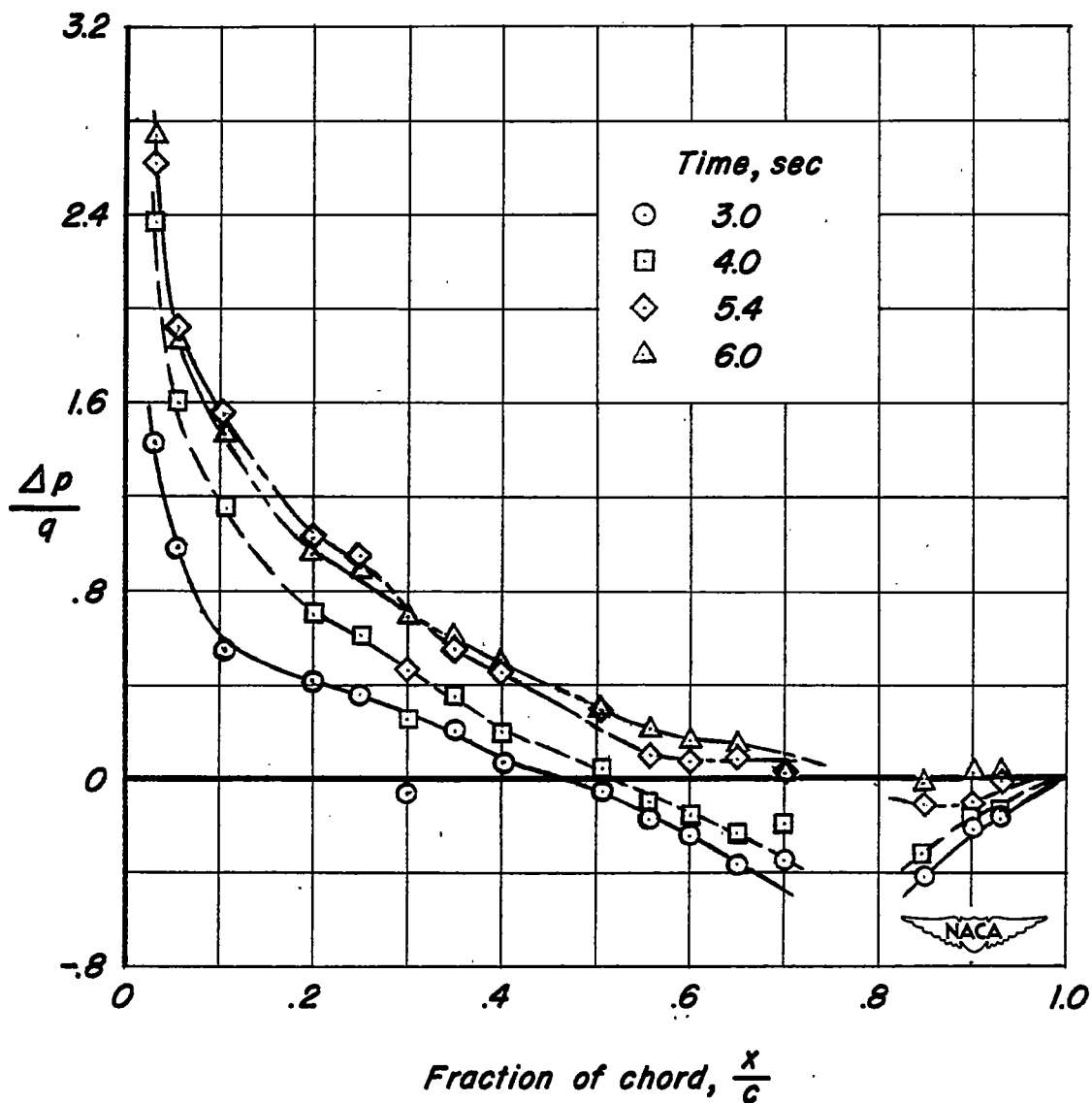
(b) Chordwise distribution of load coefficient at 42.2 % span on vertical stabilizer.

Figure 41.- Concluded.



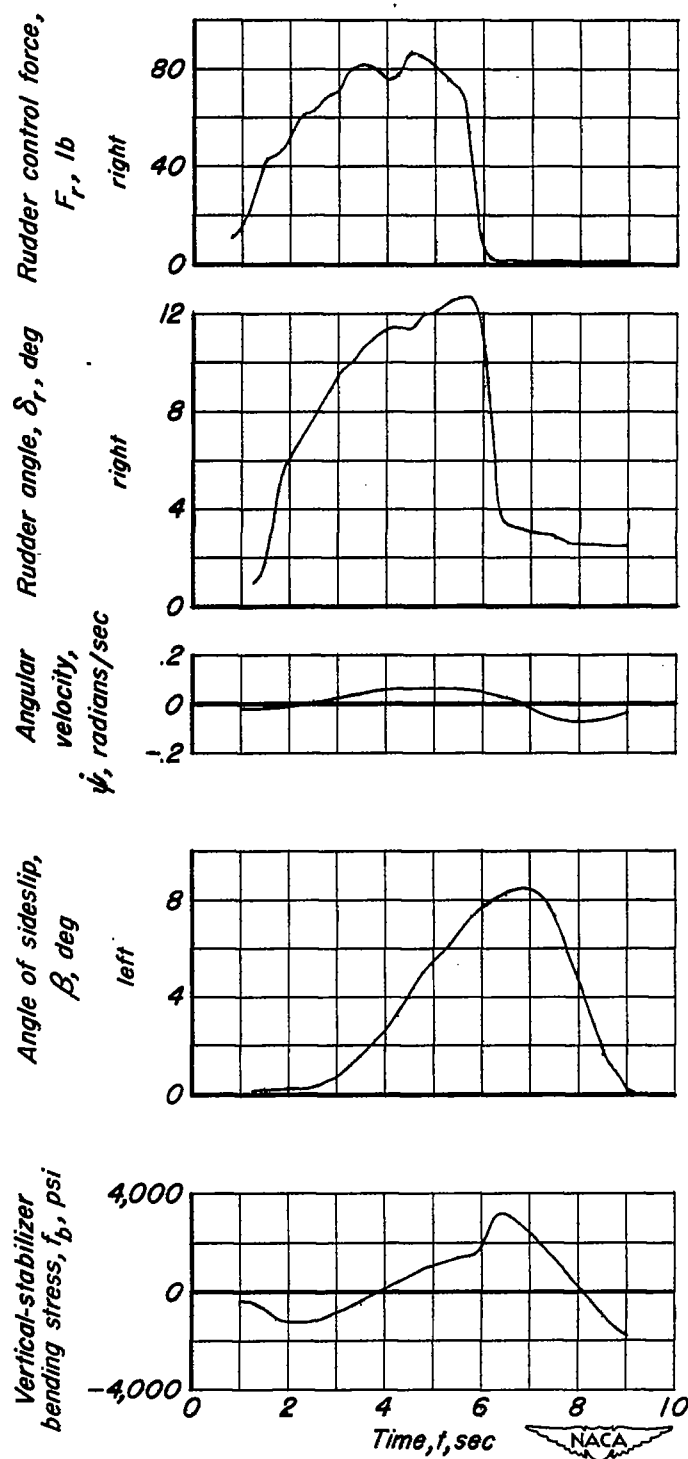
(a) Time history.

Figure 42.-Pertinent quantities measured during rudder-kick maneuver; airspeed, 144 miles per hour; altitude, 5,000 feet.



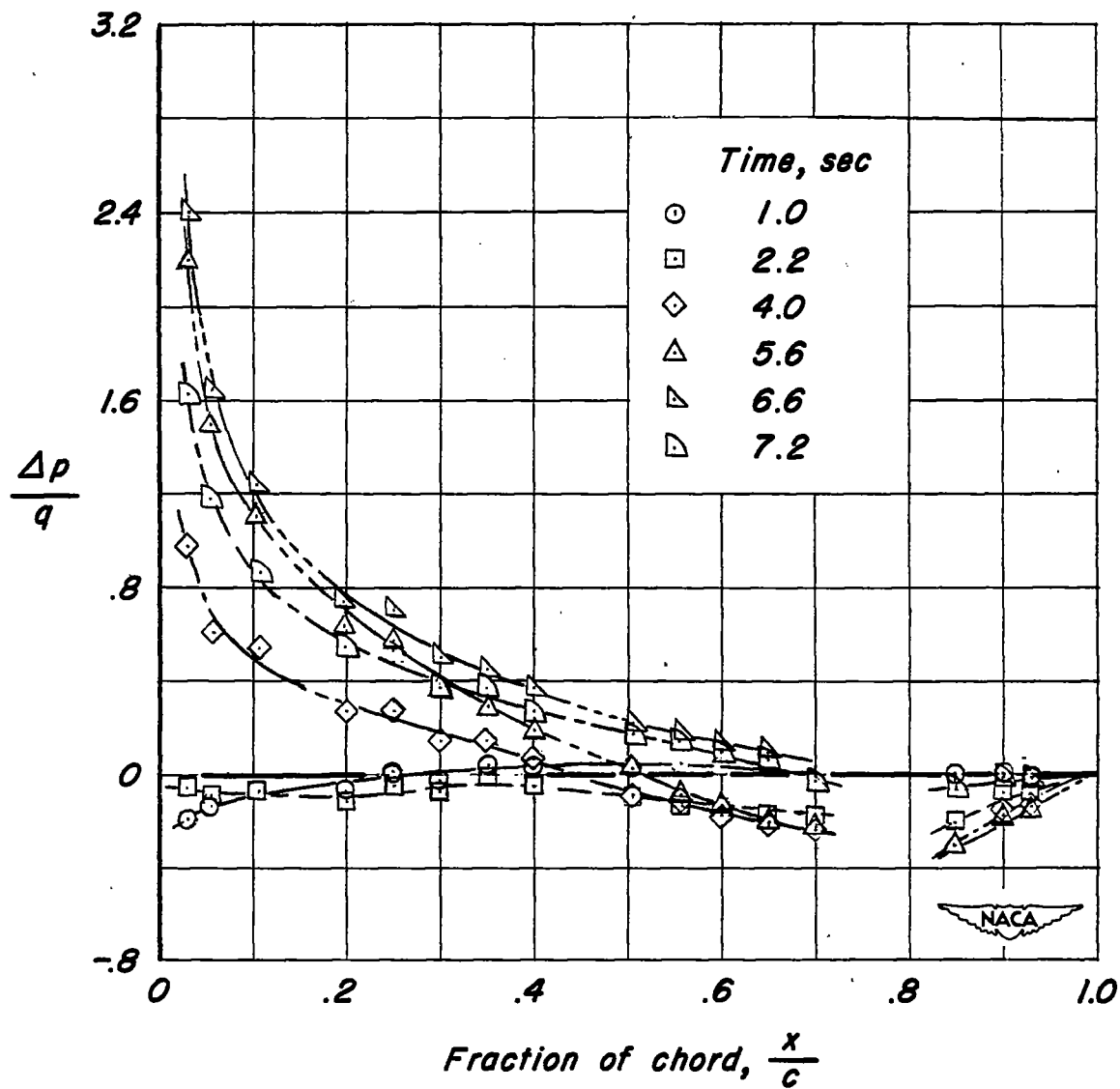
(b) Chordwise distribution of load coefficient at 42.2% span on vertical stabilizer.

Figure 42.- Concluded.



(a) Time history.

Figure 43.— Pertinent quantities measured during rudder-kick maneuver; airspeed, 140 miles per hour; altitude, 20,000 feet.



(b) Chordwise distribution of load coefficient at 42.2% span on vertical stabilizer.

Figure 43.—Concluded.

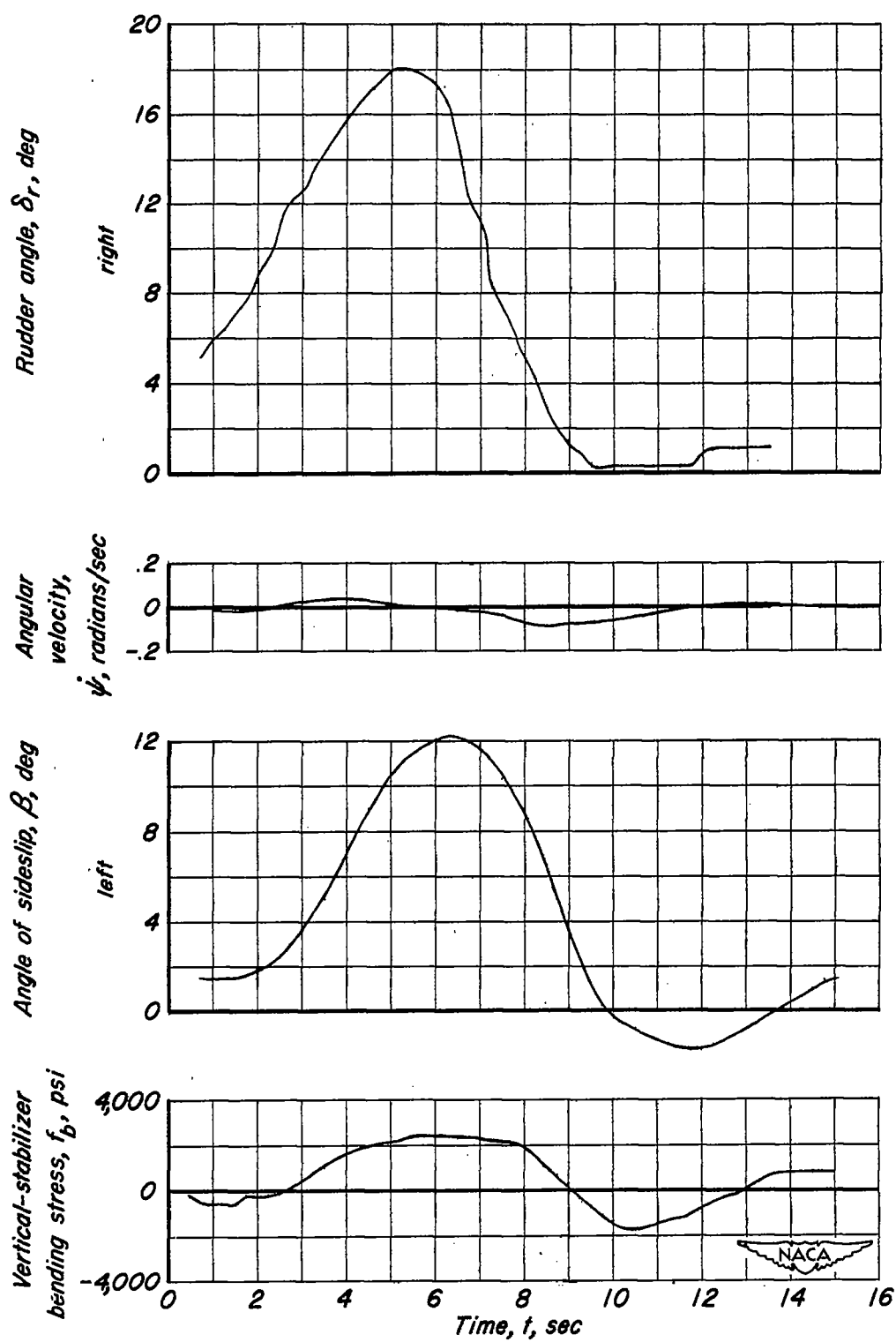
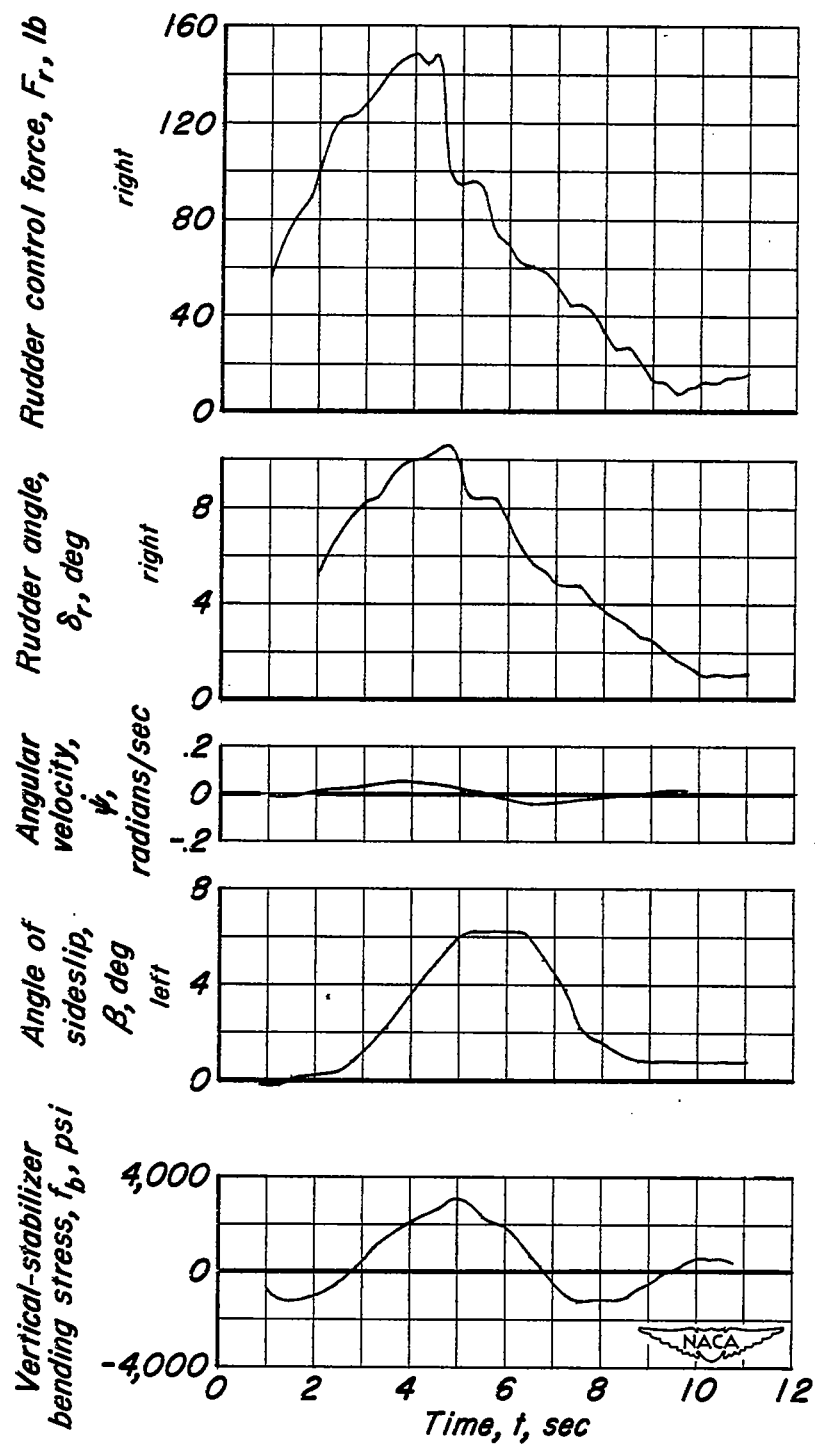
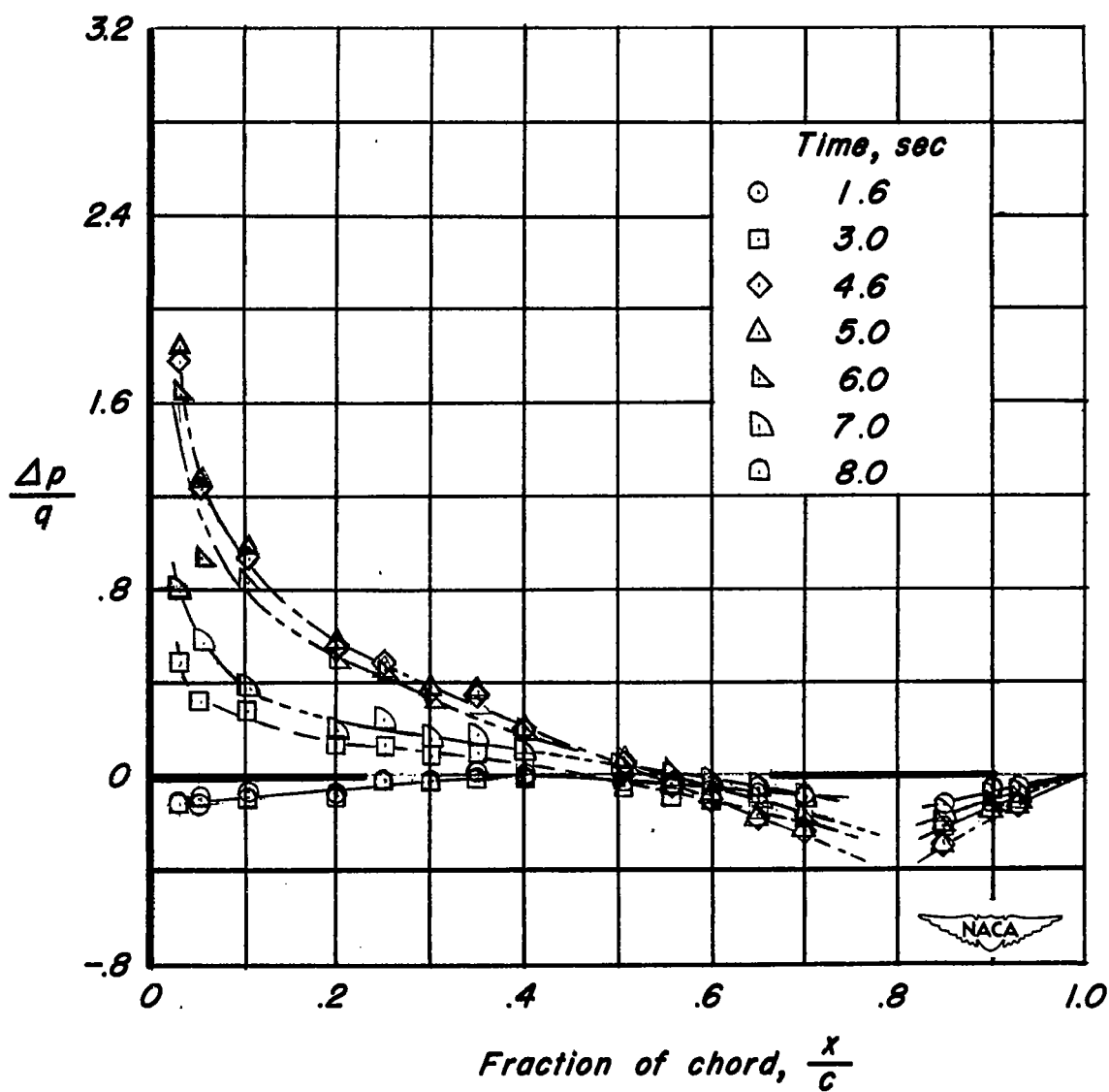


Figure 44.—Time history of rudder-kick maneuver; airspeed, 145 miles per hour; altitude, 19,800 feet.



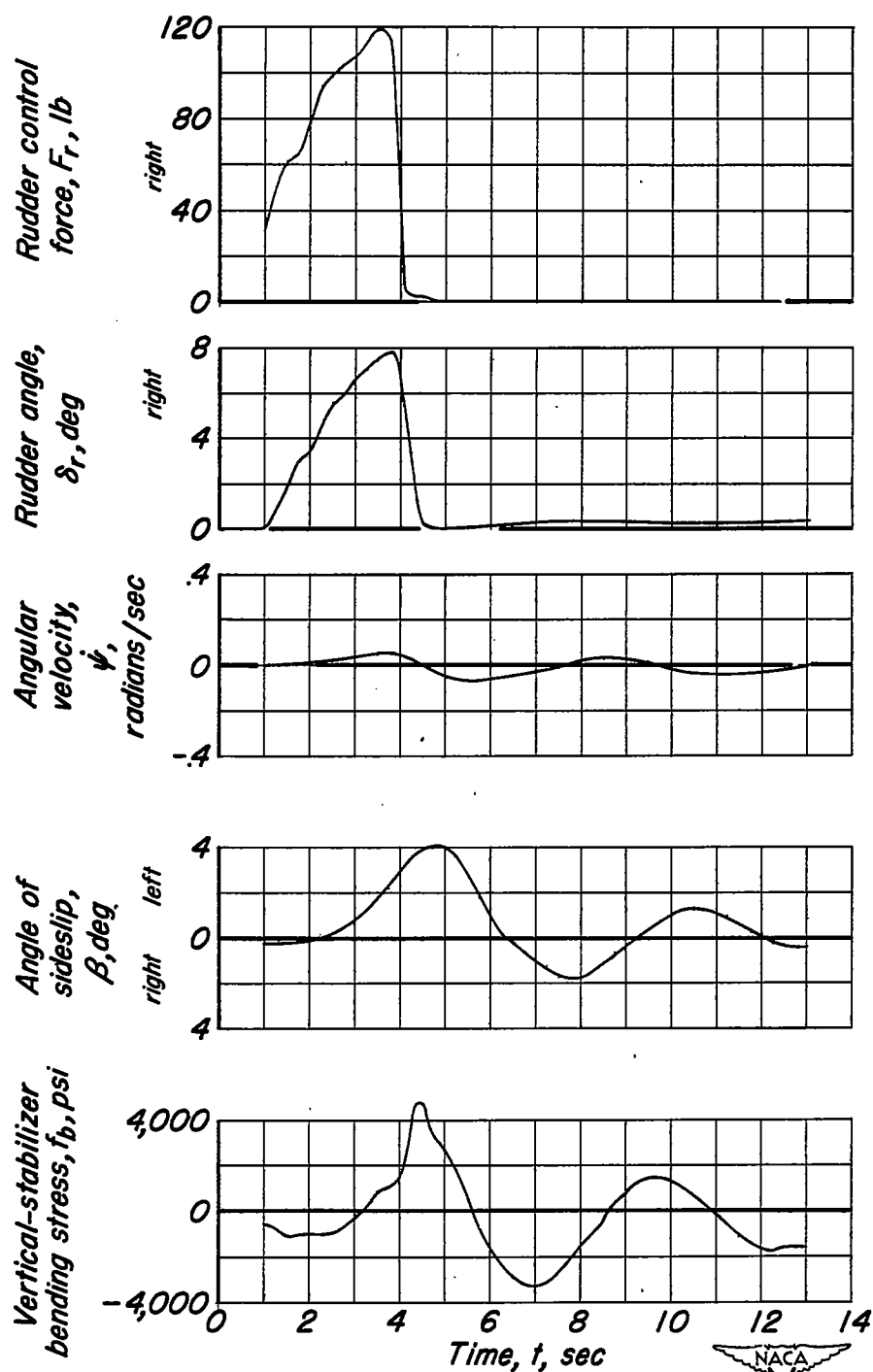
(a) Time history.

Figure 45.—Pertinent quantities measured during rudder-kick maneuver; airspeed, 201 miles per hour; altitude, 20,000 feet.



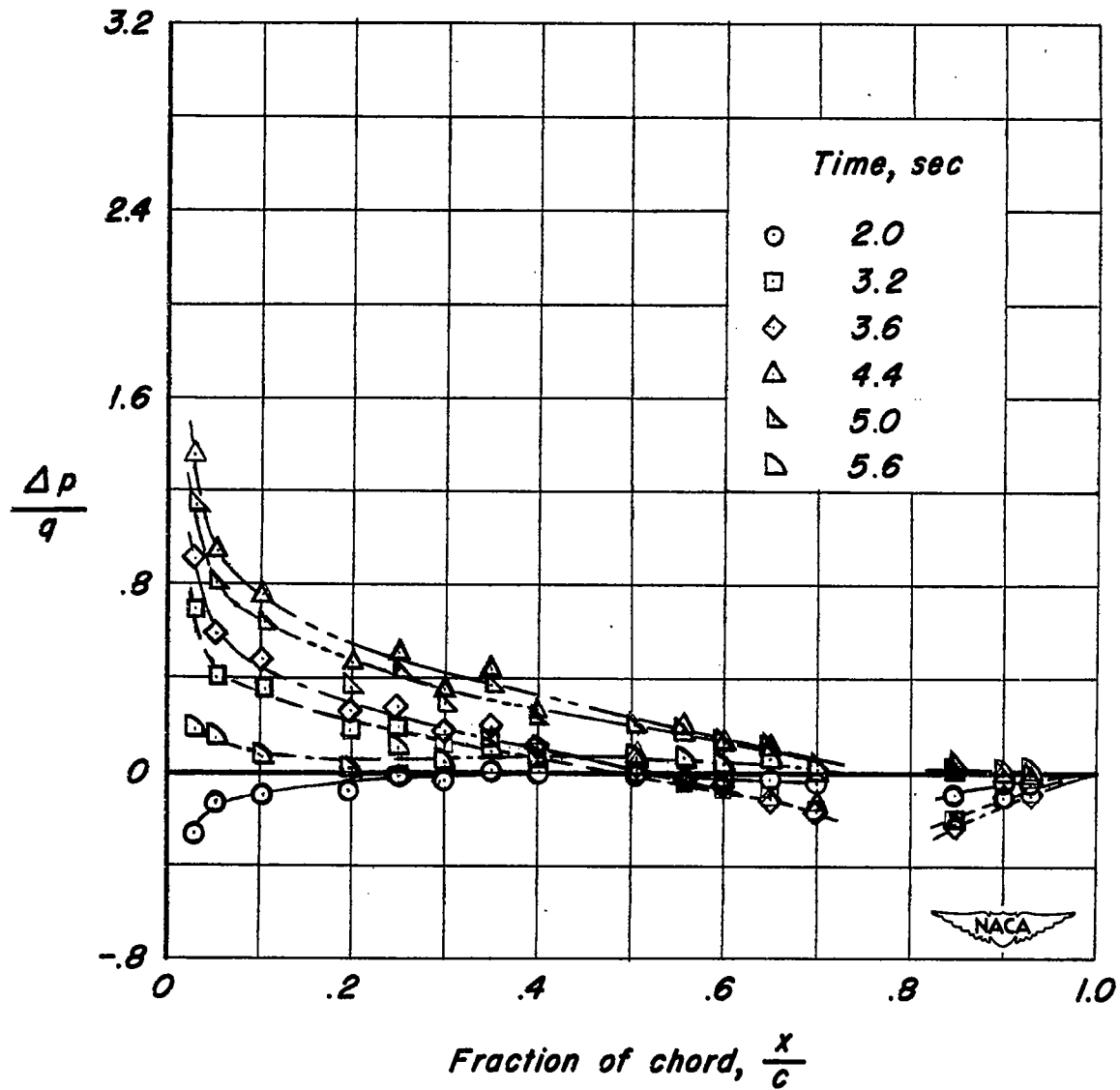
(b) Chordwise distribution of load coefficient at 42.2% span on vertical stabilizer.

Figure 45.—Concluded.



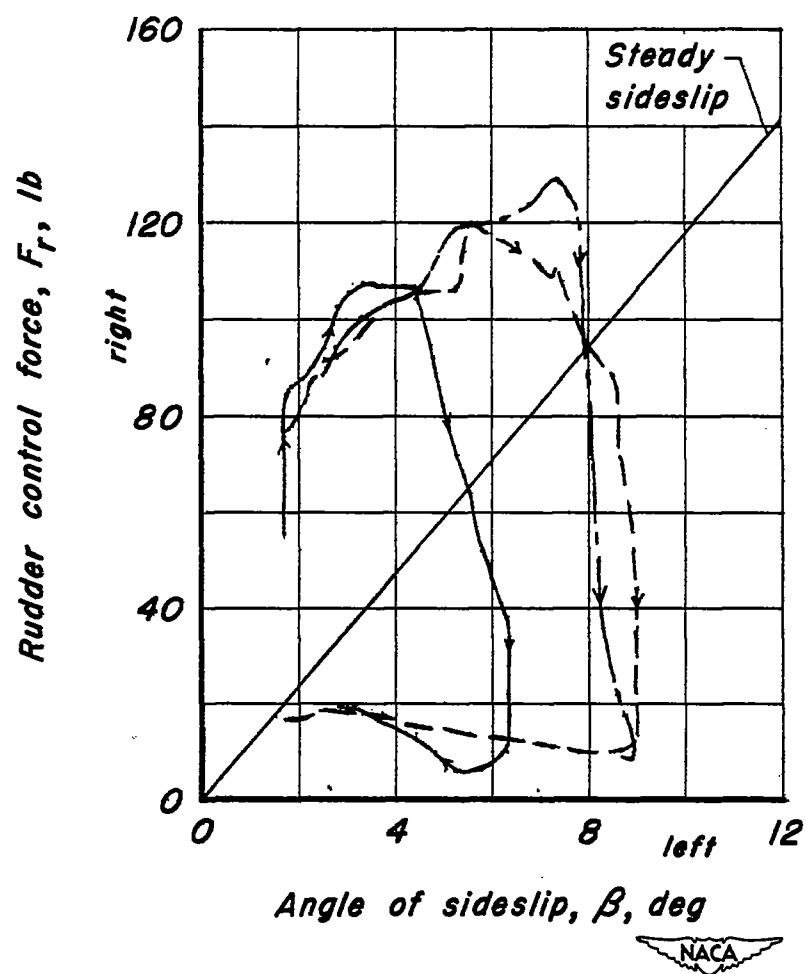
(a) Time history.

Figure 46.- Pertinent quantities measured during rudder-kick maneuver; airspeed, 204 miles per hour; altitude, 20,000 feet.



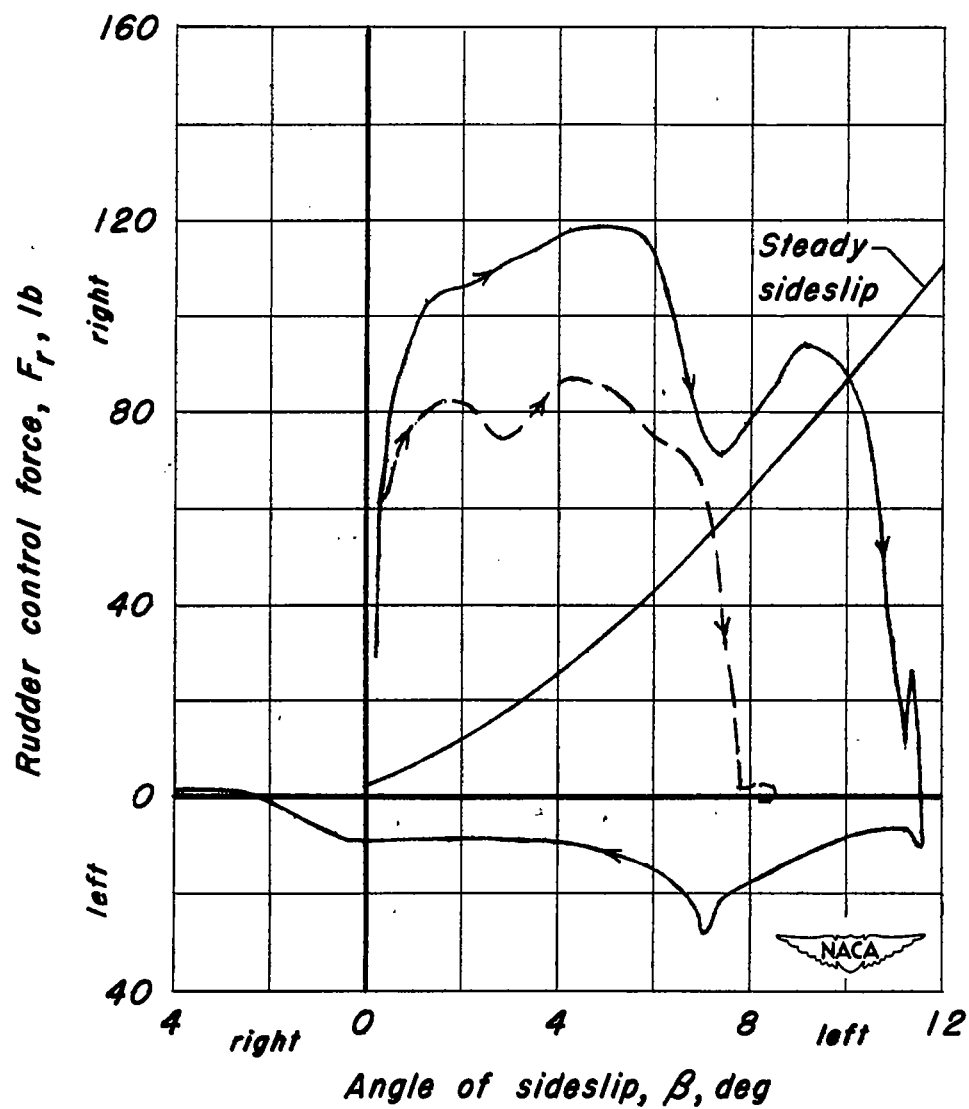
(b) Chordwise distribution of load coefficient at 42.2% span on vertical stabilizer.

Figure 46.—Concluded.



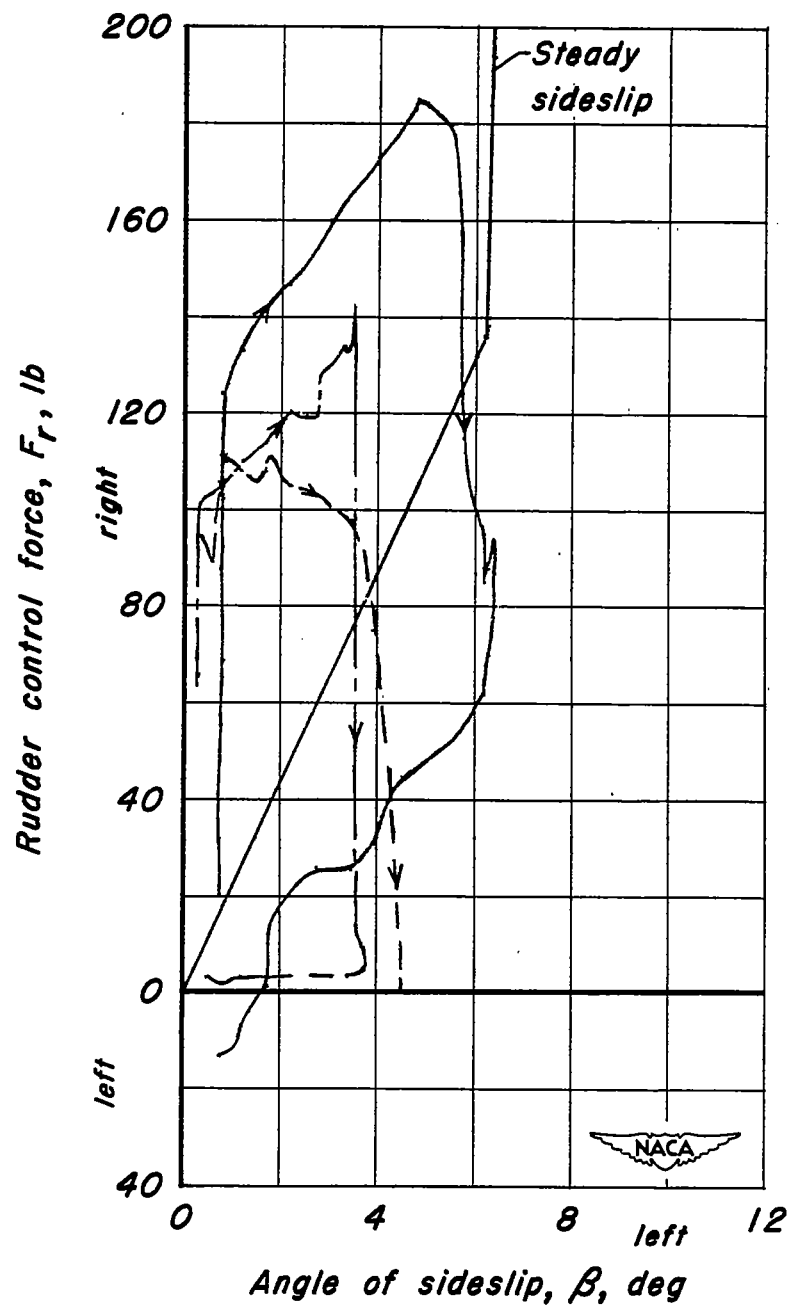
(a) $V_i = 145$ mph; $h_p = 5,000$ ft.

Figure 47.— Concurrent variation of rudder control force and angle of sideslip during yawing maneuvers.



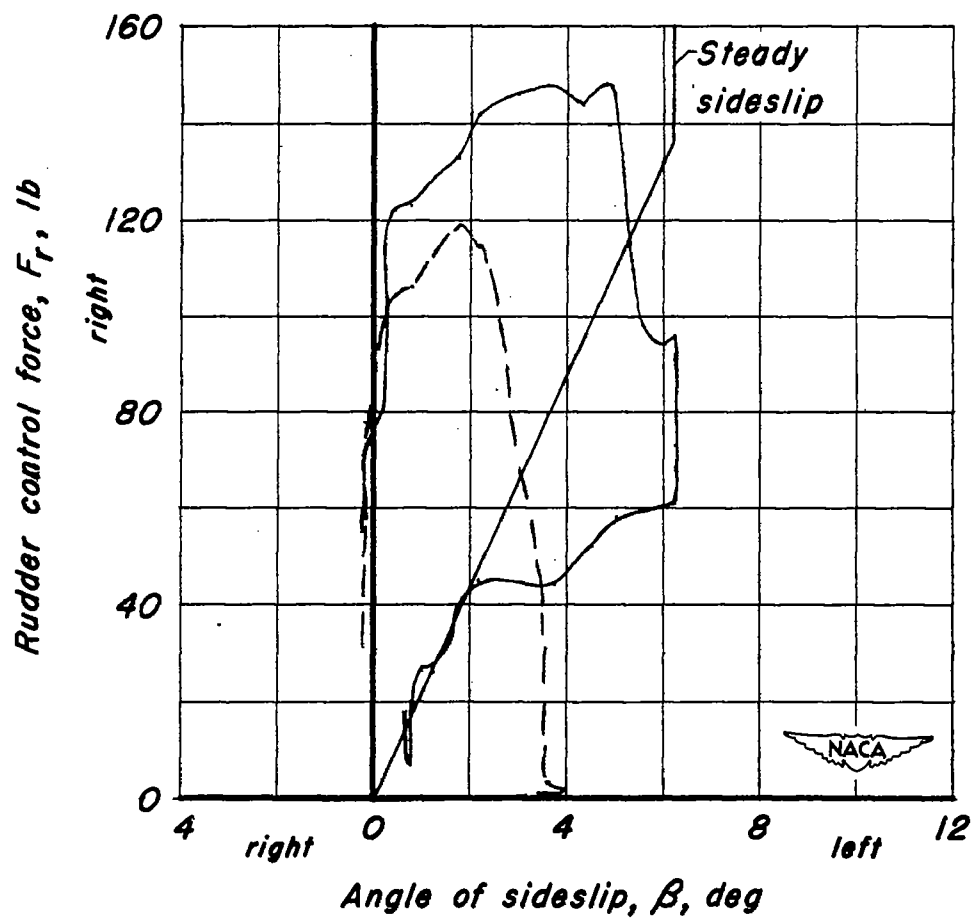
(b) $V_i = 145$ mph ; $h_p = 20,000$ ft.

Figure 47.- Continued.



(c) $V_i = 204$ mph; $h_p = 5,000$ ft.

Figure 47.- Continued.



(d) $V_i = 204 \text{ mph}$; $h_p = 20,000 \text{ ft.}$

Figure 47.- Concluded.

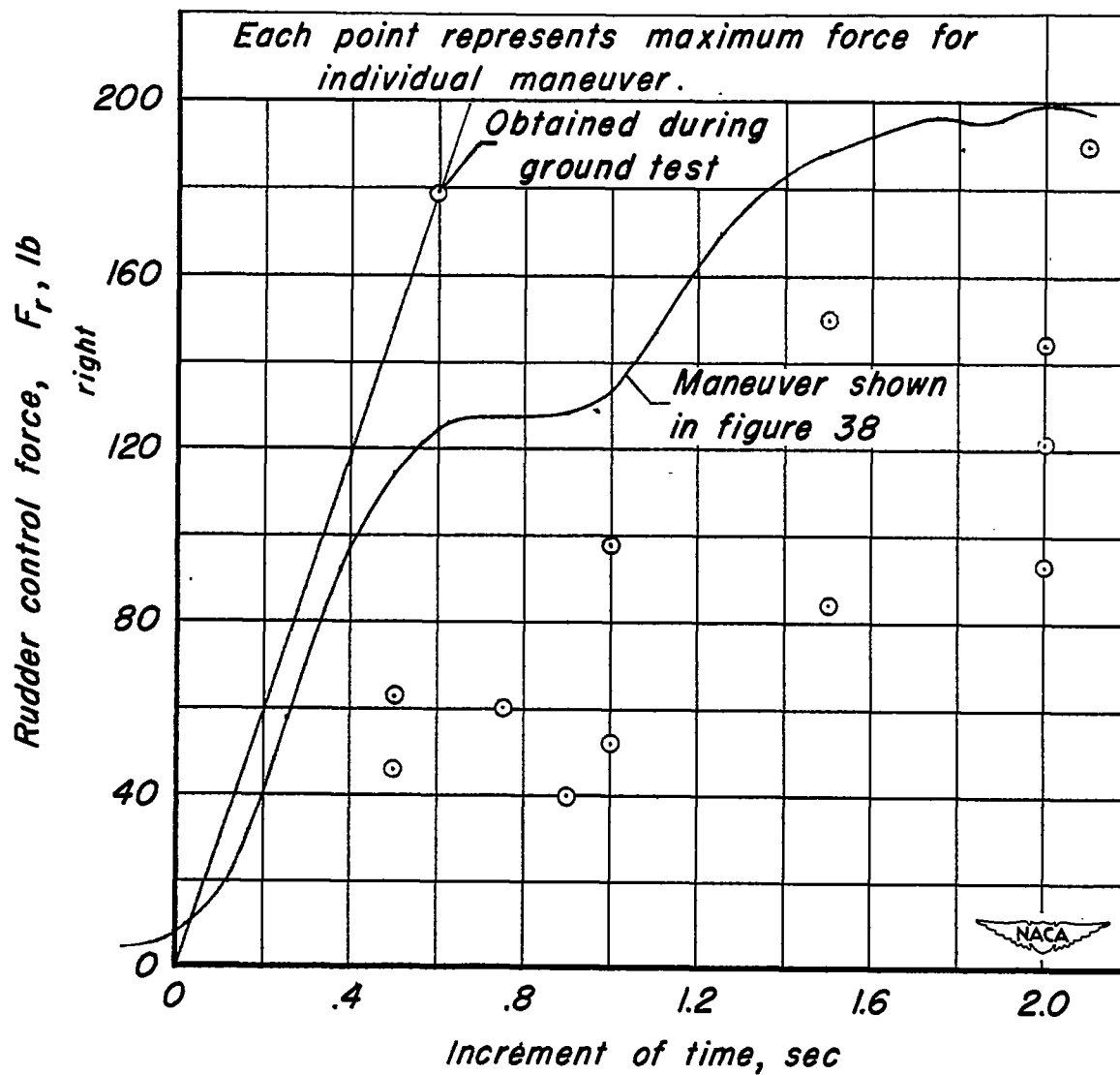
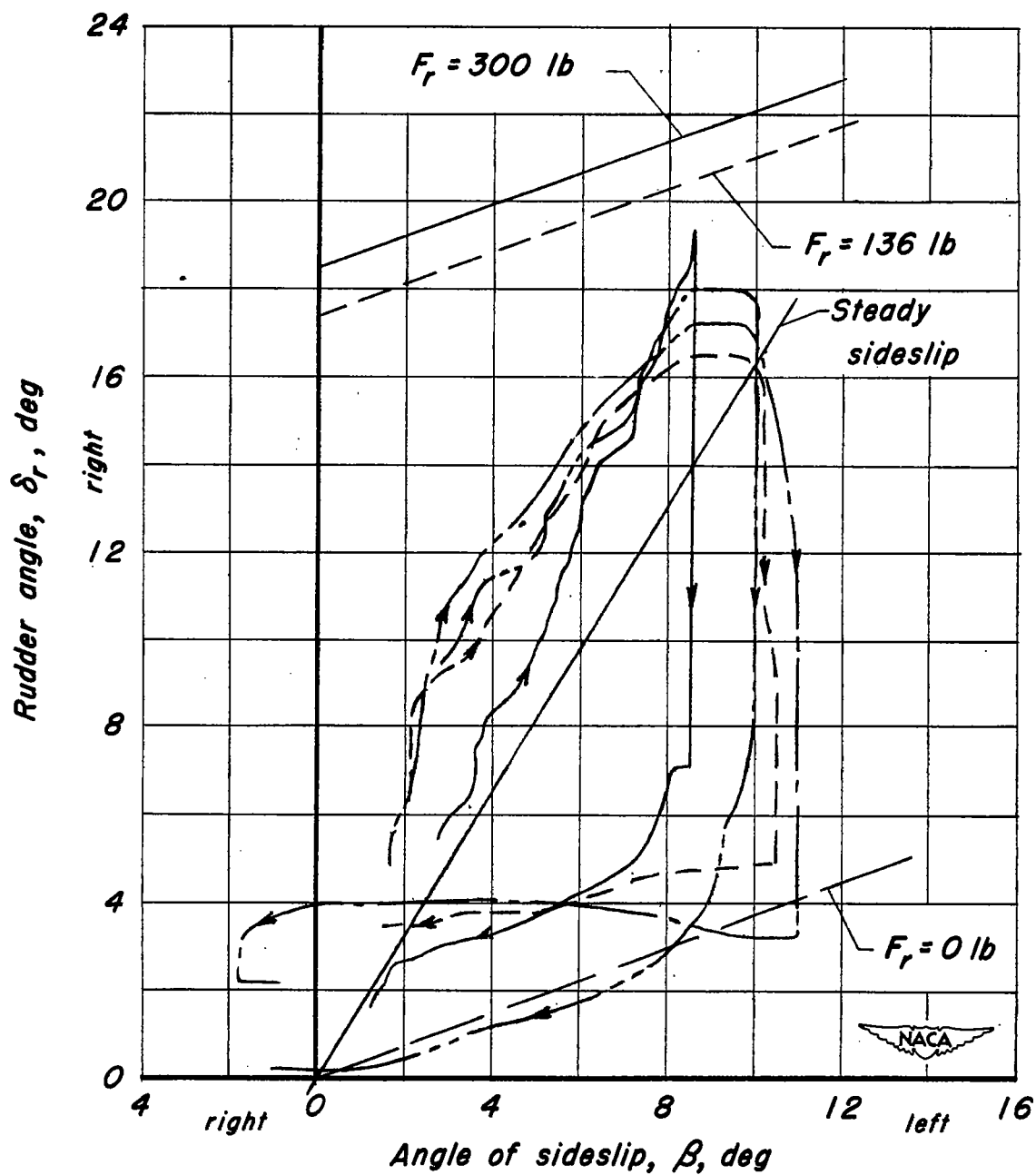
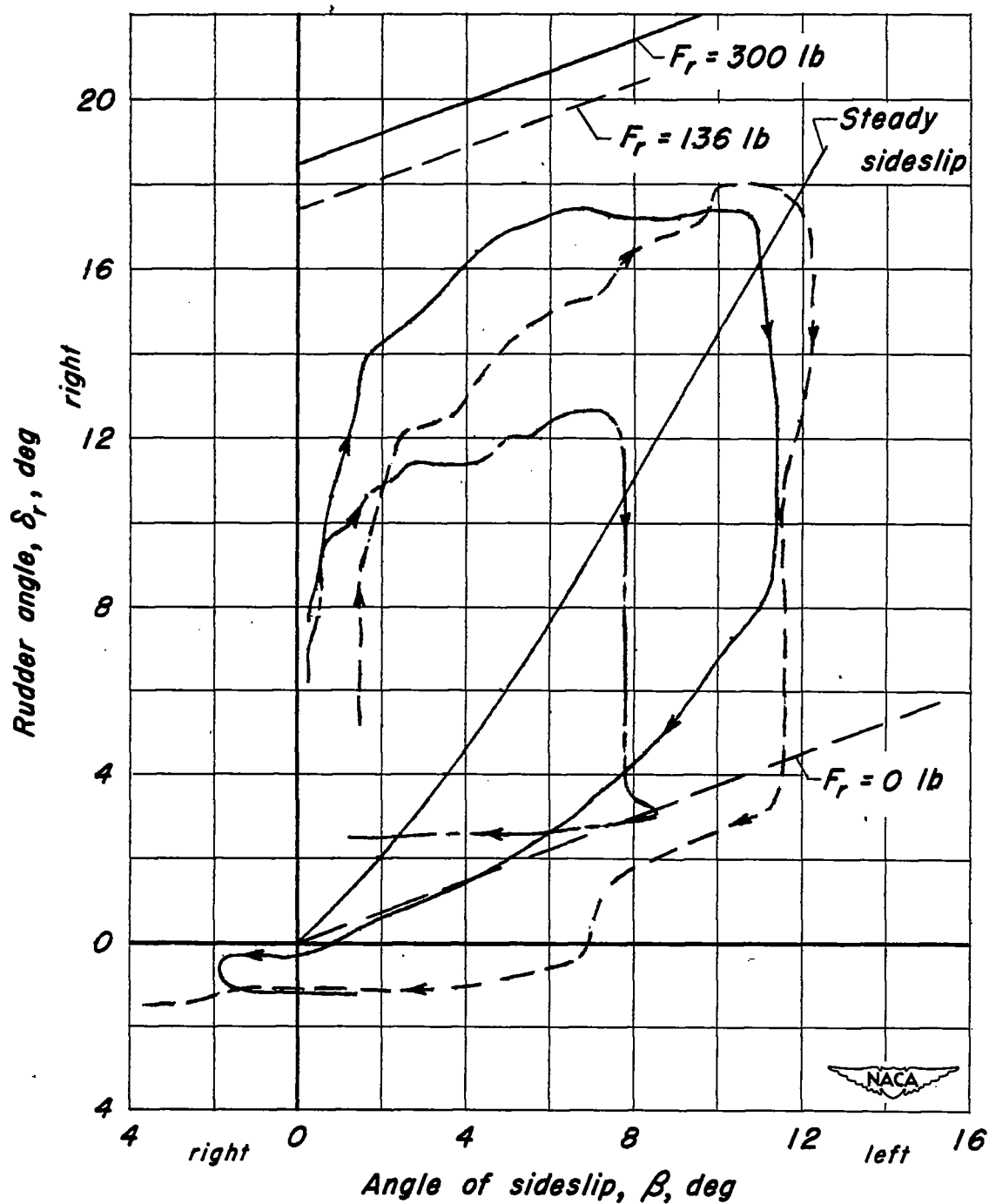


Figure 48.— Time required to apply rudder control forces during yawing maneuvers.



(a) $V_i = 145$ mph; $h_p = 5,000$ ft.

Figure 49.— Concurrent variation of rudder angle and angle of sideslip during yawing maneuvers.



(b) $V_i = 145$ mph; $h_p = 20,000$ ft.

Figure 49.- Continued.

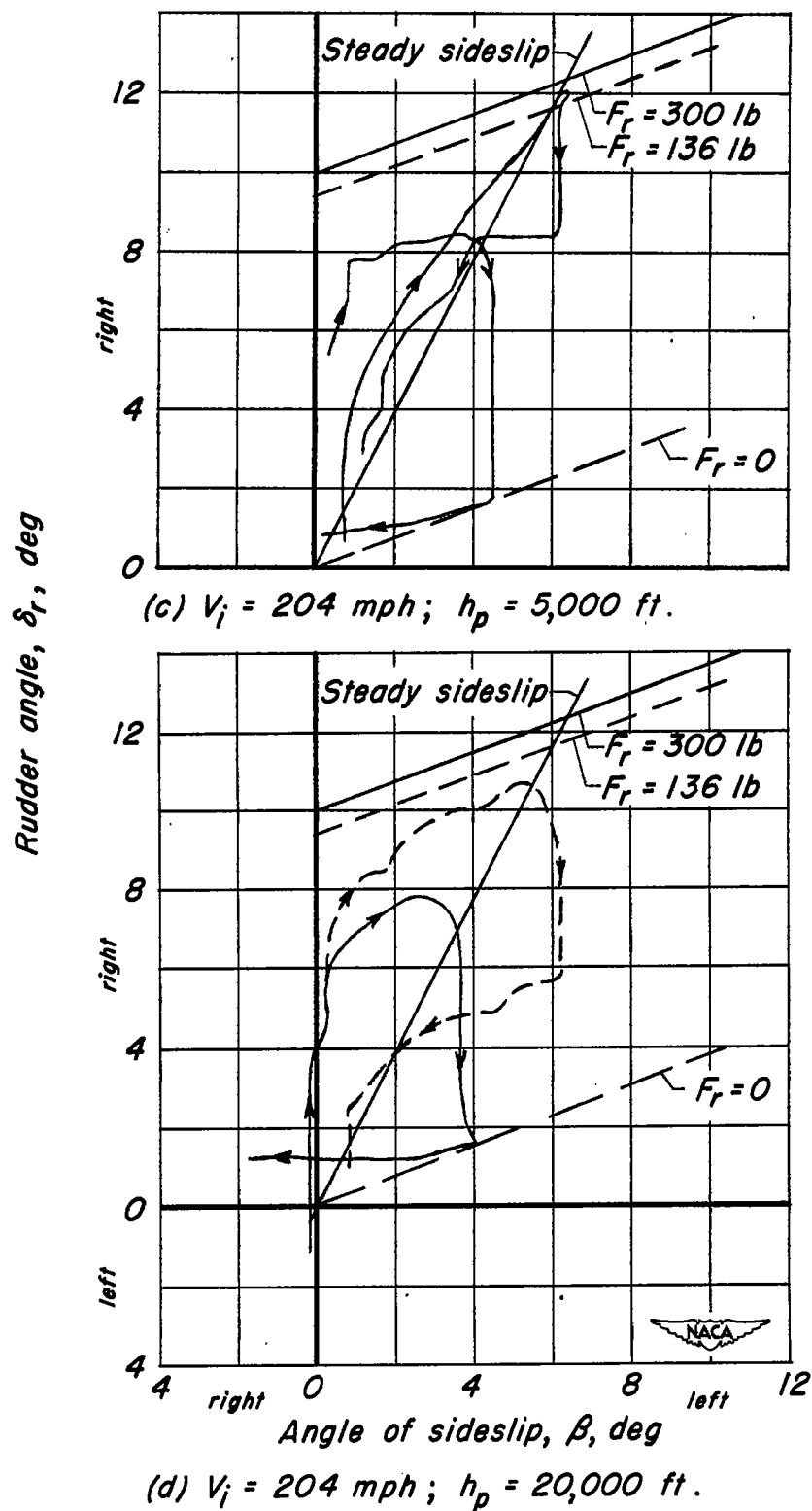


Figure 49.—Concluded.

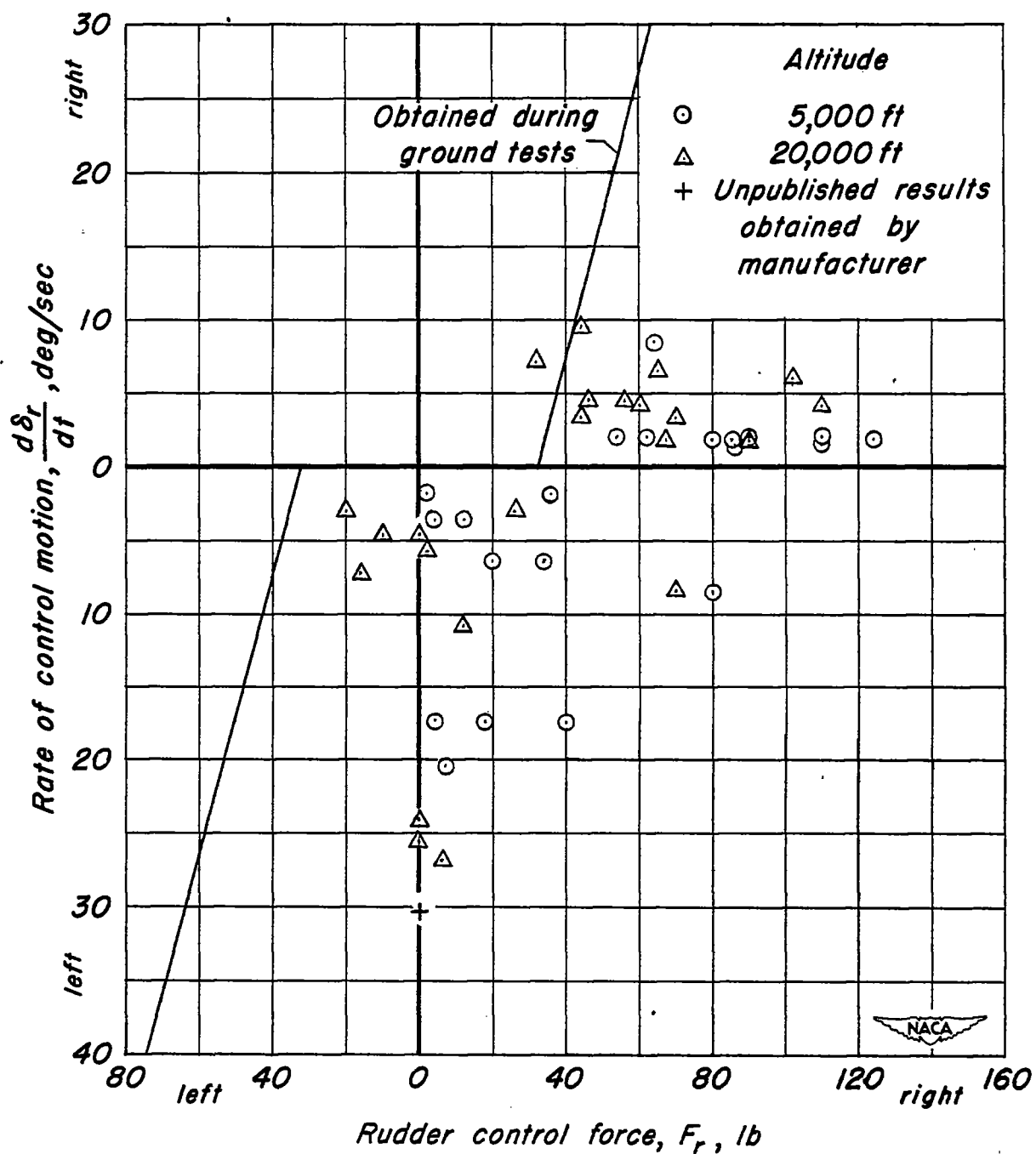


Figure 50.- Maximum rates of rudder motion as a function of rudder control force from flight tests.

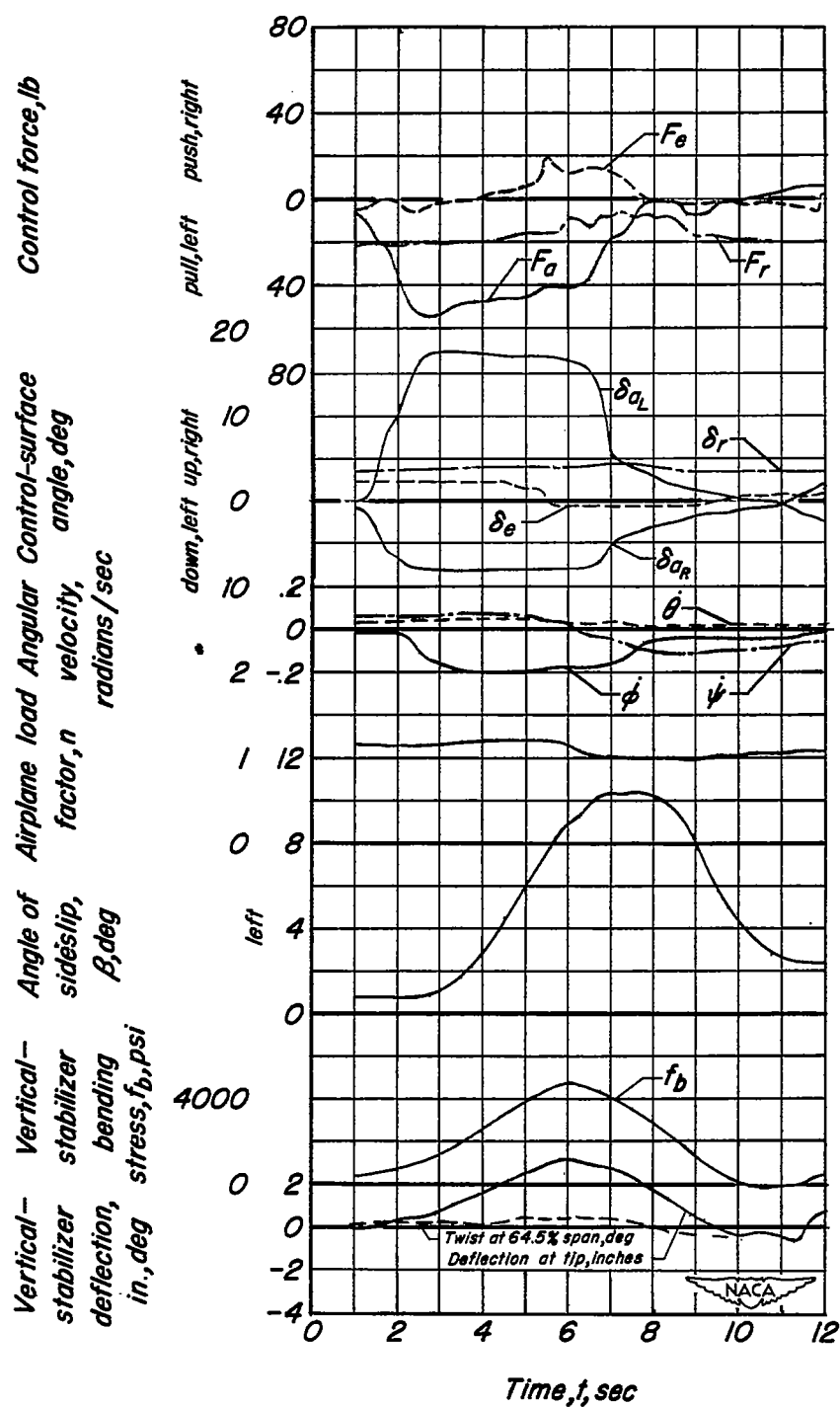
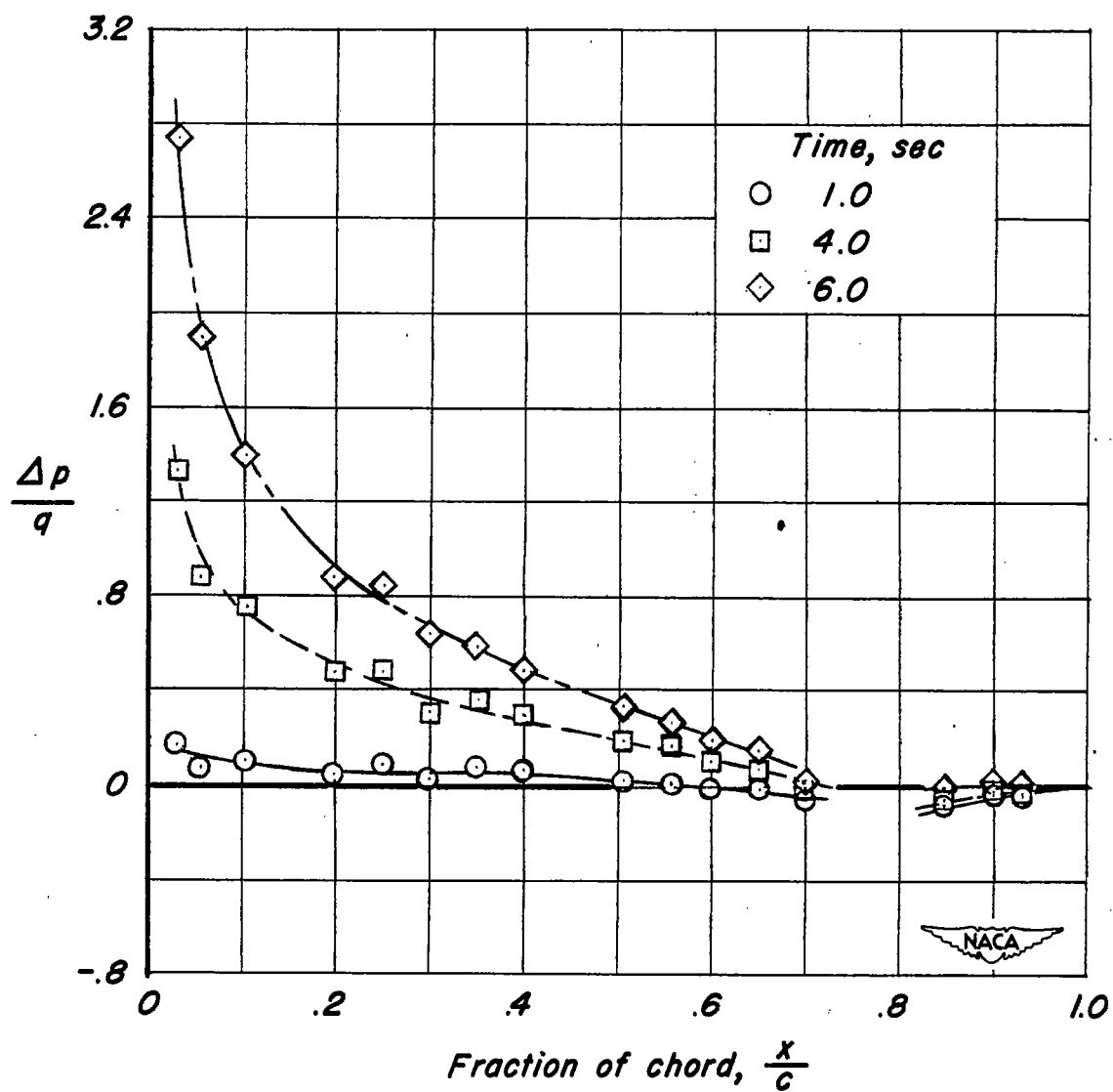
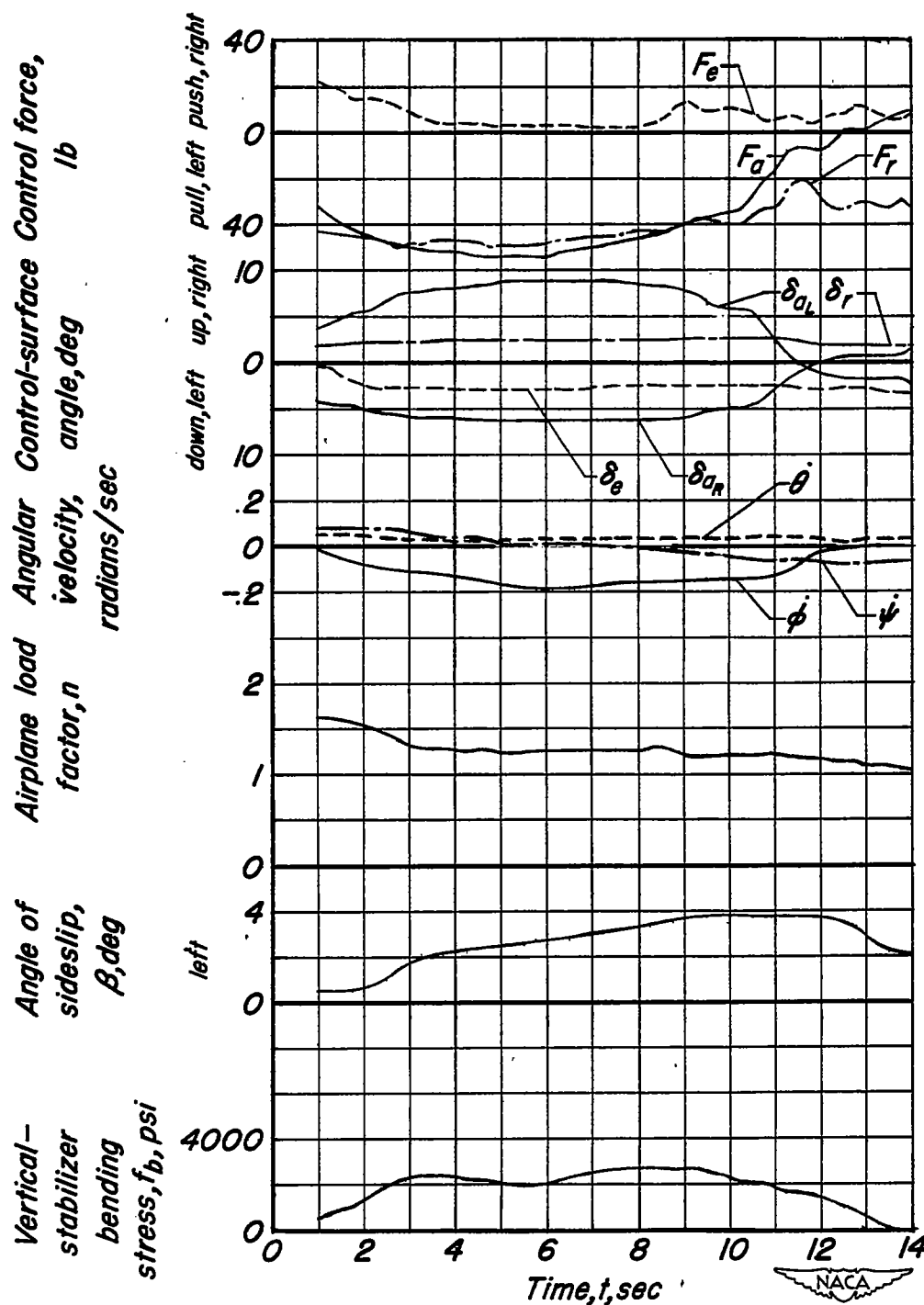


Figure 52.—Pertinent quantities measured during rolling pull-out maneuver; airspeed, 144 miles per hour; altitude, 20,000 feet.



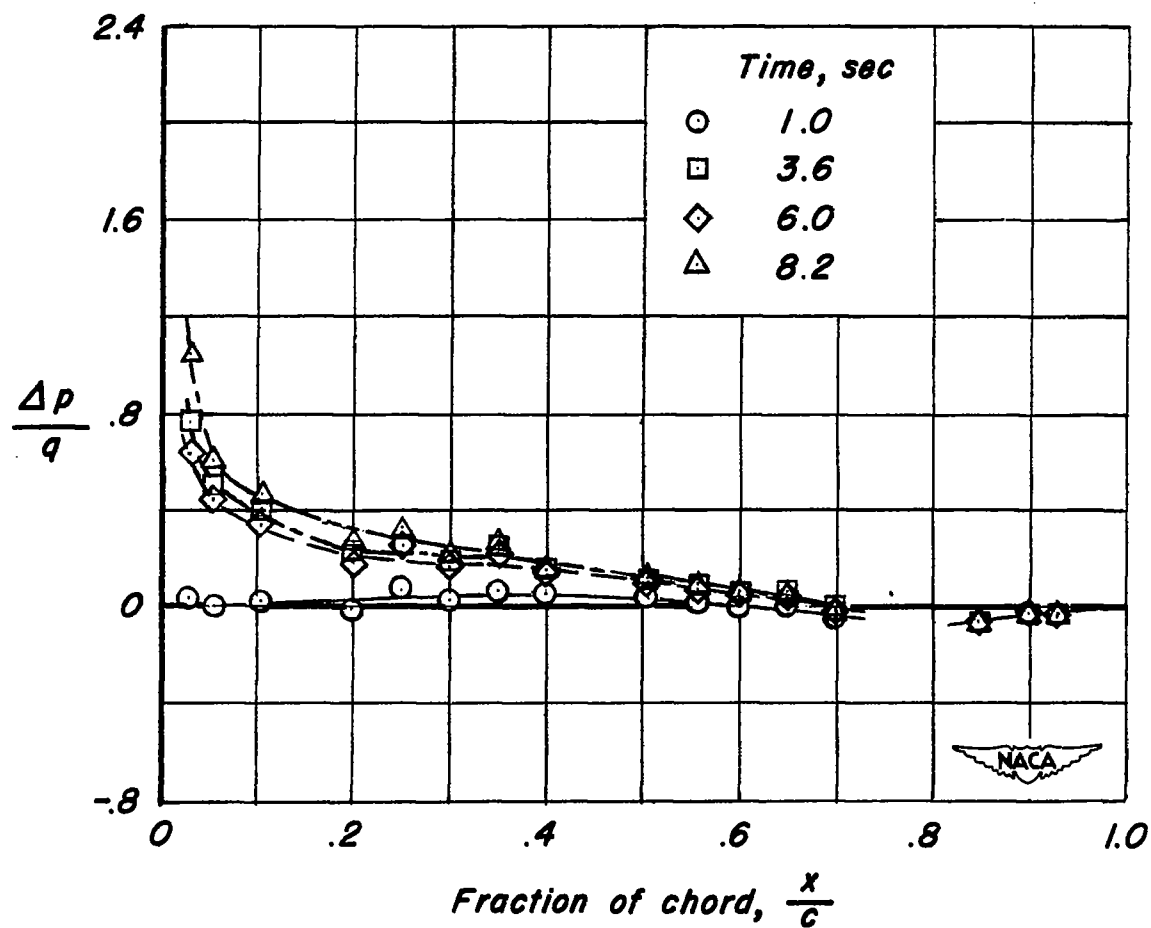
(b) Chordwise distribution of load coefficient at 42.2% span on vertical stabilizer.

Figure 52.- Concluded.



(a) Time history.

Figure 53.- Pertinent quantities measured during rolling pull-out maneuver; airspeed, 204 miles per hour; altitude, 20,000 feet.



(b) Chordwise distribution of load coefficient at 42.2% span on vertical stabilizer.

Figure 53.—Concluded.

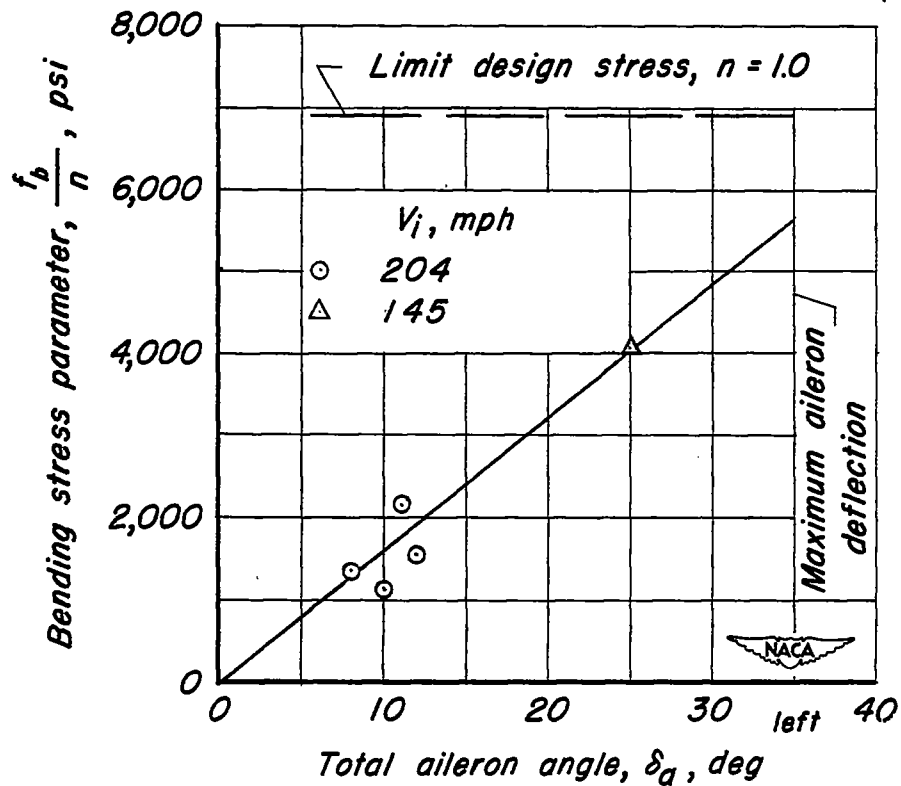
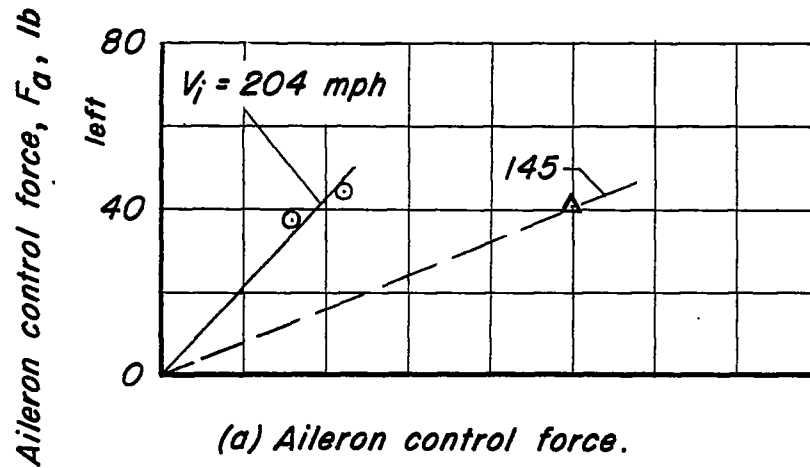
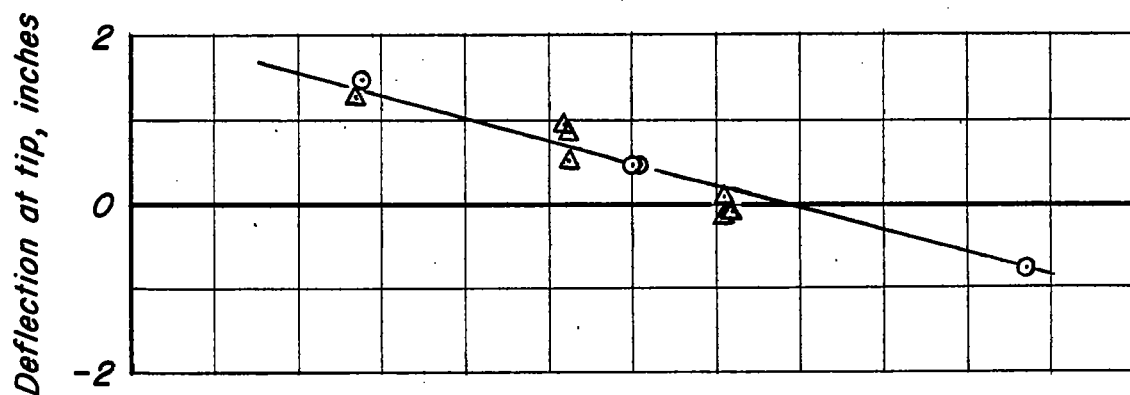
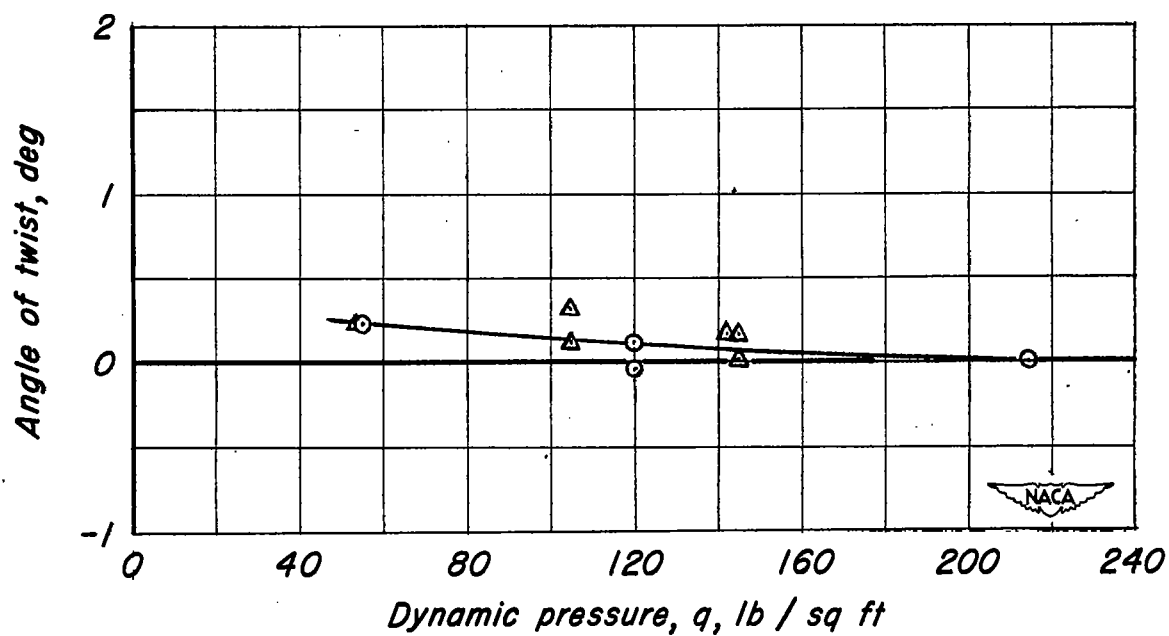


Figure 54.- Aileron control forces used in rolling pull-out maneuver as a function of total aileron angle and effect of total aileron angle on vertical-stabilizer bending stress.

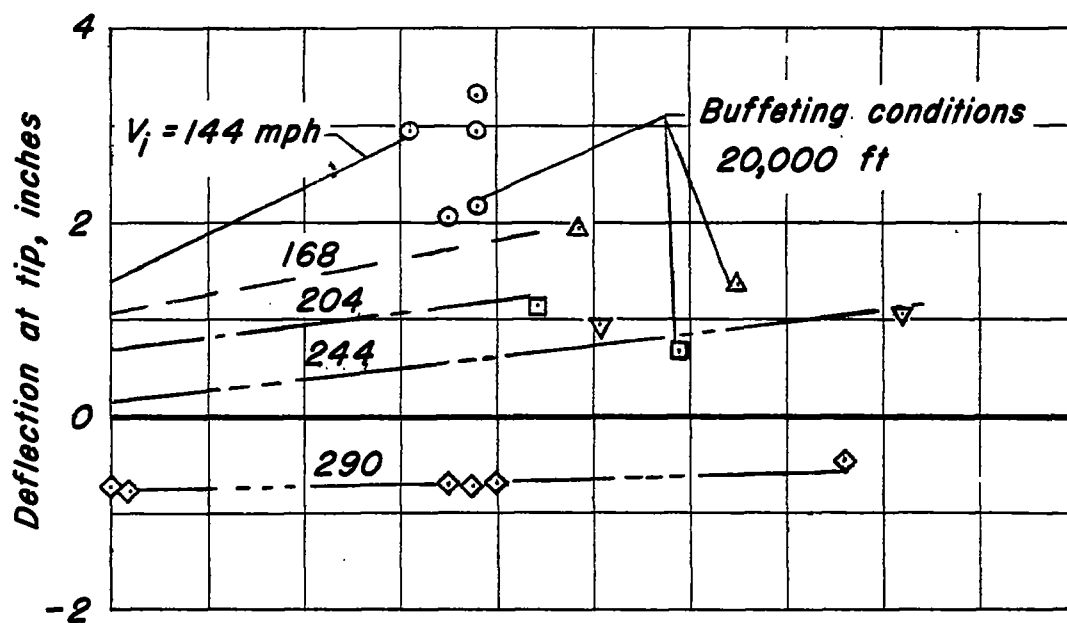


(a) Deflection of stabilizer tip.

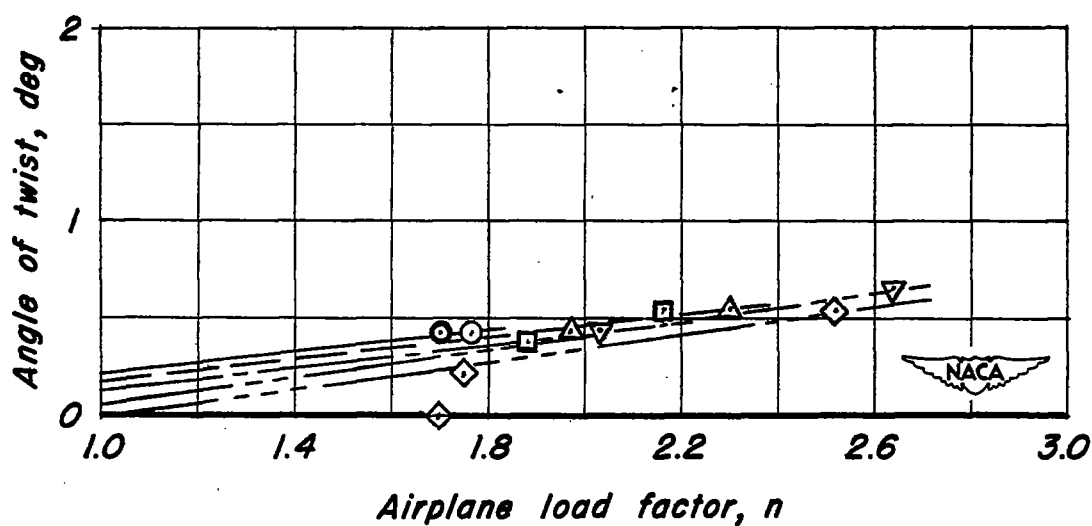


(b) Twist at 64.5% stabilizer semispan.

Figure 55.- Horizontal-stabilizer distortion in unaccelerated flight.



(a) Deflection of stabilizer tip.



(b) Twist at 64.5% stabilizer semispan.

Figure 56.-Horizontal-stabilizer distortion in steady turning flight.

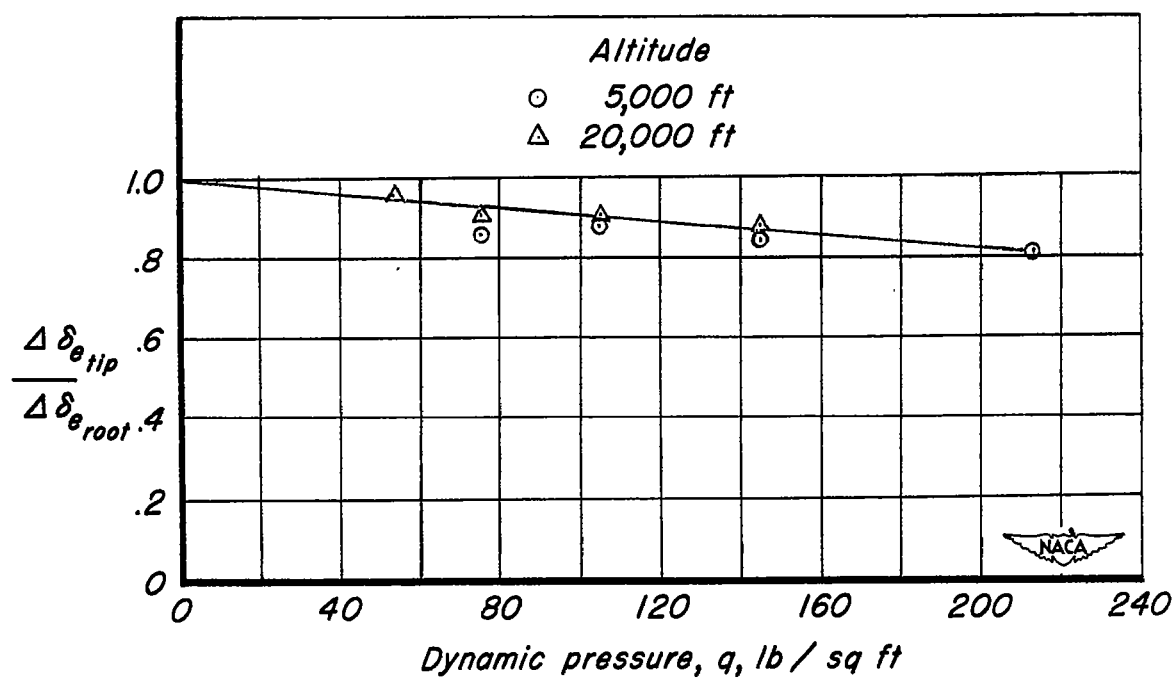
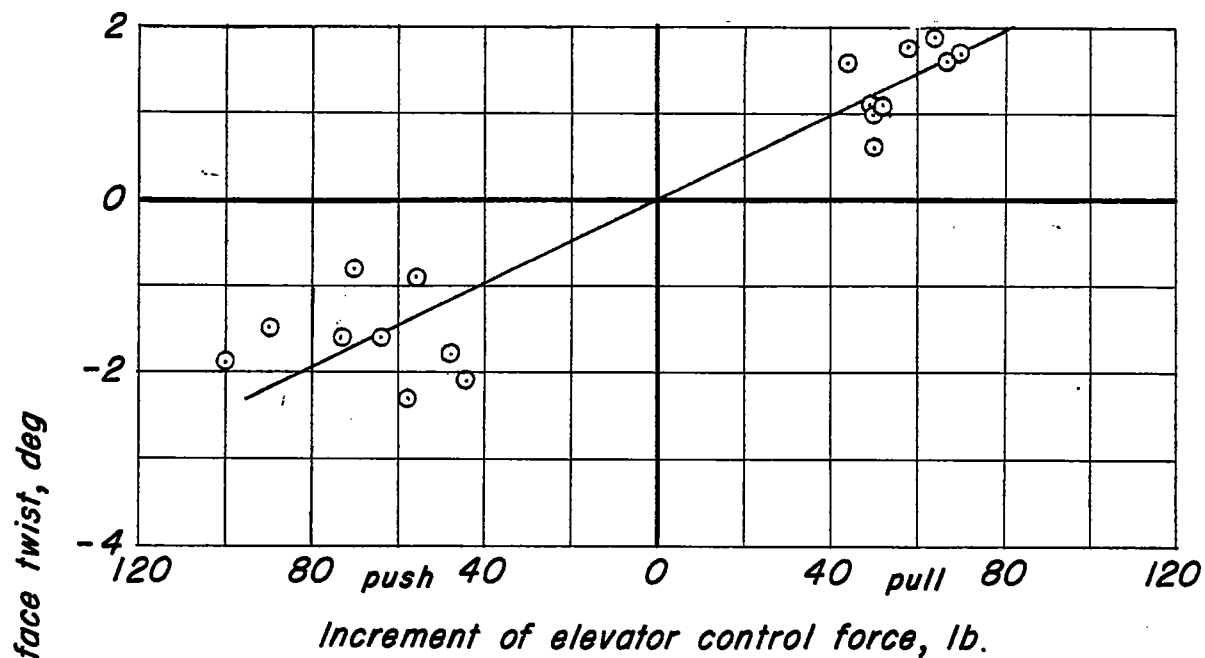
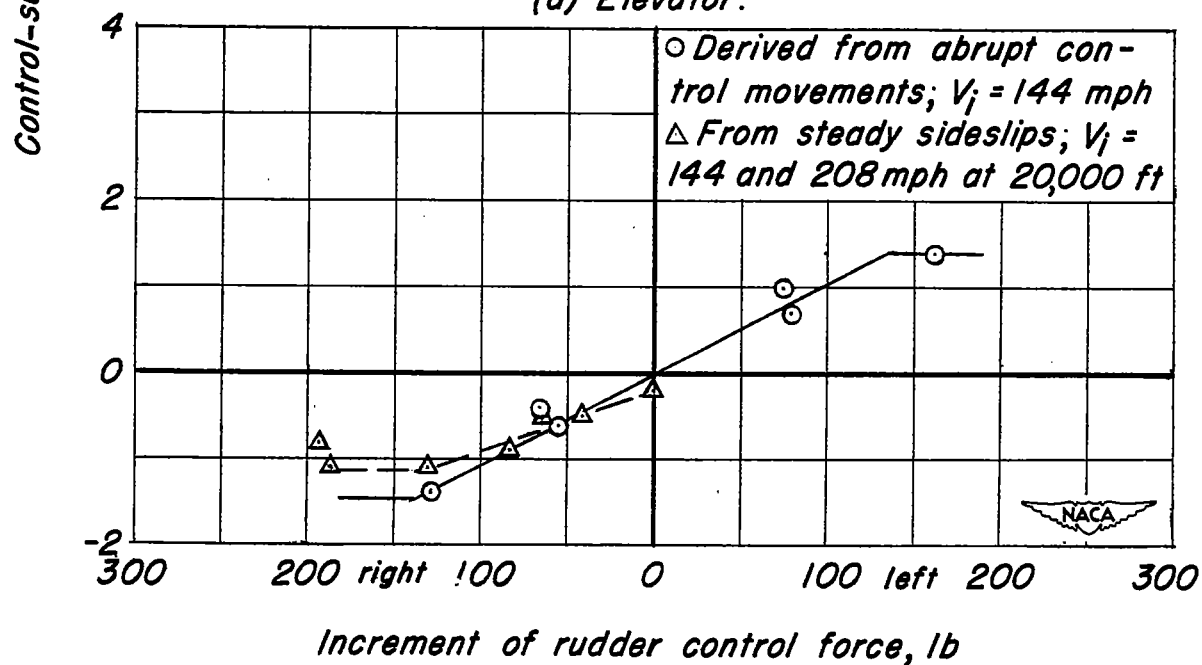


Figure 57.-Effect of dynamic pressure upon the elevator deflection at the outboard station.



(a) Elevator.



(b) Rudder.

Figure 58.—Measured twist of control surface with respect to stabilizer as a function of control force.